THE HONG KONG POLYTECHNIC UNIVERSITY

DEPARTMENT OF LAND SURVEYING AND GEO-INFORMATICS

AN ITRF COMBINATION MODEL WITH PREFERRED OBSERVATION FUNCTIONALS AND ITS SOLUTION USING GENERALIZED CONDITION EQUATIONS

HOK SUM FOK

A Thesis Submitted in Partial Fulfillment of the Requirements for the

Degree of Master of Philosophy

May, 2007

CERTIFICATE OF ORIGINALITY

I hereby declare that this thesis is my own work and that, to the best of my knowledge and belief, it reproduces no material previously published or written, nor material that has been accepted for the award of any other degree or diploma, except where due acknowledgement has been made in the text.

(Signed)

Hok Sum Fok (Name of Student)

ABSTRACT

Providing a stable and accurate reference frame is of the fundamental importance because accurate solution realization of an International Terresterial Reference Frame (ITRF) is essential to the correct interpretation of any geophysical and geologic phenomena. The existing ITRF mathematical model uses the state vectors of different stations derived from a number of terrestrial reference frames as observations. However, the station state vectors are not always directly observed but derived from different space geodetic measurements that may be lack of Earth's center of mass and orientation information, which are necessary for defining a terrestrial reference frame.

This thesis aims to demonstrate an alternative approach, called *Preferred Observation Functionals (POF) approach*, in the solution realization of an international terrestrial reference frame from the combination of a number of auxiliary reference frames. The new formulation takes into account the inherent properties of different space geodesy measurement techniques in the solution. Three alternative formulations are demonstrated using the available TRF data. State Vector (SV) based solution is also presented for comparison with the alternative solutions.

The resulting station position and velocity estimates generated from the POF approach are, in general, comparatively more precise than the SV based solution. The results also indicate the actual position difference between station position estimates obtained from the above approaches and ITRF2000 solution realization

in each coordinate component are at a few centimeter levels, while the horizontal station velocity estimates generated from both approaches shows a good agreement with the ITRF2000 solution, particularly for those based on the POF approach. Those results present that the alternative combination solutions are not significantly different from the ITRF2000 official solution, but improve upon them by directly accounting for the inherent geometric and physical properties of different space geodesy measurement techniques.

ACKNOWLEDGEMENTS

This study is supported in part by the research project: Significance of Reference Frame Deformations in the Realization of ITRF (G-T423)

I would like to express my sincere appreciation to my supervisor Dr. H. Baki Iz for his valuable guidance, supervision and financial support towards the successful accomplishment of this research work for the past four years.

I would also like to thank Mr. W.Y. Tang for his help in matrix arrangement methodology, Mr. C.P. Chui, Miss Asma Ibrahim and Dr. E.K. Forkuo for listening to me and sharing different ideas.

TABLE OF CONTENTS

LIST OF TABLES

LIST OF FIGURES

LIST OF ABBREVIATIONS AND ACRONYMS

AC	Analysis Center for Space Geodesy Techniques
AUS	Australian Surveying and Land Information Group
CDDIS	Crustal Dynamics Data Information System
CGS	Centro Geodesia Spaziale, Matera
CODE	Center for Orbit Determination in Europe
CRL	Communications Research Laboratory
CSR	Center for Space Research
CTRS	Conventional Terrestrial Reference System
DEOS	Delft Ins. Earth Oriented Space Research
DGFI	Deutsches Geod¨atisches Forschungsinstitut
DORIS	Doppler Orbit determination and Radiopositioning by Satellite
EOP	Earth Orientation Parameter
FSG	Forschungseinrichtung Satellitengeodaesie
GFZ	GeoForschungsZentrum Potsdam
GFSC	Goddard Space Flight Center
GIA	Geophysical Institute, University of Alaska
GIUB	Geodetic Institute of Bonn University
GPS	Global Positioning System
GRGS	Groupe de Recherche de Geodesie Spatiale
IAU	International Astronomical Union
ICRF	International Celestial Reference Frame
ICRS	International Celestial Reference System
IDS	Interational DORIS Service
IERS	International Earth Rotation and Reference Systems Service
IGS	International GPS Service
IGN	Institut Gographique National
ILRS	International Laser Ranging Service
ITRF	International Terrestrial Reference Frame
ITRS	International Terrestrial Reference System
IUGG	International Union of Geodesy and Geophysics

IVS	Interational VLBI Service
JCET	Joint Center for Earth System Technology, GSFC
JPL	Jet Propulsion Laboratory
LOD	Length of Day
NCL	Univ of Newcastle upon Tyne
NOAA	National Oceanic & Atmospheric Administration
OVR	Overall Variance Ratio
POF	Preferred Observation Functionals Approach
POF with GPSBL	POF solution with GPS Baseline Lengths as Observations
POF with GPSBV	POF solution with GPS Baseline Vectors as Observations
POF with GPSSV	POF solution with GPS State Vectors as Observations
SHA	Shanghai Astronomical Observatory
SLR	Satellite Laser Ranging
SV	State Vector Based Solution
TRF	Terrestrial Reference Frame
TRS	Terrestrial Reference System
UT1	Principal Form of Universal Time
UTC	Coordinated Universal Time
VLBI	Very Long Baseline Interferometry

1. INTRODUCTION

1.1 Introduction

The evolution of space geodesy techniques (e.g. SLR, VLBI, GPS, DORIS) and their contribution to the reference system realization has a marked impact on the geophysical and geodetic research over the past decade. Most of these studies rely on the International Terrestrial Reference Frame (ITRF), which is defined as a combination of each individual solution of space geodesy techniques that defines its own terrestrial reference frame (TRF) [Iz and Fok, 2004].

A terrestrial reference system (TRS) is one of the key elements in the modeling and monitoring of Earth rotation [Boucher, 1990]. Continuous effort in defining and maintaining a stable and accurate reference frame is necessary [Bock and Zhu, 1982)] because how well the reference frame is realized has important implications for our ability to study both regional and global properties of the Earth, including post-glacial rebound, sea-level change, plate tectonics, regional subsidence and loading, plate boundary deformation, and Earth orientation excitation [Altamimi *et al*., 1993, 2001c; Becker *et al*., 1997; Blewitt *et al*., 1997; Bruyninx *et al*., 1997; Dietrich *et al*., 2001; Drewes, 1998; Willis and Morel, 2001].

As each space geodesy technique defines and realizes its own TRS, having systematic differences (offsets) when one is compared to another [Altamimi *et al*., 1993, 2002a, 2002b; Boucher *et al*., 1997; Sillard *et al*., 1998], International Terrestrial Reference System (ITRS) was initiated to be a unique TRS by

International Association of Geodesy (IUGG) and the International Association of Geodesy (IAG) for all Earth science applications [Geodesist's Handbook, 1992], which is realized by a set of physical points with precisely determined coordinates. Such realization of ITRS, which is based on combination of several Sets of Stations Coordinates (SSC) and associated velocities coming from space geodesy techniques, is called International Terrestrial Reference Frame [Altamimi *et al*., 1993].

Since the first version of ITRS realization, namely ITRF88, eight other ITRF versions were established [Boucher and Altamimi, 1992, Altamimi *et al*., 2001a] and published by the International Earth Rotation and Reference Systems Service (IERS). Improvement in accuracy of ITRF has been made by including more new sites and observations available for different space techniques. ITRF2005, which is based on time series combination, has recently become available to the public.

Due to the underlying importance of the establishment of the combined reference frame (i.e. ITRF2000), a cross check has been carried out by DGFI analysis center to validate the results using the input data provided by IGN. The results showed a number of significant differences for station positions and velocities [Beutler *et al*., 2002; DGFI Annual Report, 2003], which are attributed to the utilization of different combination strategies. Therefore, the combination of different TRFs in an optimal manner is still an open research question.

This thesis aims to introduce a new approach to the ITRF solution realization based on Preferred Observation Functionals (POF) using generalized condition equations. This approach takes into consideration the unique potential of SLR which is sensitive to the position of the center of mass of the Earth, VLBI which provides accurate earth orientation information and baseline vectors, and GPS which generates accurate scale through baseline length measurements. Since GPS also provides accurate state vectors and baseline vectors, it is worthwhile to investigate formulations that make use of such information as observations. Consequently, three alternative mathematical models are formulated for combination of various space geodetic data in the ITRF solution realization.

1.2 Objectives of this study

The objective of this thesis is to demonstrate an alternative approach based on the strength of different space geodesy techniques, which will be called “Preferred Observation Functionals (POF) formulation”, to the realization of the combined reference frame solution. Three mathematical models are formulated.

In the first formulation geocenter of the ITRF is defined by SLR by fixing to zero the translation parameters and their rates between the combined reference frame (ITRF) and the SLR-based state vector solutions. The orientation of the ITRF is defined by VLBI by setting the rotation parameters and their rates between the ITRF and the VLBI-based baseline vector solutions to zero. Contribution of the GPS is limited by the use of only the GPS baseline lengths as observations.

The second formulation differs from the first by the use of GPS baseline vectors and their rate of changes instead of baseline lengths.

The third formulation takes into account the GPS state vectors as observations. Hence, it is similar to the current ITRF combination model.

1.3 Organization of this thesis

Chapter 2 provides the background to the study. Reference frame, ITRF concepts and its transformation are illustrated in detail. Different types of solutions provided by analysis centers and introduction of the advanced space geodesy techniques used for ITRF solution realization are presented. Attention is paid on the derivation of the relationship between terrestrial reference frames (TRFs) and ITRF. The final two sections of the chapter focus on the detailed ITRF combination methodology and the research topics in ITRF solution realization.

Chapter 3 reviews two different least squares adjustment methods used for the study. The adjustment formulation for the ITRF2000 solution realization is detailed. The final section focuses on the mathematical modeling and adjustment formulation of the new approach to the combined reference frame solution. State vector based solution is also presented for comparison with the alternative solutions.

In Chapter 4, the input data and their spatial distribution are presented. The correlation matrices of the input covariance matrices of the stations state vectors are illustrated through their contour plots. Considerations for the preprocessing of input data is also detailed as it represents a step forward towards the implementation for the combination solutions using the new approach.

The solutions to the preferred observation functionals formulations are compared to the solution from the formulation using station state vectors (i.e. state vector based solution) in Chapter 5. The difference between the solutions from the new approach and the ITRF2000 solution realization is examined despite a few number of stations and data used in this study.

An overall evaluation of this study and further recommendations are included in Chapter 6.

2. BACKGROUND ON ITRF

This chapter discusses ITRF background, concepts and mathematical relationship that relate the ITRF and TRF. The space geodesy techniques used for ITRF combination, the raw data format, and the solutions computed by different analysis centers are introduced. Both the ITRF transformation and the combination concepts with their derivations are described. Different research topics in ITRF solution realization are presented.

2.1 General statements on the reference systems, frames and ITRF

The *conventional reference system* is defined through the description of relationship between its configuration of the basic structure and its coordinates in details. In making a reference system available to users, it is normally materialized through a number of points, objects, or coordinates, and a set of parameters, and hence the term *conventional reference frame*. The reference frame must be accessible and clearly defined without ambiguity in writing equations of motion of a body whose coordinates are referred to in the frame [Witchayangkoon, 1997].

The Earth moves, rotates and undergoes deformations. Since motion and position are not absolute concepts, they can be mathematically described only with respect to some reference of coordinates, reference frames. According to Kovalevsky and Mueller (1989), the purpose of a reference frame is to provide the means to materialize a reference system so that it can be used for the quantitative description of positions and motions on the Earth (terrestrial frames) or a celestial bodies including the Earth in space (celestial frames). In constructing the reference frame, a set of parameters must be chosen.

With the initiative to standardizing a reference system for Earth science applications, the International Terrestrial Reference Frame (ITRF) was established and is maintained by the Terrestrial Reference Frame Section of the Central Bureau (CB) of the IERS. Currently, there are three main products generated by the IERS CB including the ITRF, International Celestial Reference Frame (ICRF), and the determination of Earth orientation parameters (EOP) which relate the ITRS and the ICRS.

The International Terrestrial Reference Frame (ITRF) is a realization of the International Terrestrial Reference System (ITRS), where ITRS is a particular conventional terrestrial reference system (CTRS) which is defined by a coherent set of global models and definitions. The CTRS is realized through an adopted set of station coordinates, while the ITRS is realized through the estimates of the coordinates and velocities of a set of observing stations of the IERS. The ITRS uses International Standard (SI) meter for its length unit defined in a local Earth frame in the meaning of a relativistic theory of gravitation. According to the resolutions by the IAU and the IUGG, the orientation of the ITRS axes is consistent with that of the BIH System at 1984.0 within ± 3 milli-arc-second (mas) and the time evolution in orientation of ITRS has no residual rotation relative to Earth's crust [Boucher and Altamimi, 1996].

Its implementation was originally based on the combination of sets of station coordinates (SSC) and velocities derived from observations of space-geodetic techniques such as Satellite Laser Ranging (SLR), Lunar Laser Ranging (LLR), Very Long Baseline Interferometry (VLBI). IERS augmented the methodology to include GPS in 1991 and the Doppler Orbitography and Radio-positioning Integrated by Satellite (DORIS) in 1994 [Boucher and Altamimi, 1996]. IERS regularly performs annual ITRF solutions, which are published in the IERS Annual Reports and Technical Notes. Since the first version of ITRS realization, namely, ITRF88, eight other ITRF versions were established including ITRF2000. In the past decade, a new ITRF has been prepared approximately every 2 years [Altamimi *et al*., 2001d]. The newly established combined reference frame, ITRF2005, has currently been released for public use.

2.2 Solutions computed by analysis centers used in the ITRF combination

The space geodesy solutions (i.e. TRF solutions) computed by individual analysis center (AC) are the primary input data for the ITRF combination (Table 2.1). The ACs submitted their solutions in SINEX data format [Blewitt *et al*., 1994; Davis and Blewitt, 2000]. These solutions contain station coordinates and velocities at a given epoch together with their corresponding covariance matrices. The statement on the constraints used to compute the solution, which is provided by different analysis centers, is also provided to allow the flexibility for the re-definition of the datum constraints to be applied to each individual input TRF solution, as one would desire before the whole combination adjustment. They are generally classified into three types:

(1) Loose constraints, solutions are derived from “Free network” approach where

the uncertainty applied to the constraints is $\hat{\sigma} \geq 1$ m for positions and ≥ 10 cm/yr for velocities;

(2) Removable constraints, solution for which the estimated station positions and velocities are constrained to external values within an uncertainty $\hat{\sigma} \approx 10^{-5}$ m for positions and mm/yr for velocities;

(3) Minimum constraints, used solely to define the TRF using a minimum amount of required information so that the normal matrix could be invertible through that constraints [Altamimi *et al.*, 2002b].

The summary of each individual solution also states the orientation rate constraints (e.g. NNR NUVEL-1A) applied to the station velocities as well.

Table 2.1 Individual TRF Solutions Used in the ITRF2000 Combination (Courtesy of Altamimi (2002))

Technique Analysis Center(AC)	AC SSC	Data Span	Station Number	Constraints
VLBI				
Geodetic Institute of Bonn University	(GIUB) 00 R 01	84-99	51	Loose
Goddard Space Flight Center	(GSFC) 00 R 01	79-99	130	Loose
Shanghai Astronomical Observatory	(SHA) 00 R 01	79-99	127	Loose
LLR				
Forschungseinrichtung Satellitengeodaesie	(FSG) 00 M 01	77-00	3	Loose
SLR				
Australian Surveying and Land Information Group	(AUS) 00 L 01	92-00	55	Loose
Centro Geodesia Spaziale, Matera	(CGS) 00 L 01	84-99	94	Loose
Communications Research Laboratory	(CRL) 00 L 02	90-00	60	Loose
Center for Space Research	(CSR) 00 L 04	76-00	139	Loose
Delft Ins. Earth Oriented Space Research	(DEOS) 00 L 05	83-99	91	Loose
Deutsches Geod¨atisches Forschungsinstitut	(DGFI) 00 L 01	90-00	43	Removable
Joint Center for Earth System Technology, GSFC	(JCET) 00 L 05	93-00	48	Loose
GPS				
Center for Orbit Determination in Europe	(CODE) 00 P 03	93-00	160	Minimum
GeoForschungsZentrum Potsdam	(GFZ) 00 P 01	93-00	98	Minimum
International GPS Service by Natural Resources Canada	(IGS) 00 P 46	96-00	179	Minimum
Jet Propulsion Laboratory	(JPL) 00 P 01	91-99	112	Minimum
Univ of Newcastle upon Tyne	(NCL) 00 P 01	95-99	90	Minimum
NOAA, National Geodetic Survey	(NOAA) 00 P 01	94-00	165	Removable
DORIS				
Groupe de Recherche de Geodesie Spatiale	(GRGS) 00 D 01	93-00	66	Loose
Institut Gographique National	(IGN) 00 D 09	92-00	80	Minimum
Multi-technique (SLR +DORIS +PRARE)				
GRIM5 project (GRGS+GFZ)	(GRIM) 00 C 01	85-99	183	Loose
CSR: SLR + DORIS on TOPEX	(CSR) 00 C 01	93-00	147	Loose
GPS Densification				
CORS Network by NOAA	(CORS) 00 P 01	94-99	80	Removable
South America Network by Deutsches Geod¨atisches Forschungsinstitut	(DGFI) 00 P 01	96-00	31	Loose
IAG Subcommission for Europe (EUREF), by Bundesamt fuer Kartographie und Geod¨asie	(EUR) 00 P 03	96-00	81	Minimum
Geophysical Institute, University of Alaska	(GIA) 00 P 01	96-99	20	Minimum
Institut G´eographique National	(IGN) 00 P 01	98-00	28	Minimum
Jet Propulsion Laboratory	(JPL) 00 P 02	91-99	28	Minimum
Antartica network, by Institut Geographique National	(IGN) 00 P 02	95-00	17	Minimum
REGAL Network, France	(REGAL) 00 P 03	96-00	29	Minimum
Antartica SCAR network, by Institut fuer Planetare Geodaesie, TU Dresden	(SCAR) 00 P 02	95-99	66	Removable

2.3 Space geodesy techniques for ITRF solution realization

This section briefly introduces different space geodesy techniques for the maintenance and solution realization of ITRF. Their principles, data source service, and scientific contribution will be discussed with emphasis on the strength of each technique in the concluding remarks.

2.3.1 Satellite Laser Ranging (SLR)

The primary measurement in SLR system is the round-trip laser pulse travel time to Earth-orbiting geodetic satellites. With appropriate corrections, the travel time can be used to obtain the range from the laser instrument to the center of mass of the target satellite [Tapley, *et al*., 1985; Kar, S. 1997]. This provides instantaneous range measurements of millimeter level precision which can be accumulated to give accurate orbits and a host of important science products [Otsubo and Gotoh, 2002; Schillak and Wnuk, 2003].

The International Laser Ranging Service (ILRS) was formed to provide a service to support, through Satellite and Lunar Laser Ranging data and related products, geodetic and geophysical research activities as well as IERS products important to the maintenance of an accurate International Terrestrial Reference Frame (ITRF). The service also developed the necessary standards/specifications and encourages international adherence to its conventions [Pearlman *et al*., 2002].

Some of the scientific results derived from SLR include detection and monitoring of tectonic plate motion, crustal deformation, determination of basin-scale ocean tides, monitoring of millimeter-level variations in the location of the center of mass of the total Earth system, and establishment and maintenance of the International Terrestrial Reference System (ITRS), despite falling short of precise determination of the Earth's orientation (precession and nutation) as opposed to VLBI and LLR.

Among all the above scientific results derived from SLR, the major strength of the SLR technique is its excellent capability in providing a precise measurement on the Earth scale information (i.e. GM constant), which allows the accurate definition of the center of mass of the Earth [Montag *et al*., 1996; Smith *el al*., 1999]. It follows that the SLR technique could be regarded as one of the fundamental geophysical and geodetic measurement technique [Schutz *et al*., 1989].

2.3.2 Very Long Baseline Interferometry (VLBI)

VLBI is a geometric technique which cannot only be able to measure a distance of thousands of kilometers or relative positions between two antennas in different places around the world with a few millimeters accuracy by receiving wavefront emitted by a distant quasar, but also be able to determine the Earth orientation accurately. With the global coverage of VLBI antennas, VLBI determines the inertial reference frame, which is important to definition of the earth orientation instantaneously [Takahashi *et al*., 2000; Joel, 2004].

The International VLBI Service for Geodesy and Astrometry (IVS) is an international collaboration of organizations that operate or support Very Long

Baseline Interferometry (VLBI) components. IVS provides a service which supports geodetic and astrometric work on reference systems, Earth science research, and operational activities [Fejes *et al*., 1989; Nothnagel, 2003]. The IVS grouped geodesy and astrometry together because they share the same observations and the same analysis gives both types of results [Carter and Robertson, 1990; Schluter *et al*., 2002].

Some of the scientific results derived from VLBI include motion of the Earth's tectonic plates, regional deformation and local uplift or subsidence, definition of the celestial reference frame, variations in the Earth's orientation and length of day, maintenance of the terrestrial reference frame, measurement of gravitational forces of the Sun and Moon on the Earth and the deep structure of the Earth and improvement of atmospheric models [Takahashi *et al*., 2000; Joel, 2004].

Among all the above scientific results derived from VLBI, the major strength of the VLBI technique is its excellent capability in providing a precise measurement on the Earth orientation information (i.e. UT1-UTC), which is essential to the precise GPS positioning. Without VLBI, the continued maintenance of UT1 standards will not be possible [Takahashi *et al*., 2000]. Besides, it also provides precise measurement for the relative positions. It follows that the VLBI technique could be regarded as another measurement technique for geodetic and geophysical applications [Nothnagel, 2003].

2.3.3 The Global Positioning System (GPS)

The Global Positioning System (GPS) is a satellite-based navigation system that consists of a network of 24 satellites placed into orbit by the U.S. Department of Defense. It works in any weather conditions and any place in the world. Its applications are beyond just a navigation system and position determination. It could be used for cartography, engineering, forestry, mineral exploration, wildlife habitat management, to mention but a few.

The International GPS Services (IGS) was formed to collect, archive, and distribute GPS observation datasets, and use them to generate high precision GPS satellite ephemeredes, Earth rotation parameters, coordinates and velocities of IGS tracking stations, GPS satellite clock, and ionospheric corrections. These products have been submitted to the Crustal Dynamics Data Information System (CDDIS) for availability to the global science community. In general, a majority of the data delivered to and archived on the CDDIS are available to the user community within a few hours after the observation day [Beutler *et al*., 1999; Ferland *et al*., 2000; Ferland, 2002].

The accuracies of the IGS products are sufficient to support several scientific objectives including the improvement and maintenance of the ITRF, monitoring of the Earth's rotation and deformations of its liquid and solid components, precise GPS satellite orbit and clock determinations for analysis of regional GPS campaigns, monitoring of the ionosphere and troposphere, precise time transfer, for example.

However, the accuracy of the position of the geocenter and the earth orientation parameters (EOP) are questionable, because GPS cannot generate accurate and precise station positions without the utilization of VLBI derived EOP as a-priori information (i.e. particularly for UT1), since it cannot separate variations in orbital elements from changes in the orientation of the Earth [Hase, 1997]. Nonetheless, it provides accurate baseline lengths [Leick, 1995] if the ambiguity resolution are well determined. For the above reason, the baseline lengths and their rates are reconstructed from the station state vectors and utilized as one of the three formulations as stated in the introduction.

2.3.4 DORIS Doppler Tracking

DORIS (Doppler Orbit determination and Radiopositioning by Satellite), which is developed by the French Centre National d'Etudes Spatiales (CNES), is a dual-frequency Doppler system that has currently been used for the past 14 years for precise orbit determination as well as precise geodetic positioning of ground tracking stations [Tavernier *et al*., 2003; Willis *et al*., 2005a; 2005b].

Unlike many other navigation systems, DORIS is based on an uplink device. The receivers are on board the satellite while the transmitters are on the ground. This creates a centralized system in which the complete set of observations is downloaded by the satellite to the ground center, from where they are distributed after editing and processing [Kuijper *et al*., 1995; Jayles *et al*., 2006].

Starting from 1990s, the DORIS receivers are equipped in four satellites, namely SPOT-2 (launched in 1990), TOPEX/ Poseidon (launched in 1992), SPOT-3 (launched in 1993 and ended in 1996) and SPOT-4 (launched in 1998). Three other satellites carrying the second generation of DORIS receivers are currently in orbit, namely Jason-1 (launched in 2001), ENVISAT (launched in 2002) and SPOT-5 (launched in 2002). Its positioning accuracy improved continuously from 10-cm level to 3-cm level, thanks to the development of better antenna receiver generation and advancement of data processing techniques. The recent and fore-coming could generate weekly DORIS station coordinates with an almost 1-cm precision as well [Tavernier *et al*., 2003; 2005; 2006; Willis *et al*., 2005b].

The International DORIS Service (IDS) was also established in 2003 which served to provide a support, through online DORIS data and products, to geodetic, geophysical, and other research and operational activities [Willis *et al*., 2004; Noll and Soudarin, 2006].

With a globally well distributed coverage of 56 ground station and its achievable accuracy, most scientists has currently engaged in the use of DORIS data for different scientific exploration. It includes precise orbit determination, sea level changes, polar ice studies, gravity field measurement and the maintenance of global accessibility to, and the improvement of, the International Terrestrial Reference Frame (ITRF) and monitoring Earth rotation, to mention but a few [Vincent *et al*., 2002].

However, DORIS is a microwave system that carries many similarities to GPS. The major difference is the reverse of the installation of receivers and transmitters on the satellite and on the ground respectively. Therefore, DORIS technique is excluded in this study for the reasons of its similarity to GPS technique and the limited availability of different techniques within a co-located site.

2.4 Mathematical model that relates ITRF and TRF

The fundamental relationship between ITRF and TRF of a measurement system is achieved using a 14-parameter transformation model between ITRF and TRFs. In this process, common stations in various systems (i.e. ITRF and TRFs) are required for the estimation of the transformation parameters. The 14 parameter transformation model originates from the 3D Helmert (similarity, also known as 7-parameter) transformation while taking into account the changes of the positions of stations and the changes of the transformation parameters over time (i.e. translation, rotation and scale rates).

Consider the seven transformation parameters between system I and II which includes three translation components, one scale factor, and the three rotation angles, designated respectively, *T1*, *T2*, *T3*, *D*, *R1*, *R2*, *R3*. The transformation of a station position X_I, expressed in a reference system I, into the same station position X_{II}, expressed in another reference system II, is given by

$$X_{II} = X_I + T + DX_I + RX_I \qquad (2\text{-}1)$$

where

$$T = \begin{pmatrix} T1 \\ T2 \\ T3 \end{pmatrix}, D = \begin{pmatrix} D & 0 & 0 \\ 0 & D & 0 \\ 0 & 0 & D \end{pmatrix}, \text{ and } R = \begin{pmatrix} 0 & -R3 & R2 \\ R3 & 0 & -R1 \\ -R2 & R1 & 0 \end{pmatrix}$$

In order to take into consideration of the crustal motion associated with plate tectonics, land subsidence, volcanic activity, postglacial rebound, and so on, the coordinates of a point is expressed as a function of time [Soler and Snay, 2004]. Hence, the transformation parameters are subject to time-dependent changes. These time-dependent variations are assumed to be mostly linear [Soler, 1998;

2003]. Differentiating equation (2-1) with respect to time gives

$$\dot{X}_{II} = \dot{X}_{I} + \dot{T} + \dot{D}X_{I} + D\dot{X}_{I} + \dot{R}X_{I} + R\dot{X}_{I} \tag{2-2}$$

Since the magnitudes of *D* and *R* are at or below 10^{-5} level and $\dot{X}_1$ is, at most, about 10 cm per year [Altamimi *et al.*, 2002b; Chapter 4 IERS Conventions, 2003], the terms $D\dot{X}_I$ and $R\dot{X}_I$, which represent about 0.1 mm over 100 years, are negligible. Therefore, equation (2-2) could be written as

$$\dot{X}_{II} = \dot{X}_{I} + \dot{T} + \dot{D}X_{I} + \dot{R}X_{I} \tag{2-3}$$

Taking X_I and X_{II} as X_{ITRF} and X_{TRF} respectively, the transformation of positional coordinates from X_{ITRF} referenced to an epoch t_0 to X_{TRF} referenced to an epoch t_{TRF} expressed in an individual TRF could be deduced directly through three distinct transformations as shown in Figure 2.1.

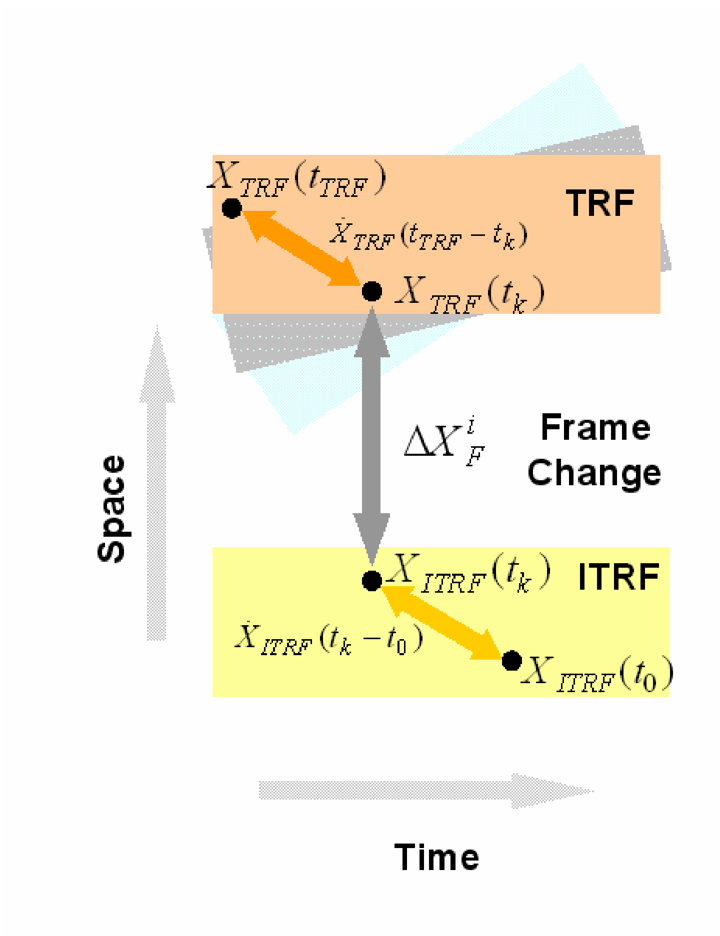

Figure 2.1 Kinematics between TRFs and ITRF

Starting from the bottom frame of Figure 2.1 above, one transforms position vector X_{ITRF} at epoch t_0 to X_{ITRF} at epoch t_k through its associated velocity vector $\dot{X}_{ITRF}$, which is expressed using a vectorial relationship as,

$$X_{ITRF}(t_k) = X_{ITRF}(t_0) + (t_k - t_0)\dot{X}_{ITRF} \tag{2-4}$$

Then transforms the position vector X_{ITRF} at epoch t_k to X_{TRF} at epoch t_k through the Helmert transformation, which is expressed as,

$$X_{TRF}(t_k) = X_{ITRF}(t_k) + T_k + D_k X_{ITRF}(t_k) + R_k X_{ITRF}(t_k) \tag{2-5}$$

Finally, one transforms the position vector from X_{TRF} at epoch t_k to X_{TRF} at epoch t_{TRF}, which is expressed as,

$$X_{TRF}(t_{TRF}) = X_{TRF}(t_k) + (t_{TRF} - t_k)\dot{X}_{TRF} \tag{2-6}$$

Addition of (2-4), (2-5) and (2-6) gives,

$$X_{TRF}(t_{TRF}) = [X_{ITRF}(t_0) + (t_k - t_0)\dot{X}_{ITRF}] + \Delta X_F + (t_{TRF} - t_k)\dot{X}_{TRF} \tag{2-7}$$

where

$$\begin{aligned} \Delta X_F &= T_k + D_k(X_{ITRF}(t_0) + (t_k - t_0)\dot{X}_{ITRF}) + R_k(X_{ITRF}(t_0) + (t_k - t_0)\dot{X}_{ITRF}) \\ &\cong T_k + D_k X_{ITRF}(t_0) + R_k X_{ITRF}(t_0) \end{aligned} \tag{2-8}$$

ΔX_F represents the frame change at epoch t_k. The terms $D_k(t_k - t_0)\dot{X}_{ITRF}$ and $R_k(t_k - t_0)\dot{X}_{ITRF}$ is negligible, since the magnitudes of *D* and *R* are at or below 10^{-5} level and $\dot{X}_{ITRF}$ is, at most, about 10 cm per year as stated in the above.

Differentiating equation (2-8) with respect to time gives,

$$\Delta\dot{X}_F = \dot{T}_k + \dot{D}_k X_{ITRF}(t_0) + \dot{R}_k X_{ITRF}(t_0) = \dot{X}_{TRF} - \dot{X}_{ITRF} \tag{2-9}$$

where in turn

$$\dot{X}_{TRF} = \dot{X}_{ITRF} + \dot{T}_k + \dot{D}_k X_{ITRF}(t_0) + \dot{R}_k X_{ITRF}(t_0) \tag{2-10}$$

which is equivalent to (2-3).

Substituting (2-8) and (2-9) into (2-7) followed by rearrangement gives,

$$\begin{aligned} X_{TRF}(t_{TRF}) = X_{ITRF}(t_0) + (t_{TRF} - t_0)\dot{X}_{ITRF} + T_k + D_k X_{ITRF} + R_k X_{ITRF} \\ + (t_{TRF} - t_k)[\dot{T}_k + \dot{D}_k X_{ITRF} + \dot{R}_k X_{ITRF}] \end{aligned} \tag{2-11}$$

Writing equation (2-10) and (2-11) together, and omitting the epochs of TRF and ITRF position gives

$$\begin{cases} X^{i}_{TRF} = X^{i}_{ITRF} + (t_{TRF} - t_0)\dot{X}^{i}_{ITRF} \\ \qquad\qquad + T_k + D_k X^{i}_{ITRF} + R_k X^{i}_{ITRF} \\ \qquad\qquad + (t_{TRF} - t_k)[\dot{T}_k + \dot{D}_k X^{i}_{ITRF} + \dot{R}_k X^{i}_{ITRF}] \\ \dot{X}^{i}_{TRF} = \dot{X}^{i}_{ITRF} + \dot{T}_k + \dot{D}_k X^{i}_{ITRF} + \dot{R}_k X^{i}_{ITRF} \end{cases} \tag{2-12}$$

where the translation vector T_k, the scale factor D_k, and the rotation matrix R_k are respectively defined (following IERS conventions) as:

$$T_k = \begin{pmatrix} T1_k \\ T2_k \\ T3_k \end{pmatrix}, \quad D_k = \begin{pmatrix} D_k & 0 & 0 \\ 0 & D_k & 0 \\ 0 & 0 & D_k \end{pmatrix} \quad \text{and} \quad R_k = \begin{pmatrix} 0 & -R3_k & R2_k \\ R3_k & 0 & -R1_k \\ -R2_k & R1_k & 0 \end{pmatrix}$$

The dotted parameters $\dot{T}_k$, $\dot{D}_k$ and $\dot{R}_k$ represent their derivatives with respect to time. This relationship is the same as the general ITRF combination model [Boucher *et al*., 1999; 2003] but derived using alternative approach.

2.5 ITRF combination concepts and ITRF2000 solution

Different terrestrial reference frames (TRFs) have been realized for different purposes. With a view to unifying the reference system, different TRFs were combined in calculating ITRF.

In the combined solution, using (2-12), one has to estimate a set of positions X_{ITRF} at a given epoch t_0, velocities $\dot{X}_{ITRF}$, and their respective transformation parameters T_k and rates $\dot{T}_k$ at an epoch t_k, from the ITRF to each individual frame at epoch t_k. This is an unusual least squares task that the input data types are the same as the output parameter types (i.e. positional coordinates and velocities in 3D for each station) and additional 3D Helmert transformation parameters and their respective rates have to be estimated [Davies and Blewitt, 2000].

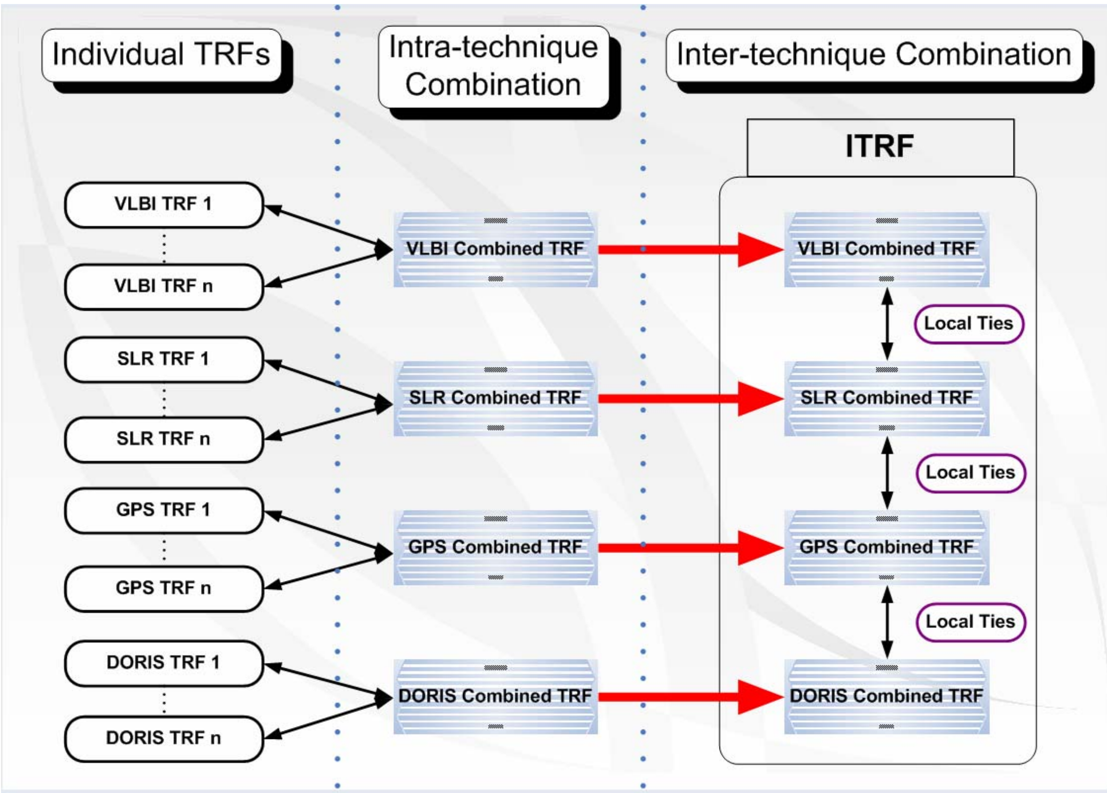

Figure 2.2 Intra-technique and Inter-technique combination

Figure 2.2 illustrates the concepts of intra-technique and inter-technique combination. For the TRFs belonging to the same technique, some stations would be the same and hence provide redundant observations for the intra-technique combination. Since there is no dynamic datum defined in combined TRF frame within the same technique, the observation design matrix has a rank deficiency of 14. The rank deficiency can be overcome either by fixing the values of 14 Helmert transformation parameters between one of the TRFs and the combined TRF frame, or defining a minimum constraint datum of the combined TRF frame through 7 coordinates and 7 velocities components of stations.

As the stations of different TRFs from different techniques are referenced to different nearby physical monuments, local ties are needed to relate different TRFs together in co-located sites and hence, providing redundancy to the solution formulation. Given sufficient redundancy of observations, the rank deficiency could be solved again either by fixing the values of 14 Helmert transformation parameters between *one of the individual TRF or combination of them* and the ITRF (i.e. the combined TRF frame), or defining a datum of ITRF through coordinates and velocities components of some stations for inter-technique combination. It is reminded that the ITRF is an unknown to be determined together with the transformation parameters between each individual TRF.

Following the aforementioned discussion, ITRF2000 solution can be carried out in three stages: (i) application of minimum constraint for the pre-processing, (ii) combination of individual solutions with local ties, and (iii) variance components estimation and outlier detection during the combination.

(i) Application of minimum constraint for the pre-processing

As discussed in Section 2.2, the constraints applied by each individual ACs to the normal equations for the input solution in the form of Cartesian coordinate system can be classified as loose constraints, removable constraints, and minimum constraints.

Those constraints, which are not originally applied with minimum constraints, are removed and re-applied with minimum constraints. This is because one would desire to provide homogeneous (and consistent) input covariance matrices and solutions before the combination of the solutions [Altamimi *et al.*, 2002a; 2002b].

Removable constraints may be removed before the combination solution using the following relationship:

$$\overline{X}_s = \Sigma_s^{mc}\left[\left(\Sigma_s^{est}\right)^{-1} X_s^{est} - \left(\Sigma_s^{const}\right)^{-1} X_s^{const}\right] \tag{2-13}$$

where

$$\left(\Sigma_s^{unc}\right)^{-1} = \left(\Sigma_s^{est}\right)^{-1} - \left(\Sigma_s^{const}\right)^{-1} \tag{2-14}$$

$$\left(\Sigma_s^{mc}\right)^{-1} = \left(\Sigma_s^{unc}\right)^{-1} - \left(B^T \Sigma_\theta^{-1} B\right) \tag{2-15}$$

For some solutions which are derived with “free network” approach (loosely constraint solutions), the underlying reference system is loosely fixed. The covariance matrices of those solutions derived from this approach contain both random errors and relatively large Reference System Effect (RSE). Therefore, equation (2-16) is used to convert the relatively large RSE to a well known a reference system with small RSE (i.e. minimum constraint datum) [Boucher *et al.*, 1999].

$$\Sigma_s^{mc} = \Sigma_s^{est} - \Sigma_s^{est} B^T \left(B \Sigma_s^{est} B^T + \Sigma_\theta\right)^{-1} B \Sigma_s^{est} \tag{2-16}$$

where $B = (A^T A)^{-1} A^T$ is the matrix containing all the information necessary to define the reference TRF, depending on the shape of the implied network. Σ_s^{unc} is the unconstrained matrix, Σ_s^{const} is the constrained matrix, Σ_s^{mc} is the minimally constrained variance matrix, Σ_s^{est} is the estimated matrix, Σ_θ is the diagonal matrix containing small variances for the 14 transformation parameters, $\overline{X}_s$ is the newly minimum constraint solution constructed after the removal of the original constraints, X_s^{est} is the estimated solution [Sillard and Boucher, 2001].

(ii) Combination of individual solutions with local ties

After the minimum constraints are applied, all the individual solutions serve as an input data for the ITRF2000 combination solution. The variance-covariance matrices for the individual solutions and the variances for the local ties provide the weight matrix (being as the inverse of the whole variance-covariance matrix) for all observations during the iteration for the intermediate results for the inter-technique combination that are weighted through the estimated variance components iteratively which will be discussed later in this section.

Co-located sites represent a key element of the ITRF combination; connecting the individual TRF networks together [Altamimi *et al.*, 2002b]. Because these sites are not truly co-located, local measurements derived from local surveys are used to provide baseline (tie) vectors between the stations at co-located sites.

$$\begin{pmatrix} \Delta x_s^{i,j} \\ \Delta y_s^{i,j} \\ \Delta z_s^{i,j} \end{pmatrix} = \begin{pmatrix} x^j - x^i \\ y^j - y^i \\ z^j - z^i \end{pmatrix} \tag{2-17}$$

$\left(\Delta x_s^{i,j}, \Delta y_s^{i,j}, \Delta z_s^{i,j}\right)$ are the geocentric components of the tie vector linking two points *i* and *j*, of a given data set *s*. The standard deviations $\left(\sigma\Delta x_s^{i,j}, \sigma\Delta y_s^{i,j}, \sigma\Delta z_s^{i,j}\right)$ for each local tie vector are used to compute a diagonal variance matrix. If those standard deviations are not available, they are computed through [Altamimi *et al.*, 2002b]:

$$\sigma_{computed} = \sqrt{\sigma_1^2 + \sigma_2^2} \tag{2-18}$$

where σ_1 = ±3 mm and

$$\sigma_2 = 10^{-6} \times \sqrt{(\Delta x_s^{i,j})^2 + (\Delta y_s^{i,j})^2 + (\Delta z_s^{i,j})^2} \tag{2-19}$$

σ_1 = ±3 mm is introduced to allow the uncertainties of each XYZ component of the local ties derived from local surveys to be at a minimum of ±3 mm.

Despite the redundancy provided by local ties, the design matrix of the combination solution observation equations is still of rank defect by 14 since the ITRF2000 datum is still yet to be defined. In order to compensate for the rank deficiency, the implementation of the ITRF2000 datum is achieved as follows:

(1) Translation constraints are introduced as 'zero' values to the translation and its corresponding translation rate parameters *stochastically* between ITRF and the weighted mean of the SLR solutions of the five analysis centers: CGS, CRL, CSR, DGFI and JCET [Altamimi *et al.*, 2001b; 2002b], so that these translation parameters and its rates are adjusted simultaneously with other parameters. Consequently, the resulting translation and their corresponding rate parameters for those solutions listed in the IERS Technical Note are not exactly equal to zero together with their precision.

(2) Scale constraints are introduced as 'zero' values to the scale and its corresponding scale rate parameters *stochastically* between ITRF and the weighted mean of the above SLR solutions and the VLBI solutions [Altamimi *et*

al., 2001b; 2002b], so that the ITRF scale is defined by the SLR and VLBI techniques.

(3) Orientation constraints, which is the alignment of ITRF2000 to ITRF97 and to the NNR-NUVEL-1A model, is given by,

$$B(X_0 - X) = 0 \qquad (2\text{-}20)$$

where (1) $B = \left(A^T A\right)^{-1} A^T$ and A is the design matrix of partial derivatives (restricted to its last three columns), as given in Section 3.2; (2) X_0, ITRF97 positions at epoch 1997.0 defining the rotation angles and NNR-NUVEL-1A velocities defining the rotation rates; and (3) X, estimated station positions and velocities. It should be noted that equation (2-20) applied only upon 50 selected sites with high geodetic quality, which introduces six equations defining the ITRF2000 orientation and its respective time evolution [Altamimi *et al*., 2001b; 2002b].

(4) Velocity constraints are introduced to limit the stations within the same site to have the same velocity as the separation in-between is small [Altamimi *et al*., 2002b].

(iii) Variance components estimation and outlier detection during the combination

This is the last step before the final combination result is wholly prepared. The calculated variance components in the first run are used to re-scale their corresponding weighted matrices and solutions, and the combination will continuously iterate until the variance component of the global combination converge to unity. During the process of iteration, outliers are detected continuously. Stations are rejected if any position or velocity normalized residual exceeds a chosen threshold value. The formula of the variance components estimation and the description of outlier detection are given in Chapter 5.

2.6 Research topics in ITRS realization

Some topics on ITRF related research has been outlined in the IERS Workshop on Combination Research and Global Geophysical Fluids 2002 [Angermann *et al.*, 2002; 2003a] as:

(a) Assessment on the quality of the local tie information and study on the impact of local ties on the combination. [Altamimi *et al.*, 2002c]

(b) Study on the weighting of solutions in the intra- ad inter-technique case and development on weighting methods and variance component estimation techniques, etc.

(c) Modeling on the non-linear site motions for sites located in deformation zones.

(d) Study on zero-order datum definition issues for combined solutions.

(e) Study on systematic modeling error and potential biases between the techniques concerned with the resulting scale, geocentre, LOD (and nutation rates) from satellite techniques, biases in time series of station position and velocity estimates (especially for co-located sites), biases in time series of EOPs, consistency between TRF and EOPs, impact of combination on the ICRF solution realization.

Currently, most studies concentrate on (e) fully exploiting the potential of analysis of the time series as provided by space geodetic observations for the investigations of various global and regional, short-term, seasonal, and annual effect and stability performance of the ITRF [Altamimi *et al.*, 2003b; 2005a; 2005b; Angermann *et al*., 2003b, 2004b; Ferland *et al*., 2004; Meisel *et al*., 2005]. Investigations are also conducted to demonstrate proper the local tie data format, different local survey strategies to the improvement of accuracy and its quality, and the disagreement of the local survey information with respect to the combined reference frame in terms of magnitude and their corresponding normalized spherical error [Altamimi, 2003b; Angermann *et al*., 2004a; McCarthy and Petit, 2003; Sarti *et al*., 2004; Ray and Altamimi, 2005], which belongs to (a).

However, little researches have been conducted to model non-linear motion of geodetic station caused by equipment changes, systematic errors and environment changes or seismic events [Petrov, 2005], to investigate the weighting methods and the variance component estimation for inter-technique combination [Feissel-Vernier and Le Bail, 2005], and to study on the datum definition issues for the combined reference frames [Dong *et al*., 2003; Rothacher, 2005], which are belonging to (b), (c) and (d) respectively.

With a view to meeting future needs, IERS Working Group on Combination has currently been formed to realize an up-to-date version of ITRF, namely ITRF2004.

Different combination proposals have been received and summarized [Rothacher *et al*., 2004]. Instead of computing the ITRF station positions, velocities and their transformation parameters, weekly time series of station position and velocity solutions, their transformation parameters and Earth Orientation Parameters (EOP) will be computed simultaneously so as to closely monitor the station movements and Earth’s kinematics. Thus, ITRF formulation and combination approaches for weekly time series combination have been developed for evaluation [Schwegmann and Richter, 2005].

Three approaches, namely rigorous, approximate (minimal and weekly) and semi-rigorous, have been suggested. The first two approaches were suggested in 2004 [Altamimi and Ray, 2004], while the latter approach was proposed in 2005 [Rothacher, 2005]. All methods generate the weekly combination solutions. The first approach requires the reference solutions to process together with new weekly solutions, while the second aligns new weekly solutions to the ITRF2004 reference solutions. The last approach aligns respective weekly solutions to their own combined TRF solutions for different techniques without additional datum and local tie. However, the ITRF datum definition would be kept unchanged as in the ITRF2000 [Altamimi *et al*., 2002b; 2003b; 2005b]. Those methods are still under investigation.

This study focuses on investigating an appropriate weighting method through variance components estimation and the zero-order datum definition for the ITRF combined solutions, which belongs to (b) and (d). This will be illustrated in subsequent sections.

3. ADJUSTMENT MODEL FOR ITRF COMBINATION

In this chapter, a synopsis of least-squares adjustment models is given. It also introduces methods in handling rank defects in parametric least squares model. Both the adjustment of ITRF2000 combination and alternative formulations are presented.

3.1 Least squares adjustment models

3.1.1 Parametric adjustment for non-linear model and rank deficiency problem

In this study, mathematical model is non-linear. Therefore, following the content and the notation given by Uotila (1997), the mathematical model of the non-linear observation equations is expressed as

$$L^a = F(X^a) \rightarrow \hat{L}^a = F(\hat{X}^a) \tag{3-1}$$

where L^a is the theoretical values of observations, X^a is the theoretical values of parameters, $\hat{L}^a$ is the vector of adjusted values of observations, $\hat{X}^a$ is the vector of estimates (i.e. unknown parameters).

In statistical terms, all observations, L^b, contain errors. Considering the true error of the observations, ε, the non-linear observation equations are given by the following matrix expression

$$L^b - \varepsilon = F(X^a) \tag{3-2}$$

and the weight matrix associated with the observations is given by

$$P = \sigma_0^2 \Sigma_{L^b}^{-1} \tag{3-3}$$

where Σ_{L^b} refers to the covariance matrix of the observations.

In order to estimate the unknown parameters, the non-linear observation equations in the above are linearized using Taylor series expansion and give

$$L^b - \varepsilon = F(X^a) = F(X^0) + \left.\frac{\partial F}{\partial X^a}\right|_{X^a = X^0} (X^a - X^0) + \cdots \tag{3-4}$$

The second order and higher terms are neglected in equation (3-4).

Denoting

$$\left.\frac{\partial F}{\partial X^a}\right|_{X^a = X^0} =: A$$

where X^0 refers to the vector of approximate (nominal) values of parameters to be estimated.

With the use of the following relations,

$$\begin{matrix} -\varepsilon = AX + F(X^0) - L^b \\ V = A\hat{X} + F(X^0) - L^b \end{matrix} \leftrightarrow \begin{matrix} X = X^a - X^0 \\ \hat{X} = \hat{X}^a - \hat{X}^0 \end{matrix} \tag{3-5}$$

and denoting

$$\begin{aligned} F(X^0) &= L^0 \\ L^0 - L^b &= L \end{aligned}$$

Therefore, one obtains the following simplified expression for the linearized observation equations

$$\underset{n\times 1}{V} = \underset{n\times m}{A} \underset{m\times 1}{\hat{X}} + \underset{n\times 1}{L} \tag{3-6}$$

where n is the number of observations and m is the number of unknown parameters. Attention is to be paid to the sign of the L term and its definition. Note also that, L^0 must be computed rigorously and enough significant digits must be recorded in the above expression [Uotila, 1997].

Notice that the number of observations n is normally larger than the number of unknown parameters m to be solved to provide redundancy of observations. The redundancy of the system is given by:

$$r = n - rk(A) = n - m \qquad (3\text{-}7)$$

where $rk(A)$ refers to the rank of design matrix A.

A least squares solution vector for $\hat{X}$ (provided the design matrix A is of full rank) is obtained by minimizing the quadratic form of $V^T PV$ and satisfying the equation (3-6) simultaneously through the method of Lagrange multiplier, and thus expressed as,

$$\hat{X} = -\left(A^T PA\right)^{-1} A^T PL \qquad (3\text{-}8)$$

such that the refined estimates and the adjusted observations are obtained respectively from $\hat{X}^a = X^0 + \hat{X}$ and $\hat{L}^a = L^b + V$. Iteration is required to get further refined estimates.

The estimated variance component is given by

$$\hat{\sigma}_0^2 = \frac{V^T PV}{n - m} \qquad (3\text{-}9)$$

and the corresponding covariance matrix for $\hat{X}^a$, $\hat{L}^a$ and V are

$$\Sigma_{\hat{X}^a} = \hat{\sigma}_0^2 \left(A^T PA\right)^{-1} \tag{3-10}$$

$$\Sigma_{\hat{L}^a} = \hat{\sigma}_0^2 A\left(A^T PA\right)^{-1} A^T \tag{3-11}$$

$$\Sigma_V = \hat{\sigma}_0^2 \left(P^{-1} - A\left(A^T PA\right)^{-1} A^T\right) = \Sigma_{L^b} - \Sigma_{L^a} \tag{3-12}$$

However, the design matrix A is not always of full rank as it is the case in this study, unique solutions to equations (3-8) can be obtained using independent a-priori information (stochastic or otherwise) on the unknown parameters or by reformulating the mathematical model as a function of estimable quantities [Grafarend and Schaffrin 1974; Tan, 2002].

In this study, the mathematical model is rank deficient because the datum has not been defined. Therefore, the adjustment with stochastic constraints for the minimum constraint estimation, which is first introduced by H.J. Buiten (1978), is being employed as our baseline solution because different methods of the adjustment with constraints used in a similar situation are shown to give similar result [Fok, et al., 2007 (in press)], whereas adjustment based on generalization is being used in the alternative model.

3.1.2 Adjustment based on generalization

Instead of writing least squares adjustment in the parametric form, a new set of generalized condition equations could be formulated if, instead of conventional practice, all parameters comprising the mathematical model are also considered as measured quantities to be adjusted.

Such an interpretation is plausible if we consider an observation to be a constant and the corresponding residual is zero when associated with an infinitely large weight. Similarly, a quantity could be considered as an unknown parameter if it is associated with a zero weight [Mikhail, 1976; Uotila, 1997].

Following again the derivations by Uotila (1997), the mathematical model of the non-linear generalized condition equations is expressed as

$$F(L_F^a, L_X^a) = 0 \rightarrow F(\tilde{L}_F^a, \tilde{L}_X^a) = 0 \qquad (3\text{-}13)$$

where L_F^a is the theoretical values of observations in the first group, L_X^a is the theoretical values of *desired* observations in the second group, $\tilde{L}_F^a$ is the vector of adjusted values of observations in the first group, $\tilde{L}_X^a$ is the *desired* vector of adjusted observations in the second group.

Denoting that

$$\begin{aligned} \tilde{L}_F^a &= L_F^b + V_F \\ \tilde{L}_X^a &= L_X^b + V_X \end{aligned}$$

where L_F^b , V_F , L_X^b and V_X refer to the vector of observed values and residuals in the first group, and the vector of observed values and residuals in the second group respectively.

The weight matrices associated with the observed values of the first and the second groups are given by

$$\begin{aligned} P_F &= \sigma_0^2 \Sigma_{L_F^b}^{-1} \\ P_X &= \sigma_0^2 \Sigma_{L_X^b}^{-1} \end{aligned} \qquad (3\text{-}14)$$

where $\Sigma_{L_F^b}$ and $\Sigma_{L_X^b}$ refers to the covariance matrices of the observations in the first and the second group.

Again, the non-linear generalized condition equations in the above are linearized using Taylor series expansion to give

$$F(\tilde{L}_F^a, \tilde{L}_X^a) = F(L_F^b + V_F, L_X^b + V_X)$$
$$= F(L_F^b, L_X^b) + \left.\frac{\partial F}{\partial L_F^a}\right|_{\substack{L_F^a = L_F^b \\ L_X^a = L_X^b}} V_F + \left.\frac{\partial F}{\partial L_X^a}\right|_{\substack{L_F^a = L_F^b \\ L_X^a = L_X^b}} V_X + \cdots = 0 \qquad (3\text{-}15)$$

Denoting

$$\left.\frac{\partial F}{\partial L_F^a}\right|_{\substack{L_F^a = L_F^b \\ L_X^a = L_X^b}} =: B_F\ , \quad \left.\frac{\partial F}{\partial L_X^a}\right|_{\substack{L_F^a = L_F^b \\ L_X^a = L_X^b}} =: B_X \text{ and } \ F\left(L_F^b, L_X^b\right) =: W_F$$

and assuming that there are r equations, n L_F^a 's and u L_X^a 's.

Therefore, one obtains the following simplified expression for the linearized generalized condition equations

$$\underset{r\times n}{B_F}\ \underset{n\times 1}{V_F} + \underset{r\times u}{B_X}\ \underset{u\times 1}{V_X} + \underset{r\times 1}{W_F} = 0 \qquad (3\text{-}16)$$

A least squares solution for V_X and V_F are obtained by minimizing the quadratic form of $V_X^T P_X V_X$, $V_F^T P_F V_F$ and satisfying equation (3-16) simultaneously through the method of Lagrange multiplier and thus expressed as,

$$V_X = -\left(B_X^T M_F^{-1} B_X + P_X\right)^{-1} B_X^T M_F^{-1} W_F \qquad (3\text{-}17)$$

$$V_F = -P_F^{-1} B_F^T M_F^{-1}\left(B_X V_X + W_F\right) \qquad (3\text{-}18)$$

The estimated variance component is given by

$$\tilde{\sigma}_0^2 = \frac{V_F{}^T P_F V_F + V_X{}^T P_X V_X}{r} \tag{3-19}$$

The corresponding covariance matrix of V_X and V_F are given by

$$\Sigma_{V_X} = \tilde{\sigma}_0^2 \left(P_X^{-1} - \left(B_X^T M_F^{-1} B_X + P_X \right)^{-1} \right) \tag{3-20}$$

$$\Sigma_{V_F} = \tilde{\sigma}_0^2 \left(P_F^{-1} B_F^T \left(M_F + M_X \right)^{-1} B_F P_F^{-1} \right) \tag{3-21}$$

where $M_F = B_F P_F^{-1} B_F^T$ and $M_X = B_X P_X^{-1} B_X^T$

The corresponding covariance matrix of $\tilde{L}_F^a$ and $\tilde{L}_X^a$ are given by

$$\Sigma_{\tilde{L}_F^a} = \tilde{\sigma}_0^2 \left(B_F^T M_X^{-1} B_F + P_F \right)^{-1} \tag{3-22}$$

$$\Sigma_{\tilde{L}_X^a} = \tilde{\sigma}_0^2 \left(B_X^T M_F^{-1} B_X + P_X \right)^{-1} \tag{3-23}$$

3.2 Adjustment model for current ITRF solution

The formulation for the ITRF combination adjustment model, considering the issues discussed in Chapter 2, is the last step in the computation of the final combination solution.

Differentiating the equation (2-12) with respect to ITRF yields,

$$\begin{pmatrix} V_{X_{TRF}} \\ V_{\dot{X}_{TRF}} \end{pmatrix} = \begin{pmatrix} (1 + D_k^0 + dt_k \dot{D}_k^0) I_{3\times3} + R_s & dt_{TRF} I_{3\times3} \\ \dot{D}_k^0 I_{3\times3} + \dot{R}_k^0 & I_{3\times3} \end{pmatrix} \begin{pmatrix} dX_{ITRF} \\ d\dot{X}_{ITRF} \end{pmatrix} + \begin{pmatrix} A_{TRF}^i & dt_k^i A_{TRF}^i \\ 0 & A_{TRF}^i \end{pmatrix} \begin{pmatrix} dT_k \\ d\dot{T}_k \end{pmatrix} + \begin{pmatrix} X_{TRF}^0 - X_{TRF}^b \\ \dot{X}_{TRF}^0 - \dot{X}_{TRF}^b \end{pmatrix} \tag{3-24}$$

where D_k^0 and $\dot{D}_k^0$ are the approximate scale and scale rate parameters expressed in a given frame at epoch t_k.

R_s is the design matrix of partial derivatives constructed using approximate rotation parameters $R1_k^0, R2_k^0, R3_k^0$ and its rates expressed in a given frame at epoch t_k.

$$R_s = \begin{pmatrix} 0 & -(R3_k^0 + dt_k \dot{R3}_k^0) & (R2_k^0 + dt_k R2_k^0) \\ (R3_k^0 + dt_k \dot{R3}_k^0) & 0 & -(R1_k^0 + dt_k R1_k^0) \\ -(R2_k^0 + dt_k R2_k^0) & (R1_k^0 + dt_k R1_k^0) & 0 \end{pmatrix}$$

A_{TRF}^i is the design matrix of partial derivatives constructed using approximate station positions $\left(x_0^i, y_0^i, z_0^i\right)$, where *1<i<n* and *n* is the number of stations

$$A_{TRF}^i = \begin{pmatrix} . & . & . & . & . & . & . \\ 1 & 0 & 0 & x_0^i & 0 & z_0^i & -y_0^i \\ 0 & 1 & 0 & y_0^i & -z_0^i & 0 & x_0^i \\ 0 & 0 & 1 & z_0^i & y_0^i & -x_0^i & 0 \\ . & . & . & . & . & . & . \end{pmatrix}$$

where $V_{X_{TRF}}$ and $V_{\dot{X}_{TRF}}$ are the vector of residual of the observations corresponding to the positions and velocities respectively.

The above adjustment model given in equation (3-24) could be simplified as

$$V = A_1 X + A_2 T_k + L \qquad (3\text{-}25)$$

where

$$A_1 = \begin{pmatrix} I_{3\times3} & dt_{TRF} I_{3\times3} \\ 0 & I_{3\times3} \end{pmatrix} \quad \text{and} \quad A_2 = \begin{pmatrix} A_{TRF}^i & dt_k A_{TRF}^i \\ 0 & A_{TRF}^i \end{pmatrix}$$

by assuming $D_k^0, R1_k^0, R2_k^0$ and $R3_k^0$ and their rates zero which yield a simpler form of matrix for A_1 since their values are extremely small that poses negligible effect on the final estimates as mentioned from chapter 2 with $dt_{TRF} = t_{TRF} - t_0$ and

$dt_k = t_{TRF} - t_k$. L is the vector of (*Computed-Observed*) observations in the linearized mathematical model context. The unknown parameters in equation (3-25) are the corrections to station positions and velocities, X , and the corrections to the nominal values of the transformation parameters, T_k , and their corresponding rates from ITRF to a particular TRF frame at epoch t_k .

As discussed in Chapter 2, the estimated parameters cannot be computed directly since the normal matrix of a single adjustment for all ITRF parameters is rank-deficient. Constraints, either fixed or stochastic, have to be applied to provide independent equations for inverting the normal matrix.

3.3 Combined reference frame solution through station state vectors and preferred observation functionals

This section aims to introduce a *preferred observation functionals formulation* based on the strength of different space geodesy techniques with three variations. Their solutions will be carried out using generalized condition equations. We will also describe a formulation which uses station *state vectors*. This formulation is solved using minimum constraint and the solution results are used for comparison.

3.3.1 State vectors formulation

The transformation between ITRF and TRFs station state vectors is assumed to be an extended 3D similarity transformation by taking into account of the time dependent changes in the station positions including the ITRF at different epochs and thus, the 14-parameter transformation model is formulated and described in Chapter 2. Since the generated normal equations are of rank defect by 14, a minimum constraint solution for the state vector (SV) formulation can be obtained by fixing 7 position vector components of co-located stations and 7 velocity vector components in equation (3-25).

3.3.2 Preferred observation functionals approach based on the strength of the techniques

As compared to the existing coordinate-based ITRF solution formulation, the following preferred observation functionals (POF) formulation is proposed. The formulation uses SLR station state vectors recognizing the fact that SLR satellite orbits are referenced dynamically to the center of mass of the Earth which provides position information referenced to the center of mass of the Earth in addition to the accurate Earth orientation information. The VLBI system, being purely geometric, provides accurate earth orientation information and baseline vectors. Although GPS shares the SLR system properties, the accuracy of station positions in vertical is significantly lower than the horizontal counterparts. Moreover, GPS solutions make use of the long term EOP provided by VLBI solutions and hence, creating a strong correlation between the two techniques. Under these circumstances, the only independent observations that GPS provides is the baseline lengths and their rates.

To investigate the effect of the duplicate information on the ITRF solution, the following variations in the mathematical formulation are considered in this study:

1 – GPS station state vectors are replaced by GPS derived baselines and baseline rates which are not sensitive to the changes in the orientations and origin of the

GPS-based reference frames.

2 – GPS baseline vectors are used which are insensitive to the origin of the GPS-based reference frames but allowing duplication of EOP information from VLBI technique.

3 – GPS station state vectors are used which allow the use of inaccurate coordinate system information with their corresponding weights for the ITRF solution.

In solving the alternative formulations, it is recognized that all the unknown parameters of the solution parameters can be treated as observations with appropriate weights in the context of *generalized condition equations* [Mikhail, 1976; Uotila, 1997]. In this least square solution method, the most up-to-date ITRF station state vectors and the 3D conformal transformation parameters are considered as observations to be adjusted rather than as unknown parameters to be solved for, since some of the parameters along with their covariance matrix are available a-priori from the most recent ITRF solution (ITRF97) in this study.

The corresponding mathematical and statistical models are derived in the following sections.

3.3.2.1 Mathematical model based on the strength of different techniques

Mathematical model for Satellite Laser Ranging (SLR) based data

Because the orbits of the SLR system satellites are referenced accurately to the center of mass of the Earth, it is desirable to have the origin of the ITRF solution to be defined by the SLR, which can be achieved by setting the translation T_k and their rates $\dot{T}_k$ to zero for the TRF frames realized by SLR technique in equation (2-12). The following condition equations establishes the relationships between the ITRF and the SLR that gives accordingly,

$$\begin{cases} X^{i}_{ITRF} + (t_k - t_0)\dot{X}^{i}_{ITRF} + (t_{SLR} - t_k)\dot{X}^{i}_{SLR} + (D_k + R_{VLBI})X^{i}_{ITRF} - X^{i}_{SLR} = 0 \\ \dot{X}^{i}_{ITRF} + (\dot{D}_k + \dot{R}_{VLBI})X^{i}_{ITRF} - \dot{X}^{i}_{SLR} = 0 \end{cases} \quad (3\text{-}26)$$

where R_{VLBI} is the rotation between the SLR and VLBI TRFs since the orientation of the ITRF is defined by VLBI baseline vectors as discussed in the following section.

Mathematical model for Very Long Baseline Interferometry (VLBI) based data

The VLBI provides accurate earth orientation information and baseline vectors but VLBI observations, being purely geometric, do not contain any information about the Earth's center of mass. We therefore formulate VLBI measurement contributions accordingly as a function of their observables (i.e. baseline vectors between station *i* and station *j* along with their respective velocities at the same epoch t_{TRF}) using equation (2-12) and thus it gives

$$\begin{cases} \Delta X^{ij}_{ITRF} + (t_k - t_0)\Delta\dot{X}^{ij}_{ITRF} + (t_{VLBI} - t_k)\Delta\dot{X}^{ij}_{VLBI} + D_k\Delta X^{ij}_{ITRF} - \Delta X^{ij}_{VLBI} = 0 \\ \Delta\dot{X}^{ij}_{ITRF} + \dot{D}_k\Delta X^{ij}_{ITRF} - \Delta\dot{X}^{ij}_{VLBI} = 0 \end{cases} \quad (3\text{-}27)$$

This formulation does not include any translation parameters because the baseline vectors do not contain any information about the origin of the reference frame. Also, no rotation parameters appear between the VLBI and the combined reference frame, because VLBI is chosen to define the orientation of the ITRF. Meanwhile, the simultaneously observed baseline vectors must be non-trivial, i.e. independent of each other; otherwise, the generated design matrix will be rank-deficient.

Mathematical model for Global Positioning System (GPS) based data

Although the GPS technique is excellent for relative positioning with high precision, absolute station position information cannot be determined very accurately. Moreover, current GPS orbit solutions require the use of a-priori Earth orientation Parameter (EOP) provided by the VLBI. As a result, the GPS station state vector estimates are highly correlated with those from VLBI measurements, as a result of duplicate information. The following three variant formulations are considered for investigation.

1 – GPS contributes accurate scale information in the ITRF solution realization through baseline length measurements. Baseline lengths do not contain translation and rotation information, therefore, the corresponding mathematical model for the GPS baseline observation is formulated using equation (3-27) through the norm of the baseline vector at the same epoch t_{TRF} for simplicity and it gives,

$$\begin{cases} \left\| \left[\Delta X_{ITRF} + (t_k - t_0)\Delta \dot{X}_{ITRF} + (t_{GPS} - t_k)\Delta \dot{X}_{GPS} + D_k \Delta X_{ITRF}\right]^T \cdot \right. \\ \qquad \left. \left[\Delta X_{ITRF} + (t_k - t_0)\Delta \dot{X}_{ITRF} + (t_{GPS} - t_k)\Delta \dot{X}_{GPS} + D_k \Delta X_{ITRF}\right] \right\| \\ \qquad\qquad\qquad\qquad\qquad - \left\| \Delta X_{GPS}{}^T \Delta X_{GPS} \right\| = 0 \\ \left\| \left[\Delta \dot{X}_{ITRF} + \dot{D}_k \Delta X_{ITRF}\right]^T \left[\Delta \dot{X}_{ITRF} + \dot{D}_k \Delta X_{ITRF}\right] \right\| - \left\| \Delta \dot{X}_{GPS}{}^T \Delta \dot{X}_{GPS} \right\| = 0 \end{cases} \tag{3-28}$$

Here, superscripts *ij* are omitted for a better clarity. Note that no rotation and rotation rate parameters appear in the above equation.

2 – The second formulation utilizes GPS baseline vectors and their rates as observations as opposed to the station state vectors. This corresponding mathematical model is similar to equation (3-27) for the VLBI-based data, while leaving the rotation parameters and their rates to be adjusted rather than letting them to define the orientation. Therefore, it gives

$$\begin{cases} \Delta X^{ij}_{ITRF} + (t_k - t_0)\Delta \dot{X}^{ij}_{ITRF} + (t_{GPS} - t_k)\Delta \dot{X}^{ij}_{GPS} \\ \qquad\qquad + D_k \Delta X^{ij}_{ITRF} + R_k \Delta X^{ij}_{ITRF} - \Delta X^{ij}_{GPS} = 0 \\ \Delta \dot{X}^{ij}_{ITRF} + \dot{D}_k \Delta X^{ij}_{ITRF} + \dot{R}_k \Delta X^{ij}_{ITRF} - \Delta \dot{X}^{ij}_{GPS} = 0 \end{cases} \tag{3-29}$$

3 – The third formulation makes use of equation (2-12) which leaves all the 14 transformation parameters intact but still relies on VLBI for orientations in the estimation. Therefore, the mathematical model reads as,

$$\begin{cases} X^{i}_{ITRF} + (t_k - t_0)\dot{X}^{i}_{ITRF} + (t_{GPS} - t_k)\dot{X}^{i}_{GPS} \\ \qquad\qquad + T_k + (D_k + R_{VLBI})X^{i}_{ITRF} - X^{i}_{GPS} = 0 \\ \dot{X}^{i}_{ITRF} + \dot{T}_k + (\dot{D}_k + \dot{R}_{VLBI})X^{i}_{ITRF} - \dot{X}^{i}_{GPS} = 0 \end{cases} \tag{3-30}$$

3.3.2.2 Statistical model based on generalization

Since all the mathematical models for different based data as described in the previous section are non-linear, they have to be linearlized accordingly.

Linearized mathematical model for SLR-based data

Taylor expansion of the equation (3-26) with respect to L^a_{SLR} and L^a_{ITRF} respectively and retaining only the linear terms gives,

$$B_{SLR}V_{X_{SLR}} = \left.\frac{\partial F}{\partial L^a_{SLR}}\right|_{\substack{L^a_{SLR}=L^b_{SLR}\\ L^a_{ITRF}=L^b_{ITRF}}} V_{X_{SLR}} = \begin{pmatrix} -I_{3\times3} & (t_{SLR}-t_k)I_{3\times3} \\ 0 & -I_{3\times3} \end{pmatrix}\begin{pmatrix} V_{X_{SLR}} \\ V_{\dot{X}_{SLR}} \end{pmatrix} \quad (3\text{-}31)$$

$$B_{ITRF}V_{X_{ITRF}} = \left.\frac{\partial F}{\partial L^a_{ITRF}}\right|_{\substack{L^a_{SLR}=L^b_{SLR}\\ L^a_{ITRF}=L^b_{ITRF}}} V_{X_{ITRF}}$$

$$= \begin{pmatrix} \left(I_3 + D^b_k + R^b_{VLBI}\right) & (t_k - t_0)I_3 & DR & 0 \\ \dot{D}^b_k + \dot{R}^b_{VLBI} & I_3 & 0 & DR \end{pmatrix}\begin{pmatrix} V_{X_{ITRF}} \\ V_{\dot{X}_{ITRF}} \\ V_{D_k} \\ V_{R_{VLBI}} \\ V_{\dot{D}_k} \\ V_{\dot{R}_{VLBI}} \end{pmatrix} \quad (3\text{-}32)$$

$$W_{SLR} = F(L^b_{SLR}, L^b_{ITRF}) \quad (3\text{-}33)$$

such that $B_{SLR}V_{X_{SLR}} + B_{ITRF}V_{X_{ITRF}} + W_{SLR} = 0$, where

$$DR = \begin{pmatrix} X^b_{ITRF} & 0 & Z^b_{ITRF} & -Y^b_{ITRF} \\ Y^b_{ITRF} & -Z^b_{ITRF} & 0 & X^b_{ITRF} \\ Z^b_{ITRF} & Y^b_{ITRF} & -X^b_{ITRF} & 0 \end{pmatrix}$$

It is noted that V_{D_k} corresponds to the residual for a scale value. $V_{R_{VLBI}}$ corresponds to the 3×1 vector of residuals for the three rotation components.

Linearized mathematical model for VLBI-based data

Taylor expansion of the equation (3-27) with respect to L^a_{VLBI} and L^a_{ITRF} respectively and retaining only the linear terms gives,

$$B_{VLBI}V_{\Delta X_{VLBI}} = \left.\frac{\partial F}{\partial L^a_{VLBI}}\right|_{\substack{L^a_{VLBI}=L^b_{VLBI}\\ L^a_{ITRF}=L^b_{ITRF}}} V_{\Delta X_{VLBI}} = \begin{pmatrix} -I_3 & (t_{VLBI}-t_k)I_3 \\ 0 & -I_3 \end{pmatrix}\begin{pmatrix} V_{\Delta X_{VLBI}} \\ V_{\Delta \dot{X}_{VLBI}} \end{pmatrix} \quad (3\text{-}34)$$

$$B_{ITRF}V_{\Delta X_{ITRF}} = \left.\frac{\partial F}{\partial L^a_{ITRF}}\right|_{\substack{L^a_{VLBI}=L^b_{VLBI}\\ L^a_{ITRF}=L^b_{ITRF}}} V_{\Delta X_{ITRF}}$$

$$= \begin{pmatrix} (I_3 + D^b_k) & (t_k - t_0)I_3 \\ \dot{D}^b_k & I_3 \end{pmatrix} K_1 \begin{pmatrix} V^1_{X_{ITRF}} \\ V^2_{X_{ITRF}} \\ V^1_{\dot{X}_{ITRF}} \\ V^2_{\dot{X}_{ITRF}} \end{pmatrix} + \begin{pmatrix} \Delta X^b_{ITRF} & 0 \\ 0 & \Delta X^b_{ITRF} \end{pmatrix}\begin{pmatrix} V_{D_k} \\ V_{\dot{D}_k} \end{pmatrix} \quad (3\text{-}35)$$

$$W_{VLBI} = F(L^b_{VLBI}, L^b_{ITRF}) \quad (3\text{-}36)$$

such that $B_{VLBI}V_{\Delta X_{VLBI}} + B_{ITRF}V_{\Delta X_{ITRF}} + W_{VLBI} = 0$, where

$$K_1 = \begin{pmatrix} I_3 & -I_3 & 0 & 0 \\ 0 & 0 & I_3 & -I_3 \end{pmatrix} \quad (3\text{-}37)$$

Note that $V^i_{X_{ITRF}}$ and $V^i_{\dot{X}_{ITRF}}$ in (3-35) refer to 3×1 vector of residuals for the station positions and velocities at position *i* respectively.

Linearized mathematical model for GPS-based data

Since there are many terms in equation (3-28), they are grouped by and denoted as

$$l_{ITRF} = \Big\| \left[\Delta X_{ITRF} + (t_k - t_0)\Delta\dot{X}_{ITRF} + (t_{GPS} - t_k)\Delta\dot{X}_{GPS} + D_k \Delta X_{ITRF}\right]^T \cdot \left[\Delta X_{ITRF} + (t_k - t_0)\Delta\dot{X}_{ITRF} + (t_{GPS} - t_k)\Delta\dot{X}_{GPS} + D_k \Delta X_{ITRF}\right] \Big\|$$

$$\dot{l}_{ITRF} = \left\| \left[\Delta\dot{X}_{ITRF} + \dot{D}_k \Delta X_{ITRF} \right]^T \left[\Delta\dot{X}_{ITRF} + \dot{D}_k \Delta X_{ITRF} \right] \right\|$$

$$l_{GPS} = \left\| \Delta X_{GPS}{}^T \Delta X_{GPS} \right\|$$

$$\dot{l}_{GPS} = \left\| \Delta\dot{X}_{GPS}{}^T \Delta\dot{X}_{GPS} \right\|$$

for simplicity and better presentation.

Similarly, Taylor expansion of the equation (3-28) with respect to L^a_{GPS} and L^a_{ITRF} respectively and retaining only the linear terms gives,

$$B_{GPS} V_{\Delta X_{GPS}} = \left. \frac{\partial F}{\partial L^a_{GPS}} \right|_{\substack{L^a_{GPS} = L^b_{GPS} \\ L^a_{ITRF} = L^b_{ITRF}}} V_{\Delta X_{GPS}} = \begin{pmatrix} -\dfrac{\Delta X^b_{GPS}{}^T}{l_{GPS}} & K_2 \\ 0 & -\dfrac{\Delta\dot{X}^b_{GPS}{}^T}{\dot{l}_{GPS}} \end{pmatrix} \begin{pmatrix} V_{\Delta X_{GPS}} \\ V_{\Delta\dot{X}_{GPS}} \end{pmatrix} \tag{3-38}$$

$$B_{ITRF} V_{\Delta X_{ITRF}} = \left. \frac{\partial F}{\partial L^a_{GPS}} \right|_{\substack{L^a_{GPS} = L^b_{GPS} \\ L^a_{ITRF} = L^b_{ITRF}}} V_{\Delta X_{ITRF}}$$

$$= \begin{pmatrix} K_3 & K_4 \\ \dfrac{1}{\dot{l}_{ITRF}} \left[\dot{D}^b_k \Delta\dot{X}^b_{ITRF}{}^T + \dot{D}^{b\,2}_k \Delta X^b_{ITRF}{}^T \right] & \dfrac{1}{\dot{l}_{ITRF}} \left[\Delta\dot{X}^b_{ITRF}{}^T + \dot{D}^b_k \Delta X^b_{ITRF}{}^T \right] \end{pmatrix} \cdot \tag{3-39}$$

$$K_1 \begin{pmatrix} V^1_{X_{ITRF}} \\ V^2_{X_{ITRF}} \\ V^1_{\dot{X}_{ITRF}} \\ V^2_{\dot{X}_{ITRF}} \end{pmatrix} + \begin{pmatrix} K_5 & 0 \\ 0 & \dfrac{1}{\dot{l}_{ITRF}} \left[\Delta\dot{X}^b_{ITRF}{}^T \Delta X^b_{ITRF} + \dot{D}^b_k \Delta X^b_{ITRF}{}^T \Delta X^b_{ITRF} \right] \end{pmatrix} \begin{pmatrix} V_{D_k} \\ V_{\dot{D}_k} \end{pmatrix}$$

$$W_{GPS} = F(L^b_{GPS}, L^b_{ITRF}) \tag{3-40}$$

such that $B_{GPS} V_{\Delta X_{GPS}} + B_{ITRF} V_{\Delta X_{ITRF}} + W_{GPS} = 0$ for the POF approach based on the first formulation, where

$$K_2 = \frac{1}{l_{ITRF}} \left\{ (t_{GPS} - t_k)(1 + D^b_k) \Delta X^b_{ITRF}{}^T + (t_k - t_0)(t_{GPS} - t_k) \Delta\dot{X}^b_{ITRF}{}^T + (t_{GPS} - t_k)^2 \Delta\dot{X}^b_{GPS}{}^T \right\}$$

$$K_3 = \frac{1}{l_{ITRF}} \left\{ \left(1 + D_k^b\right)^2 \Delta X_{ITRF}^{b\ T} + \left(t_k - t_0\right)\left(1 + D_k^b\right) \Delta \dot{X}_{ITRF}^{b\ T} + \left(t_{GPS} - t_k\right)\left(1 + D_k^b\right) \Delta \dot{X}_{GPS}^{b\ T} \right\}$$

$$K_4 = \frac{1}{l_{ITRF}} \left\{ \left(t_k - t_0\right)\left(1 + D_k^b\right) \Delta X_{ITRF}^{b\ T} + \left(t_k - t_0\right)^2 \Delta \dot{X}_{ITRF}^{b\ T} + \left(t_k - t_0\right)\left(t_{GPS} - t_k\right) \Delta \dot{X}_{GPS}^{b\ T} \right\}$$

$$K_5 = \frac{1}{l_{ITRF}} \left\{ \left(1 + D_k^b\right) \Delta X_{ITRF}^{b\ T} \Delta X_{ITRF}^{b} + \left(t_k - t_0\right) \Delta X_{ITRF}^{b\ T} \Delta \dot{X}_{ITRF}^{b} + \left(t_{GPS} - t_k\right) \Delta X_{ITRF}^{b\ T} \Delta \dot{X}_{GPS}^{b} \right\}$$

The linearized GPS observation for the second formulation is similar to equation (3-34) to (3-37). Taylor expansion of the equation (3-29) with respect to L_{GPS}^a and L_{ITRF}^a respectively and retaining only the linear terms gives the following generalized condition equations,

$$B_{GPS} V_{\Delta X_{GPS}} = \left. \frac{\partial F}{\partial L_{GPS}^a} \right|_{\substack{L_{GPS}^a = L_{GPS}^b \\ L_{ITRF}^a = L_{ITRF}^b}} V_{\Delta X_{GPS}} = \begin{pmatrix} -I_3 & (t_{GPS} - t_k) I_3 \\ 0 & -I_3 \end{pmatrix} \begin{pmatrix} V_{\Delta X_{GPS}} \\ V_{\Delta \dot{X}_{GPS}} \end{pmatrix} \qquad \text{(3-41)}$$

$$B_{ITRF} V_{\Delta X_{ITRF}} = \left. \frac{\partial F}{\partial L_{ITRF}^a} \right|_{\substack{L_{GPS}^a = L_{GPS}^b \\ L_{ITRF}^a = L_{ITRF}^b}} V_{\Delta X_{ITRF}}$$

$$= \begin{pmatrix} \left(I_3 + D_k^b + R_k^b\right) & (t_k - t_0) I_3 \\ \dot{D}_k^b + \dot{R}_k^b & I_3 \end{pmatrix} K_1 \begin{pmatrix} V_{X_{ITRF}}^1 \\ V_{X_{ITRF}}^2 \\ V_{\dot{X}_{ITRF}}^1 \\ V_{\dot{X}_{ITRF}}^2 \end{pmatrix} + \begin{pmatrix} \Delta DR & 0 \\ 0 & \Delta DR \end{pmatrix} \begin{pmatrix} V_{D_k} \\ V_{R_{VLBI}} \\ V_{\dot{D}_k} \\ V_{\dot{R}_{VLBI}} \end{pmatrix} \qquad \text{(3-42)}$$

$$W_{GPS} = F(L_{GPS}^b, L_{ITRF}^b) \qquad \text{(3-43)}$$

such that $B_{GPS} V_{\Delta X_{GPS}} + B_{ITRF} V_{\Delta X_{ITRF}} + W_{GPS} = 0$, where

$$\Delta DR = \begin{pmatrix} \Delta X_{ITRF}^b & 0 & \Delta Z_{ITRF}^b & -\Delta Y_{ITRF}^b \\ \Delta Y_{ITRF}^b & -\Delta Z_{ITRF}^b & 0 & \Delta X_{ITRF}^b \\ \Delta Z_{ITRF}^b & \Delta Y_{ITRF}^b & -\Delta X_{ITRF}^b & 0 \end{pmatrix}$$

The linearized GPS observation for the third formulation is similar to equation (3-24). Taylor expansion of the equation (3-30) with respect to L^a_{GPS} and L^a_{ITRF} respectively and retaining only the linear terms gives the following generalized condition equations,

$$B_{GPS}V_{X_{GPS}} = \left.\frac{\partial F}{\partial L^a_{GPS}}\right|_{\substack{L^a_{GPS}=L^b_{GPS} \\ L^a_{ITRF}=L^b_{ITRF}}} V_{X_{GPS}} = \begin{pmatrix} -I_3 & (t_{GPS}-t_k)I_3 \\ 0 & -I_3 \end{pmatrix}\begin{pmatrix} V_{X_{GPS}} \\ V_{\dot{X}_{GPS}} \end{pmatrix} \tag{3-44}$$

$$\begin{aligned} B_{ITRF}V_{X_{ITRF}} &= \left.\frac{\partial F}{\partial L^a_{ITRF}}\right|_{\substack{L^a_{GPS}=L^b_{GPS} \\ L^a_{ITRF}=L^b_{ITRF}}} V_{X_{ITRF}} \\ &= \begin{pmatrix} \left(I_3 + D^b_k + R^b_k\right) & (t_k - t_0)I_3 \\ \dot{D}^b_k + \dot{R}^b_k & I_3 \end{pmatrix}\begin{pmatrix} V_{X_{ITRF}} \\ V_{\dot{X}_{ITRF}} \end{pmatrix} + \begin{pmatrix} A_k & 0 \\ 0 & A_k \end{pmatrix}\begin{pmatrix} V_{T_k} \\ V_{\dot{T}_k} \end{pmatrix} \end{aligned} \tag{3-45}$$

$$W_{GPS} = F(L^b_{GPS}, L^b_{ITRF}) \tag{3-46}$$

such that $B_{GPS}V_{X_{GPS}} + B_{ITRF}V_{X_{ITRF}} + W_{GPS} = 0$, where

$$A_k = \begin{pmatrix} 1 & 0 & 0 & X^b_{ITRF} & 0 & Z^b_{ITRF} & -Y^b_{ITRF} \\ 0 & 1 & 0 & Y^b_{ITRF} & -Z^b_{ITRF} & 0 & X^b_{ITRF} \\ 0 & 0 & 1 & Z^b_{ITRF} & Y^b_{ITRF} & -X^b_{ITRF} & 0 \end{pmatrix}$$

and V_{T_k} and $V_{\dot{T}_k}$ denote the seven transformation parameters and their rates respectively.

4. ITRF INPUT DATA AND PREPROCESSING

This chapter examines the input data through visualization of the correlation of the a-priori covariance matrices of the space geodetic input data, basic statistical measures, and spatial distribution of the selected stations. It also details proper considerations before further processing of the input data.

4.1 Input data used in the study and their spatial distribution

There are a variety of stations available in the world. The longer the time span of the observation techniques, the more stable the TRF solutions would be. Therefore, this investigation includes TRF solutions from VLBI and SLR techniques at first because of their long time spans.

Because of limited availability of DORIS co-located with SLR and VLBI technique and its similar performance to GPS, DORIS measurements were excluded in this study. Therefore, stations with three techniques (i.e. SLR, VLBI, GPS) simultaneously occupied within a co-located site are selected for the investigation so that those technique contribution to the final combination solution for the new approach can be assessed. The selected stations are displayed in Figure 4.1.

The TRF solutions used for the study are as follows (see also Table 4.1):

SLR: Six of the SLR solutions submitted for ITRF2000 solution are provided by Australian Surveying and Land Information Group (AUS), Australia; Centro Geodesia Spaziale, Matera (CGS), Italy; Communication Research Laboratory

(CRL), Japan; Delft Institute of Earth Oriented Space Research (DEOS), Netherlands; Deutshes Geodadtisches Forschungsinstitut (DGFI), Germany and Joint Center for Earth System Technology, GSFC (JCET), NASA, USA.

VLBI: Three VLBI solutions submitted for ITRF2000 solution are provided by the Geodetic Institutes of the University of Boon (GIUB), Germany; the Goddard Space Flight Center (GSFC), NASA, USA and the Shanghai Astronomical Observatory (SHA), China.

GPS: Six of the GPS solutions submitted for ITRF2000 solution are provided by the Center for Orbit Determination (CODE) in Europe; GeoForschungsZentrum Potsdam (GFZ), Germany; International GPS Service (IGS) by Natural Resources Canada; Jet Propulsion Laboratory (JPL), USA; University of Newcastle upon Tyne (NCL), England and National Oceanic and Atmospheric Administration (NOAA), USA.

Table 4.1 Summary of solutions used for the TRF combination investigation

Technique	AC Solution	Data Span	No. of Stations Original	No. of Stations Used	Constraints Applied
VLBI	(GIUB) 00 R 01	1984 –1999	51	14	Loose
	(GSFC) 00 R 01	1979 –1999	130	22	Loose
	(SHA) 00 R 01	1979 –1999	127	22	Loose
SLR	(AUS) 00 L 01	1992 –2000	55	13	Loose
	(CGS) 00 L 01	1984 –1999	94	12	Loose
	(CRL) 00 L 02	1990 –2000	60	14	Loose
	(DEOS) 00 L 05	1983 –1999	91	12	Loose
	(DGFI) 00 L 01	1990 –2000	43	11	Removable
	(JCET) 00 L 05	1993 –2000	48	15	Loose
GPS	(CODE) 00 P 03	1993 –2000	160	15	Minimum
	(GFZ) 00 P 01	1993 –2000	98	13	Minimum
	(IGS) 00 P 46	1996 –2000	179	13	Minimum
	(JPL) 00 P 01	1991 –2000	112	12	Minimum
	(NCL) 00 P 01	1995 –1999	90	13	Minimum
	(NOAA) 00 P 01	1994 –2000	165	12	Removable

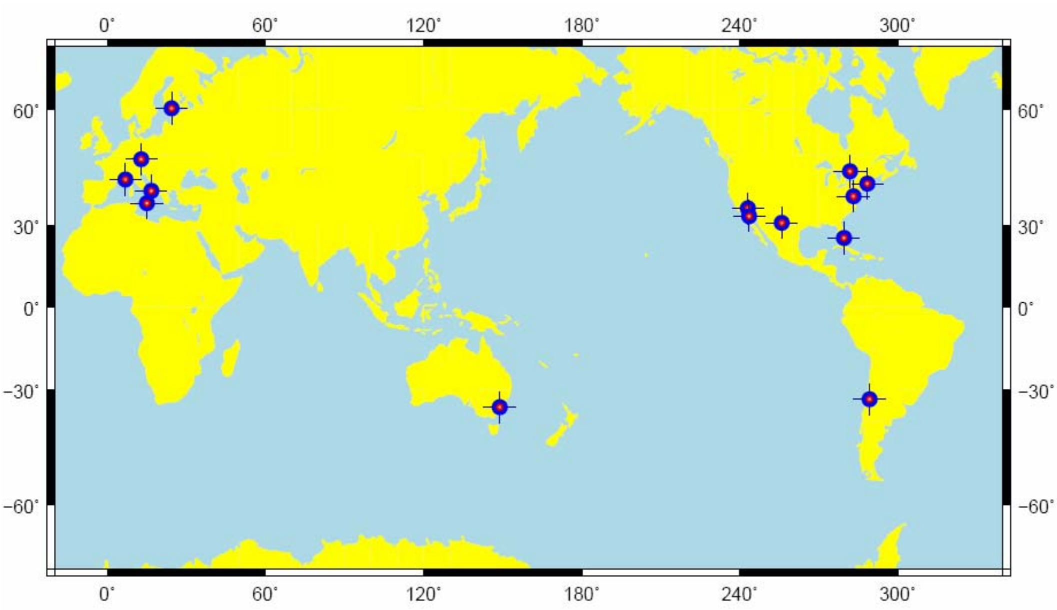

Figure 4.1 Spatial distribution of 14 co-located sites (with VLBI, SLR and GPS)

4.1.1 Space geodesy techniques solutions and local ties

In this section, the input covariance matrices of the space geodetic solutions and local ties are described. Plot of the correlation matrices together with basic statistics are made so as to gain a better understanding of the precision and correlation within a space geodetic technique solution (TRF) or a technique. Description about the local tie is also provided.

4.1.1.1 Input covariance matrices for the VLBI data

The original covariance matrices for VLBI corresponding to the three-dimensional Cartesian coordinates (x, y, z) along with their respective velocities $(\dot{x}, \dot{y}, \dot{z})$ were computed from the VLBI analysis centers. The covariance matrices, Σ_{obs}, for the required stations are extracted for this study, which is in the following format:

$$\Sigma_{obs} = \begin{pmatrix} \Sigma_C & \Sigma_{CV} \\ \Sigma_{CV} & \Sigma_V \end{pmatrix} \quad (4\text{-}1)$$

where Σ_C , Σ_V and Σ_{CV} correspond to the covariance matrix for the coordinates, the covariance matrix for the velocities, and the covariance matrix between the coordinates and velocities vectors.

The average standard deviation for the XYZ coordinate, σ_x , and velocity components, $\sigma_{\dot{x}}$, are computed as follows:

$$mean(\sigma_x) = \frac{tr\left(\sqrt{diag(\Sigma_C)}\right)}{3n} \tag{4-2}$$

$$mean(\sigma_{\dot{x}}) = \frac{tr\left(\sqrt{diag(\Sigma_V)}\right)}{3n} \tag{4-3}$$

where n is the number of stations and $tr\left(\sqrt{diag(\Sigma)}\right)$ represents the trace or the sum of the square root of variances in the diagonal of a covariance matrix.

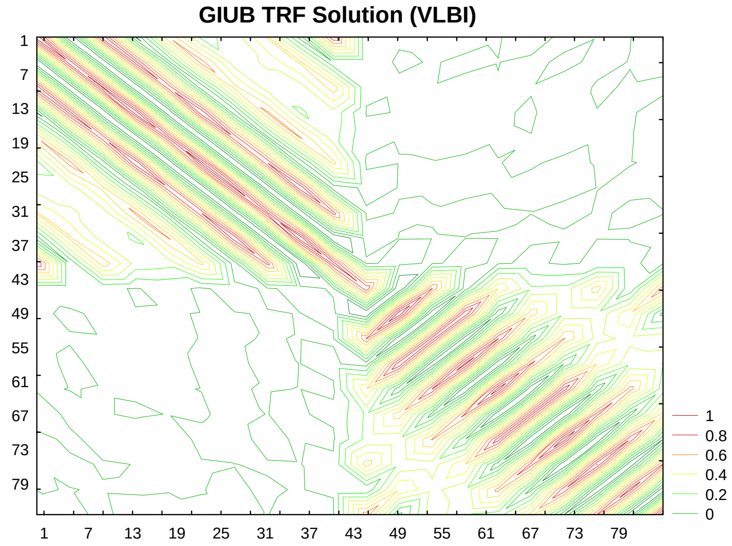

Figure 4.2 Plot of correlation matrix for GIUB TRF Solution (VLBI)

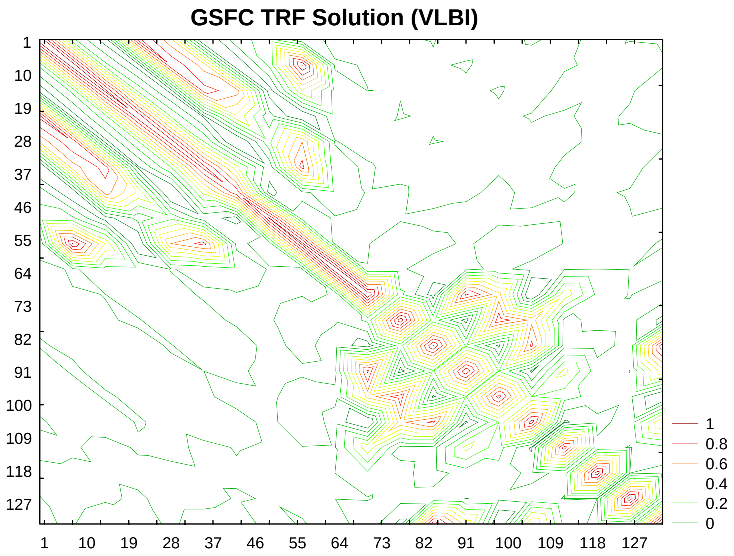

Figure 4.3 Plot of correlation matrix for GSFC TRF Solution (VLBI)

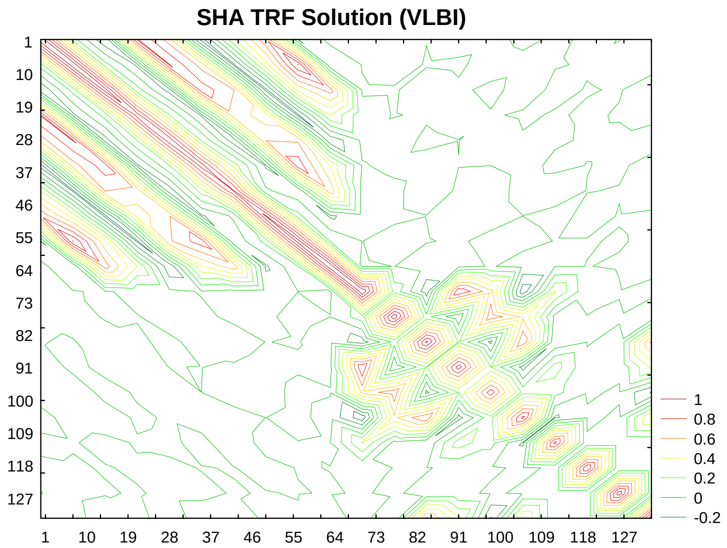

Figure 4.4 Plot of correlation matrix for SHA TRF Solution (VLBI)

Figures 4.2 to Figure 4.4 show the correlation matrices. They display high correlation among the station positions and velocities respectively. On the contrary, they present low correlation between the position and velocity vectors. The difference in the pattern of those correlation matrix plots is due to different processing strategies made by each individual analysis center.

The summary statistics for the precision of station positions and velocities is also given in Table 4.2 and 4.3 respectively. Overall, the average precision of the station positions and velocities of the VLBI-based TRF solutions are at a meter and centimeter/year level respectively. The precision of VLBI GSFC TRF solutions is relatively more diverse than the other VLBI solutions because the constraints for the estimation of positions and velocities are applied more loosely for some particular stations along with their respective velocities.

Table 4.2 Summary statistics for the input VLBI covariance matrices for station positions (in m)

A/C Solutions	Min (σ_x)	Max (σ_x)	Mean (σ_x)	Median (σ_x)
GIUB	±1.395	±1.399	±1.397	±1.396
GSFC	±0.854	±6.337	±1.896	±0.856
SHA	±0.873	±1.272	±0.954	±0.884

Table 4.3 Summary statistics for the input VLBI covariance matrices for station velocities (in m/year)

A/C Solutions	Min ($\sigma_{\dot{x}}$)	Max ($\sigma_{\dot{x}}$)	Mean ($\sigma_{\dot{x}}$)	Median ($\sigma_{\dot{x}}$)
GIUB	±0.014	±0.016	±0.015	±0.014
GSFC	±0.087	±0.764	±0.219	±0.088
SHA	±0.010	±0.100	±0.031	±0.011

4.1.1.2 Input covariance matrices for the SLR data

The original covariance matrices for SLR follow the same arrangement as in the case of VLBI (Figure 4.5 to Figure 4.10). In general, high correlation values within the correlation matrix plot are randomly appeared for a TRF without specific pattern, because of different processing strategies from different analysis centers. They also present low correlation between the position and velocity vectors, except DEOS TRF solution that displays relatively high correlation in reverse sense.

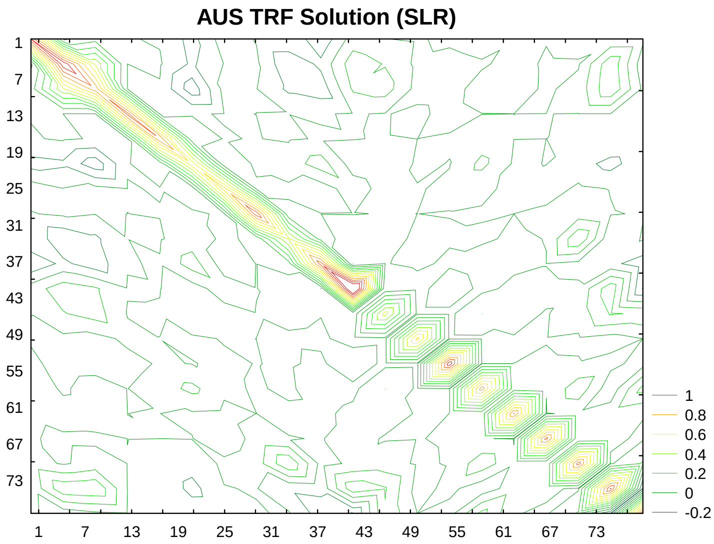

Figure 4.5 Plot of correlation matrix for AUS TRF Solution (SLR)

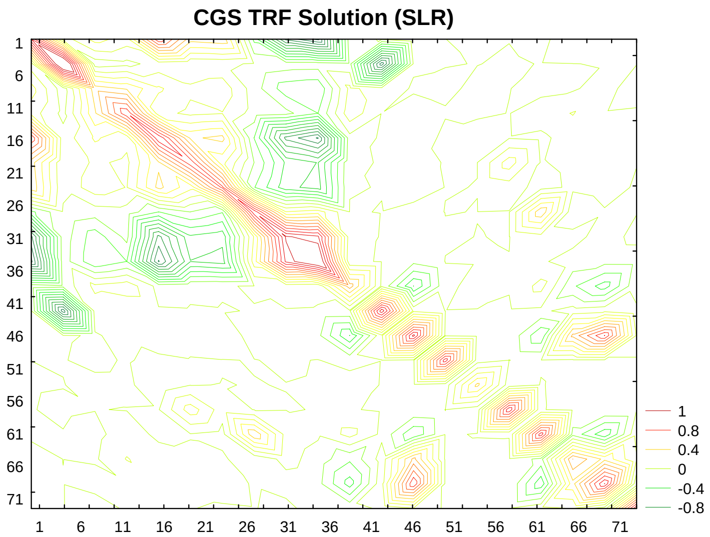

Figure 4.6 Plot of correlation matrix for CGS TRF Solution (SLR)

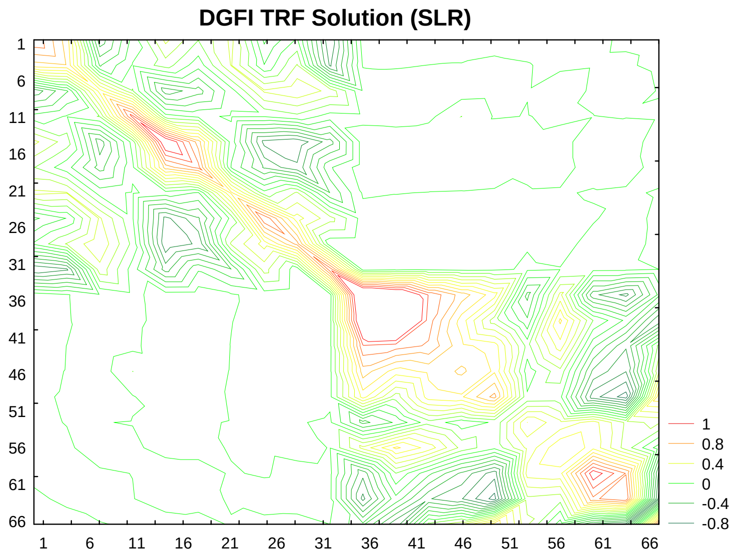

Figure 4.7 Plot of correlation matrix for DGFI TRF Solution (SLR)

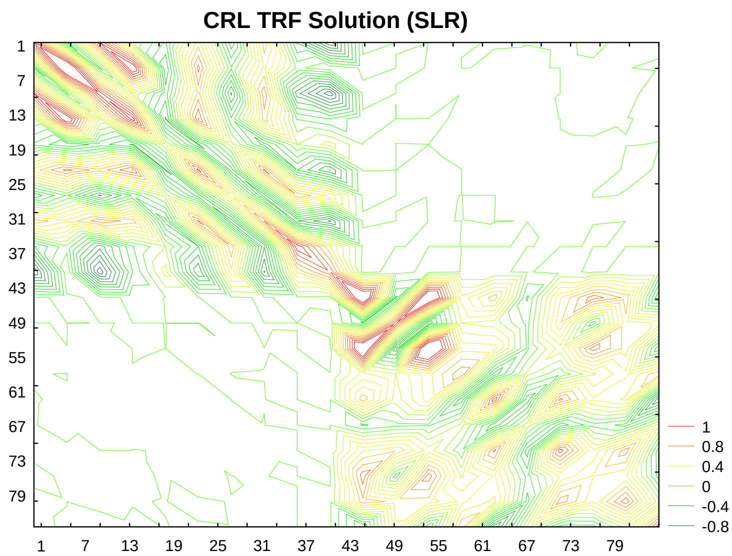

Figure 4.8 Plot of correlation matrix for CRL TRF Solution (SLR)

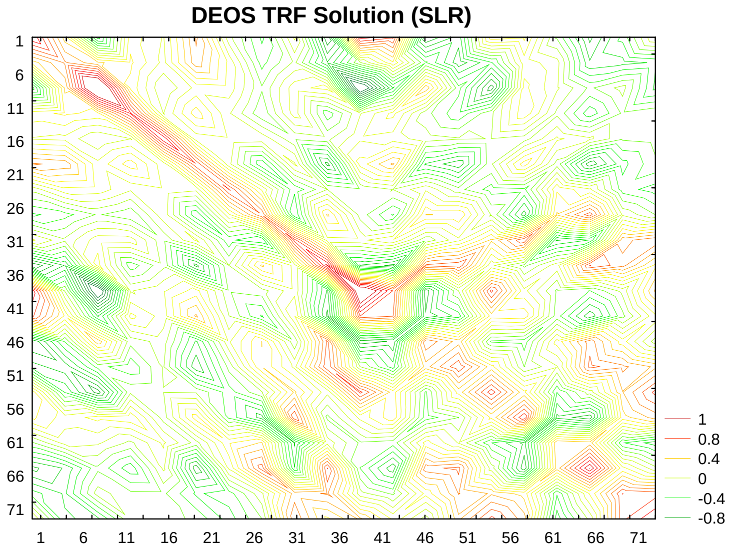

Figure 4.9 Plot of correlation matrix for DEOS TRF Solution (SLR)

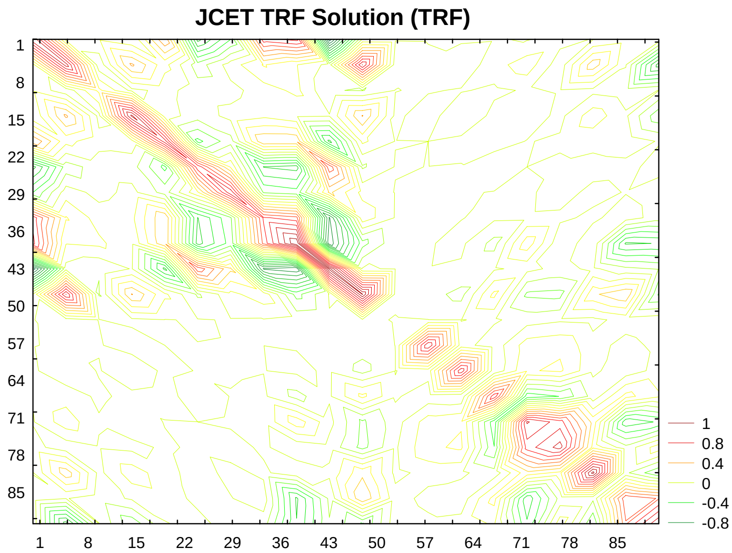

Figure 4.10 Plot of correlation matrix for JCET TRF Solution (SLR)

The summary statistics shown in the Table 4.4 and 4.5 give a diverse level of precision among different TRF solutions. The precision of the station positions and velocities range from less than a millimeter to meter level and less than a millimeter/year and a meter/year level respectively. The precision of the positions are generally lower than the velocities counterpart, except for the DEOS TRF solutions.

Table 4.4 Summary statistics for the input SLR covariance matrices for station positions (in m)

A/C Solutions	Min (σ_x)	Max (σ_x)	Mean (σ_x)	Median (σ_x)
AUS	±0.135	±0.999	±0.464	±0.284
CGS	±0.001	±0.119	±0.019	±0.008
DGFI	±0.000	±0.002	±0.001	±0.001
CRL	±1.970	±4.642	±3.707	±3.920
DEOS	±0.007	±0.064	±0.019	±0.014
JCET	±0.016	±1.042	±0.136	±0.089

Table 4.5 Summary statistics for the input SLR covariance matrices for station velocities (in m/year)

A/C Solutions	Min ($\sigma_{\dot{x}}$)	Max ($\sigma_{\dot{x}}$)	Mean ($\sigma_{\dot{x}}$)	Median ($\sigma_{\dot{x}}$)
AUS	±0.038	±0.996	±0.297	±0.094
CGS	±0.000	±0.019	±0.003	±0.001
DGFI	±0.000	±0.001	±0.001	±0.001
CRL	±0.197	±0.469	±0.371	±0.392
DEOS	±0.061	±0.140	±0.102	±0.107
JCET	±0.003	±0.124	±0.021	±0.013

4.1.1.3 Input covariance matrices for the GPS data

Figures 4.11 to Figure 4.16 show the correlation matrices for TRF solutions realized by GPS technique. They show low correlation between the coordinates and velocities vectors in general, except CODE TRF solution. The pattern for the high correlation among station positions or those in the station velocities is not apparent in general.

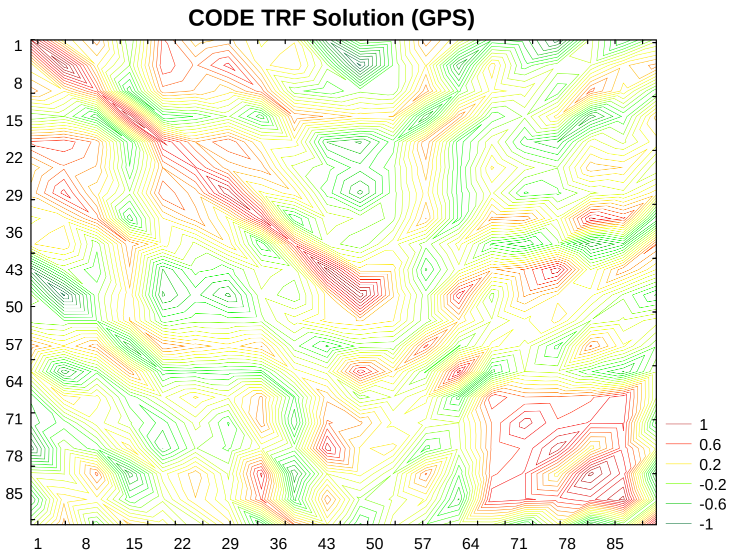

Figure 4.11 Plot of correlation matrix for CODE TRF Solution (GPS)

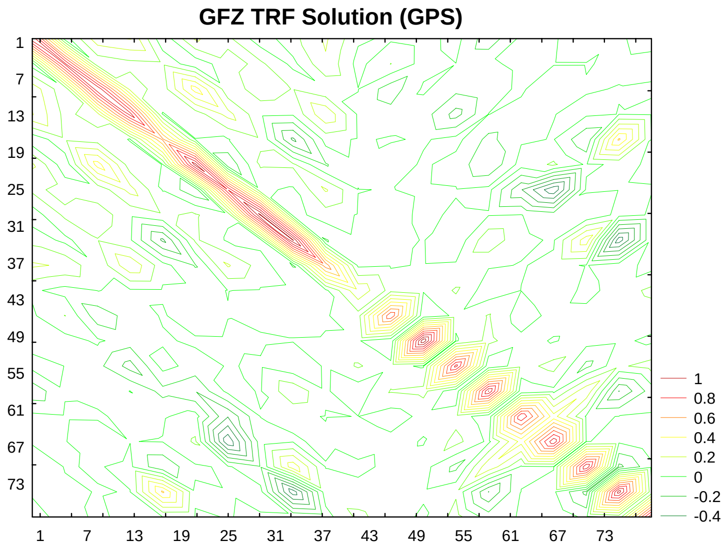

Figure 4.12 Plot of correlation matrix for GFZ TRF Solution (GPS)

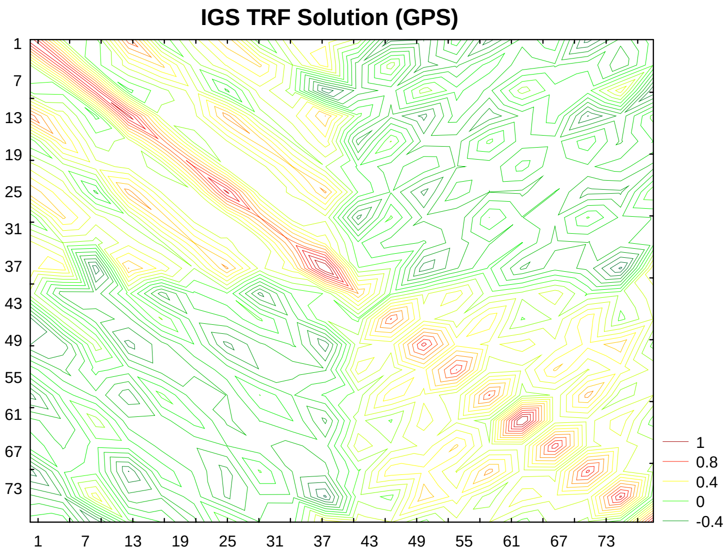

Figure 4.13 Plot of correlation matrix for IGS TRF Solution (GPS)

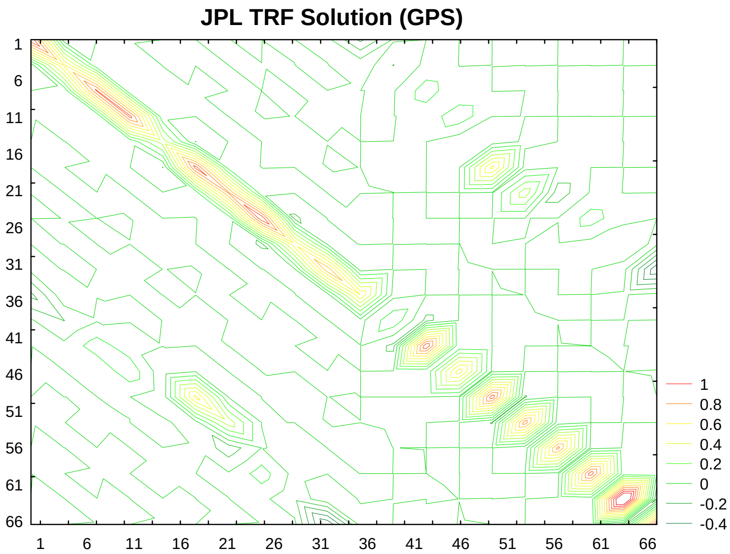

Figure 4.14 Plot of correlation matrix for JPL TRF Solution (GPS)

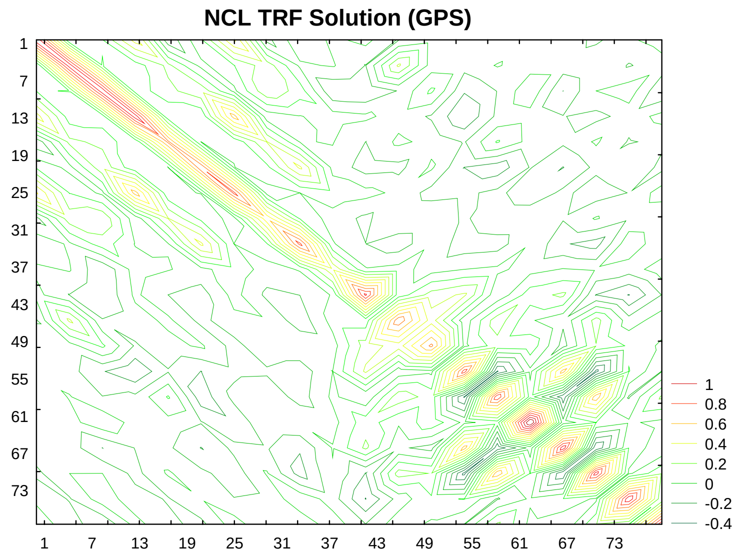

Figure 4.15 Plot of correlation matrix for NCL TRF Solution (GPS)

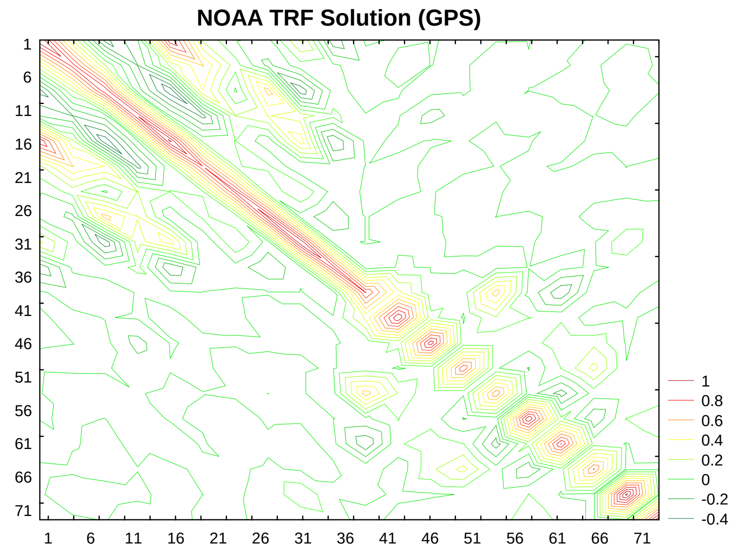

Figure 4.16 Plot of correlation matrix for NOAA TRF Solution (GPS)

Table 4.6 and Table 4.7 display the summary statistics for the precision of the station positions and velocities. Both tables present the precision of both the station positions and velocities of the GPS-based TRF solutions, which are at or below millimeter and millimeter/year level respectively, are higher than those VLBI-based and SLR-based TRF solutions. This indicates the input covariance matrices for the GPS data may be overestimated. Again, the precision for the positions are generally lower than the velocity counterparts.

Table 4.6 Summary statistics for the input GPS covariance matrices for station positions (in m)

A/C Solutions	Min (σ_x)	Max (σ_x)	Mean (σ_x)	Median (σ_x)
CODE	±0.000	±0.001	±0.000	±0.000
GFZ	±0.006	±0.115	±0.019	±0.011
IGS	±0.002	±0.004	±0.003	±0.003
JPL	±0.000	±0.001	±0.000	±0.000
NCL	±0.001	±0.004	±0.001	±0.001
NOAA	±0.000	±0.000	±0.000	±0.001

Table 4.7 Summary statistics for the input GPS covariance matrices for station velocities (in m/year)

A/C Solutions	Min ($\sigma_{\dot{x}}$)	Max ($\sigma_{\dot{x}}$)	Mean ($\sigma_{\dot{x}}$)	Median ($\sigma_{\dot{x}}$)
CODE	±0.000	±0.000	±0.000	±0.000
GFZ	±0.002	±0.013	±0.005	±0.004
IGS	±0.001	±0.003	±0.002	±0.002
JPL	±0.000	±0.000	±0.000	±0.000
NCL	±0.001	±0.002	±0.001	±0.001
NOAA	±0.000	±0.000	±0.000	±0.000

4.1.2 Local ties for co-located sites

The local ties, which are precisely surveyed in three dimensions using classical surveying method and GPS technique by national geodetic agencies, provide a link between those geodetic markers or monument realized by different space techniques within a co-located site. Typical distance between geodetic markers in a co-located site is of the order of few hundred meters. Normally, it is available in the form of coordinate differences together with their precisions.

4.2 Considerations for the preprocessing of the input data

Different analysis centers have their own way to realize their respective TRF solutions through three types of constraints as explained. Current ITRF solutions remove the datum constraints from all TRF solutions and re-apply minimum constraints to all of them again as explained in Chapter 2. However, these constraints were not clearly reported in the SINEX files. Even if they are reported, the recovery of unconstrained normal equations sometimes fails due to numerical computation problem. For example, GSFC and SHA solutions cannot be properly deconstrained to recover the original normal equations (DGFI Annual Report 2003). Hence, all the datum constraints are retained along with their respective covariance matrices as provided in this study. In fact, this approach is, in reality, more appropriate since datum constraints are part of the TRF solution realization.

From the published ITRF2000 results, most values of the transformation parameters between TRFs and ITRF are at a few millimeters level, except for those between VLBI TRFs and ITRF, which displays apparent offset (especially in the translation). This implies that those TRFs, which are not being to VLBI technique, are not much different from the ITRF. Accordingly, one could regard all TRFs within the same technique as one frame for the inter-technique combination. In other words, only 14 parameters of the 3D Helmert transformation with rates between the frame of each technique and the combined frame (ITRF) needs to be computed during the inter-technique combination instead of all the transformation parameters between TRFs and the ITRF. The same can be applied to VLBI TRFs either by taking the difference such that the definition of origin vanishes (which is utilized in the new approach) or applying an appropriate transformation before usage.

Local ties employed in the ITRF2000 combination are being used for connecting TRFs from different techniques together, as different techniques are occupied in different physical monuments within a co-located site. Since direct propagation to a common station within a co-located site allows explicit assessment on the contribution of each technique, local ties have to be shown in agreement with the previous ITRF version. It was found that the differences are at or below a centimeter level for each XYZ coordinate component.

Thus, station positions of different individual TRF within a co-located site can be propagated to a common station using local tie measurements given the validation of local ties. All the local ties within selected co-located sites are utilized. Details implementation for the combination solutions will be illustrated in Chapter 5.

5. POST-PROCESSING STRATEGY AND RESULT

This chapter gives an overview of the post-processing procedures taken to ensure good quality of the final combination solution. The comparison of the outcome solution from the new approach to both the minimum constraint solution from state vector formulation and the ITRF2000 solution realization is made.

5.1 Outlier detection

Residuals reflect the amount of discrepancy between the observed and adjusted values that remains during the iteration or after the process of the estimation. Inspection of the residuals is essential, as outliers contaminated in the observation impair the precision of the estimates.

In the context of ITRF combination, there are two approaches in handling the influential data. The normalized residual (i.e. raw residual divided by its original observation standard deviation) has been utilized together with a pre-set threshold value of 4 [Altamimi *et al.*, 2002b]. Another approach makes use of the spherical position differences with a specified threshold together with the normalized value (i.e. the spherical position differences divided by their standard deviation) as a second indicator [Angermann *et al.*, 2004a]. However, none of them give explicit statistical evaluation of the residuals.

Assume normally distributed residuals, with $V \sim N\left(0, \sigma_0^2 P^{-1}\right)$, the following statistic (Studentized residuals) is t-distributed [Belsley, 1980; Snow, 2002].

$$t_j = \frac{V_j}{\sqrt{\hat{\sigma}_0^2 (Q_V)_{jj}}} \tag{5-1}$$

where subscript *jj* denote the *j*th diagonal element of the cofactor matrix Q_V for the residuals. This statistic was used to detect the outliers during the variance components estimation at 0.01 significance level after the fourth iteration. Except for two velocity component residuals, no outliers were detected.

5.2 Variance components estimation in combining heterogeneous data

Given the varying quality of the input data sets from different TRF, an iterative variance components estimation algorithm of Helmert type is used to calculate appropriate variance components for weighting the data sets iteratively to obtain the final combination solution.

5.2.1 Variance components estimation for the observation equation formulation

This variance components estimation was classically derived by Helmert (1924). Relevant formulas are provided as below [Boucher *et al.*, 1999]:

Given the linear model in (3-6) with *k* sets of independent heterogeneous data sets and their corresponding variance of unit weights, the weight matrix is expressed as

$$P = \begin{pmatrix} \sigma_{01}^2 \Sigma_1^{-1} & 0 & \cdots & 0 \\ 0 & \sigma_{02}^2 \Sigma_2^{-1} & \cdots & 0 \\ \vdots & \vdots & \ddots & \vdots \\ 0 & 0 & \cdots & \sigma_{0k}^2 \Sigma_k^{-1} \end{pmatrix} \tag{5-2}$$

where

σ_{0k}^2 refers to the variance component of data set *k*

Σ_k^{-1} refers to the inverse of the covariance matrix of data set *k*

The variance components estimation of the Helmert type based on observation equations is estimated using,

$$\underset{k\times k}{S}\,\underset{k\times 1}{\hat{\sigma}^2} = \underset{k\times 1}{W} \tag{5-3}$$

where

$$S_{ij} = \begin{cases} n_i - 2tr(N^{-1}N_i) + tr(N^{-1}N_i)^2,\ i = j \\ tr(N^{-1}N_i N^{-1}N_j)\,, i \neq j \end{cases} \tag{5-4}$$

$$\hat{\sigma}^2 = (\hat{\sigma}_{01}^2 \quad \hat{\sigma}_{02}^2 \quad \cdots \quad \hat{\sigma}_{0k}^2)^T \tag{5-5}$$

$$W = (V_1^T P_1 V_1 \quad V_2^T P_2 V_2 \quad \cdots \quad V_k^T P_k V_k)^T \tag{5-6}$$

$$N = A^T PA,\ N_i = A_i^T P_i A_i \ \ (i = 1,...,k) \tag{5-7}$$

The equation (5-3) could be simplified to

$$\hat{\sigma}_{0i}^2 = \frac{V_i^T P_i V_i}{n_i - tr(N^{-1}N_i)} \tag{5-8}$$

by assuming that all the variance components are equal, that is;

$$\hat{\sigma}_{01}^2 = \hat{\sigma}_{02}^2 = \cdots = \hat{\sigma}_{0k}^2 \tag{5-9}$$

where n_i is the number of observations, P_i is the weight matrix and A_i is the design matrix of a particular dataset *i*.

The iteration is performed until variance components, σ_{0i}^2, for their respective cofactor matrices converge to 1. The rescaling of the cofactor matrices during the iteration process could be described as,

$$Q_i^{(n)} = \prod_{n=0}^{m} \hat{\sigma}_{0i}^{2\ (n)} Q_i \tag{5-10}$$

where *n* refers to the iteration at which they belong to, *m* refers to the number of iteration, and Q_i is the cofactor matrix for a particular dataset *i*.

5.2.2 Variance components estimation for the generalized condition equation formulation

The variance components estimation for the Helmert's "*conditioned observation equations with unknowns which are known a-priori*" has been derived by Yu (1996) based on maximum likelihood estimation. The solution is equivalent to the variance components estimation based on generalized condition equations.

Given the generalized condition equation model in (3-16) with *two* sets of independent heterogeneous datasets,

$$B_1V_1 + B_2V_2 + W = 0 \tag{5-11}$$

together with the corresponding weights

$$P_1 = \sigma_{01}^2\Sigma_1^{-1} \text{ and } P_2 = \sigma_{02}^2\Sigma_2^{-1}$$

The *M* matrix of the generalized equation could be expressed as,

$$M = B_1P_1B_1^T + B_2P_2B_2^T = M_1 + M_2 \tag{5-12}$$

The least squares solution for the residual vectors V_1 and V_2 are

$$V_1 = -P_1^{-1}B_1^T M^{-1}W \tag{5-13}$$

$$V_2 = -P_2^{-1}B_2^T M^{-1}W \tag{5-14}$$

The covariance matrix of V_1 is

$$\begin{aligned}\Sigma_{V_1} &= P_1^{-1}B_1^T M^{-1}\begin{pmatrix}B_1 & B_2\end{pmatrix}\begin{pmatrix}\sigma_{01}^2 P_1^{-1} & 0\\ 0 & \sigma_{02}^2 P_2^{-1}\end{pmatrix}\begin{pmatrix}B_1^T\\ B_2^T\end{pmatrix}M^{-1}B_1P_1^{-1}\\ &= \sigma_{01}^2 P_1^{-1}B_1^T M^{-1}M_1M^{-1}B_1P_1^{-1} + \sigma_{02}^2 P_1^{-1}B_1^T M^{-1}M_2M^{-1}B_1P_1^{-1}\end{aligned} \quad (5\text{-}15)$$

Thus,

$$\begin{aligned}E(V_1^T P_1 V_1) &= tr\{P_1 \cdot E(V_1V_1^T)\}\\ &= tr(P_1\Sigma_{V_1})\\ &= tr(P_1P_1^{-1}B_1^T M^{-1}M_1M^{-1}B_1P_1^{-1})\sigma_{01}^2\\ &\quad + tr(P_1P_1^{-1}B_1^T M^{-1}M_2M^{-1}B_1P_1^{-1})\sigma_{02}^2\\ &= tr(M^{-1}M_1M^{-1}M_1)\sigma_{01}^2 + tr(M^{-1}M_1M^{-1}M_2)\sigma_{02}^2\end{aligned} \quad (5\text{-}16)$$

Similarly,

$$E(V_2^T P_2 V_2) = tr(M^{-1}M_1M^{-1}M_2)\sigma_{01}^2 + tr(M^{-1}M_2M^{-1}M_2)\sigma_{02}^2 \quad (5\text{-}17)$$

Rearrangement of equation (5-16) and (5-17) in matrix form gives,

$$\underset{2\times2}{S}\ \underset{2\times1}{\hat{\sigma}^2} = \underset{2\times1}{W} \quad (5\text{-}18)$$

where

$$S = \begin{pmatrix} tr(M^{-1}M_1)^2 & tr(M^{-1}M_1M^{-1}M_2)\\ tr(M^{-1}M_1M^{-1}M_2) & tr(M^{-1}M_2)^2\end{pmatrix} \quad (5\text{-}19)$$

$$\hat{\sigma}^2 = (\hat{\sigma}_{01}^2 \quad \hat{\sigma}_{02}^2)^T \quad (5\text{-}20)$$

$$W = (V_1^T P_1 V_1 \quad V_2^T P_2 V_2)^T \quad (5\text{-}21)$$

Extending this solution to *k* sets of independent heterogeneous datasets results in the following expressions:

$$\underset{k\times k}{S}\ \underset{k\times1}{\hat{\sigma}^2} = \underset{k\times1}{W} \quad (5\text{-}22)$$

where

$$S_{ij} = \begin{cases} tr(M^{-1}M_i)^2,\ i = j\\ tr(M^{-1}M_iM^{-1}M_j),\ i \neq j\end{cases} \quad (5\text{-}23)$$

$$\hat{\sigma}^2 = (\hat{\sigma}_{01}^2 \quad \hat{\sigma}_{02}^2 \quad \cdots \quad \hat{\sigma}_{0k}^2)^T \tag{5-24}$$

$$W = (V_1^T P_1 V_1 \quad V_2^T P_2 V_2 \quad \cdots \quad V_k^T P_k V_k)^T \tag{5-25}$$

The equation (5-22) could be simplified to

$$\hat{\sigma}_{0i}^2 = \frac{V_i^T P_i V_i}{tr(M^{-1} M_i)} \tag{5-26}$$

by assuming that all the variance components are equal using equation (5-9).

5.3 Result and analysis

In the light of earlier discussions, combination process is carried out as follows:

1. The station positions of different individual TRF within a co-located site are propagated to a common station using local tie measurements which are assumed to be errorless. No corrections are applied to the station velocities within the co-located site because of the proximities.

2. The input covariance matrices are rescaled using their given estimated variance components calculated from earlier TRF solutions for the initial weight assignment.

3. Since an a priori ITRF datum has to be defined in the ITRF system through the nominal values (as given by the a-priori known ITRF97 solution), the covariance matrix for ITRF97 solution is multiplied by factor of “9” (i.e. 3σ) so as not to make them too dominative in both the state vectors and the preferred observation functionals approach *initially*. The transformation parameters extracted from ITRF97, which is utilized initially in the new approach, are averaged because this

study regards TRFs within the same technique as one frame for the inter-technique combination as mentioned in section 4.2. Their corresponding variances for the transformation parameters are done in a similar fashion. Hence, only 14 parameters of the 3D Helmert transformation with rates between the frame of each technique and the combined frame (ITRF) are given in the result.

4. The above processed input is put into the linearized equations for estimation. The variance components are estimated so as to re-weight their respective data sets iteratively to obtain the final combination solution. Outlier detection process is also being carried out after a few numbers of iteration. Iteration is stopped until the variance component of the global combination and all other variance components converge to unity.

Therefore, the combination solution obtained from the preferred observation functionals formulations are subsequently compared to the minimum constraint solution obtained from state vector formulation since both solutions use the same data. A comparison between solution based on the new formulation and the official ITRF2000 solution is also made to further assess the new solution's impact on the station position and velocity estimates.

5.3.1 Analysis of the quality of the estimates for the preferred observation functionals approach

The resulting estimates based on State Vectors (SV) formulation and Preferred Observation Functionals (POF) approach are compared using the individual technique residuals, the correlation matrix for the station position and velocity estimates, the precision of the station position and velocity estimates for the POF approach against the SV formulation, and the estimated transformation parameters. Three different POF solutions, where their difference is solely based on the variants of the GPS formulations, are abbreviated as

1. POF with GPSBL, the POF solution with **GPS B**aseline **L**engths as observations;

2. POF with GPSBV, the POF solution with **GPS B**aseline **V**ectors as observations;

3. POF with GPSSV, the POF solution with **GPS S**tate **V**ectors as observations.

Analysis of the individual technique residuals

The residuals based on state vectors and POF formulations are given in Appendix A1. Figure A1.1 to Figure A1.6 displays the plots of residuals for each technique estimated using SV formulation. While the residuals for the positions from GIUB and SHA TRF are at or below centimeter levels, those from GSFC gives comparatively larger residuals than the other but they are not deleted due to its corresponding low precision. Similar situation is shown in the velocity counterparts (Figure A1.1 and A1.2). Except for CRL and JCET TRF, the residuals for the position and velocities of SLR TRFs are at centimeter and centimeter/year levels. The SV residuals for GPS TRFs, which are at or below centimeter and centimeter/year levels for both position and velocity residuals respectively, are smaller than the SV residuals of the VLBI and SLR. This indicates that the GPS data dominates the combined solution.

The residuals generated from the POF approach exhibit similar properties to those obtained from SV formulation, but the magnitude of residuals for the POF approach are much less than those obtained from the SV formulation (Figure A1.1 to Figure A1.24).

When the three formulations from the POF approach are inter-compared, all residuals for SLR and VLBI TRFs are comparable to each other. However, the residuals for GPS TRFs based on the POF with GPSBV formulation are the smallest among the POF solutions (Figure A1.7 to Figure A1.24).

Analysis of the correlation matrix for the estimates

Figure 5.1 to Figure 5.4 show the contour plot of the correlation matrices for the estimates (i.e. both the station position and velocity estimates, and the transformation parameters) for different combination solutions. The upper left represents sub-correlation matrix for the station position and velocity estimates, while the lower right gives the sub-correlation matrix for the transformation parameters. The other two sides give the correlation between the station and transformation parameter estimates. The uneven size of the correlation matrices among different results is due to different number of transformation parameters being estimated as explained in Section 3.3.2.

From the figures, both solutions generated from the SV formulation and the POF approaches present a low correlation between station and transformation parameter estimates. The correlations amongst the station position and velocity estimates and amongst the transformation parameters, in general, are low for all the solutions. If comparison among different solutions in terms of correlation is required, the solution from POF with GPSBL gives a better correlation matrix for the estimates since the high correlation value is much more concentrated on the diagonals of the correlation matrix, while other solutions spread more on the diagonals. This is owing to the use of only GPS baseline lengths as observations in the POF with GPSBL solution.

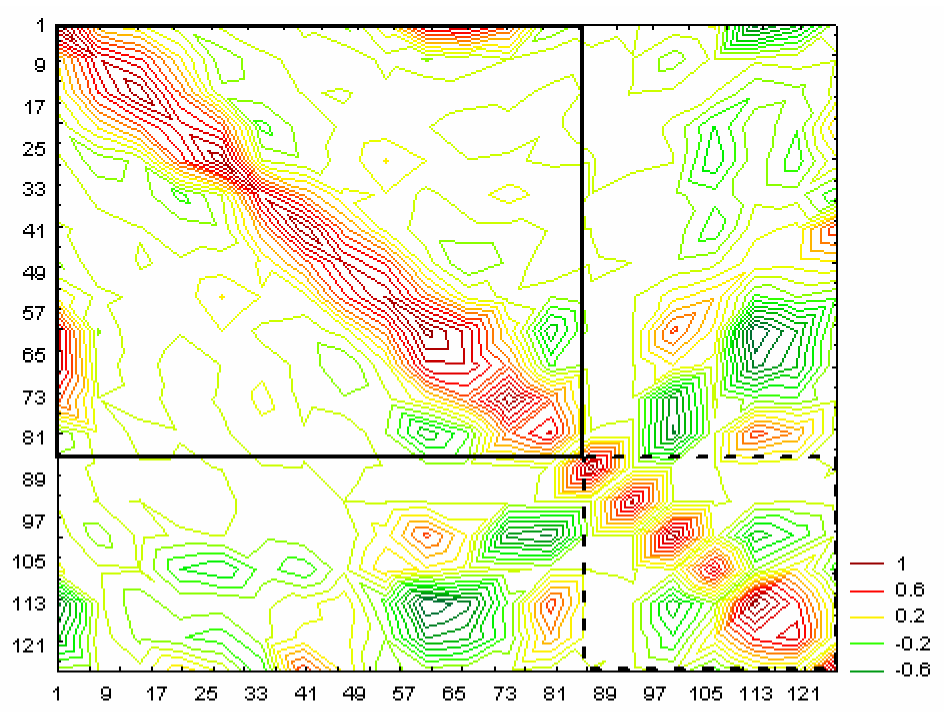

Figure 5.1 Plot of correlation matrix for the combination solution (SV formulation)

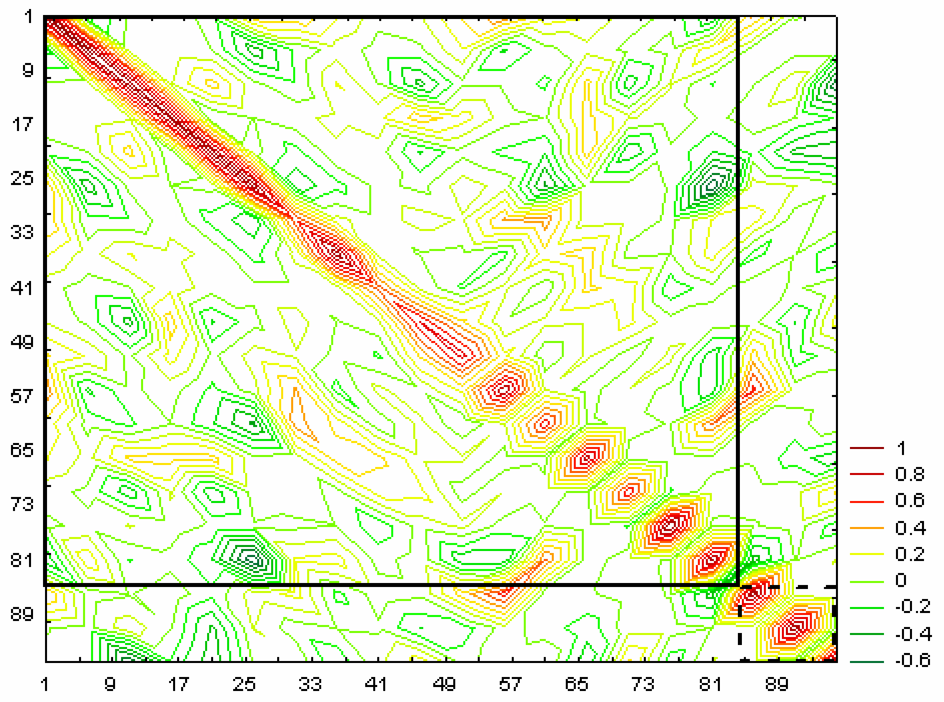

Figure 5.2 Plot of correlation matrix for the combination solution (POF with GPSBL formulation)

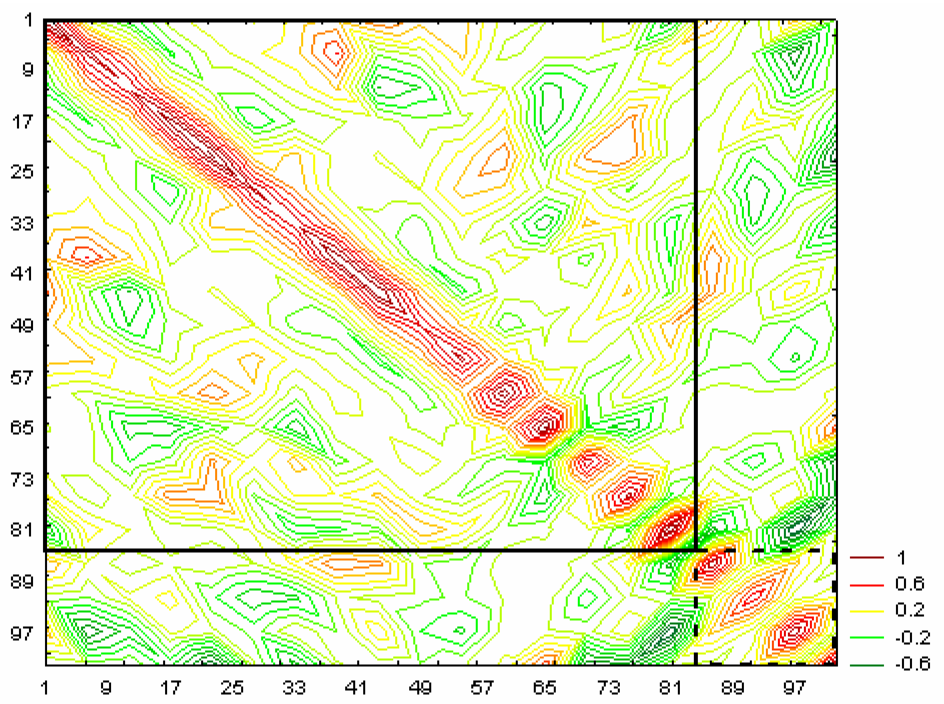

Figure 5.3 Plot of correlation matrix for the combination solution (POF with GPSBV formulation).

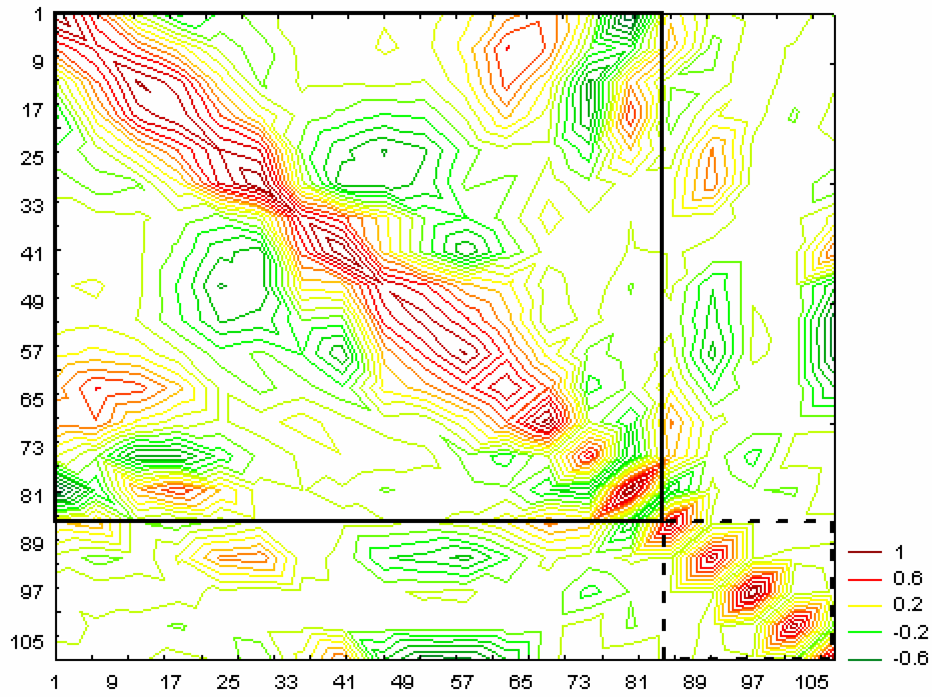

Figure 5.4 Plot of correlation matrix for the combination solution (POF with GPSSV formulation)

Analysis of the station state vector and transformation parameter estimates for the POF formulations against the SV formulation

Table 5.1 to Table 5.4 shows the precision of the station position and velocity estimates for both the SV formulation and the POF solution approach. The precision of the station positions for the SV formulation are at a few or even above centimeter level, while those estimated from the POF approach are at or below a centimeter level. Their velocity counterparts are at a few millimeter levels for both the SV formulation and the POF approach. The difference can be explained by the use of additional information used in the solution of the POF formulations.

The solution obtained from the POF with GPSBV comparatively achieves a better station position and velocity estimates than the other formulation in terms of precision overall as shown in Table 5.1 to Table 5.4. The actual position and velocity difference against ITRF2000 solution are compared in section 5.3.3.

Table 5.1 Precision of the station position and velocity estimates for the state vectors formulation (SV formulation)

DOMES	ID	σ_x (m)	σ_y (m)	σ_z (m)	$\sigma_{\dot{x}}$ (m/year)	$\sigma_{\dot{y}}$ (m/year)	$\sigma_{\dot{z}}$ (m/year)
10002S001	7835	0.018	0.028	0.018	0.001	0.001	0.001
10503S001	7805	0.016	0.015	0.017	0.001	0.001	0.001
12717M001	7543	0.020	0.032	0.017	0.002	0.001	0.002
12734S001	7939	0.019	0.028	0.017	0.001	0.001	0.001
14201S002	7834	0.017	0.022	0.017	0.001	0.001	0.001
40104M003	7410	0.077	0.028	0.049	0.002	0.002	0.001
40405M013	7288	0.090	0.059	0.055	0.002	0.002	0.002
40440M001	7091	0.077	0.027	0.050	0.002	0.002	0.001
40442M008	7850	0.095	0.049	0.060	0.002	0.002	0.002
40451M105	7105	0.083	0.030	0.053	0.002	0.002	0.001
40497M001	7110	0.092	0.060	0.057	0.002	0.002	0.002
40499M002	7295	0.093	0.038	0.061	0.002	0.002	0.002
41705M004	7404	0.085	0.080	0.067	0.002	0.002	0.002
50103S007	7843	0.010	0.121	0.066	0.002	0.003	0.003
RMS value		0.067	0.052	0.048	0.002	0.002	0.002

Table 5.2 Precision of the station position and velocity estimates for the preferred observation functionals approach (POF with GPSBL formulation)

DOMES	ID	σ_x (m)	σ_y (m)	σ_z (m)	$\sigma_{\dot{x}}$ (m/year)	$\sigma_{\dot{y}}$ (m/year)	$\sigma_{\dot{z}}$ (m/year)
10002S001	7835	0.005	0.005	0.005	0.001	0.001	0.001
10503S001	7805	0.007	0.006	0.008	0.001	0.001	0.001
12717M001	7543	0.010	0.006	0.009	0.002	0.001	0.002
12734S001	7939	0.006	0.005	0.005	0.001	0.001	0.001
14201S002	7834	0.005	0.005	0.005	0.001	0.001	0.001
40104M003	7410	0.007	0.006	0.007	0.001	0.001	0.001
40405M013	7288	0.007	0.009	0.011	0.001	0.001	0.001
40440M001	7091	0.007	0.006	0.009	0.001	0.001	0.001
40442M008	7850	0.005	0.005	0.005	0.001	0.001	0.001
40451M105	7105	0.005	0.005	0.005	0.001	0.001	0.001
40497M001	7110	0.005	0.005	0.005	0.001	0.001	0.001
40499M002	7295	0.007	0.008	0.007	0.001	0.002	0.001
41705M004	7404	0.035	0.033	0.025	0.002	0.002	0.002
50103S007	7843	0.005	0.005	0.005	0.001	0.001	0.001
RMS value		0.011	0.011	0.009	0.001	0.001	0.001

Table 5.3 Precision of the station position and velocity estimates for the preferred observation functionals approach (POF with GPSBV formulation)

DOMES	ID	σ_x (m)	σ_y (m)	σ_z (m)	$\sigma_{\dot{x}}$ (m/year)	$\sigma_{\dot{y}}$ (m/year)	$\sigma_{\dot{z}}$ (m/year)
10002S001	7835	0.005	0.005	0.005	0.001	0.001	0.001
10503S001	7805	0.006	0.005	0.005	0.001	0.001	0.001
12717M001	7543	0.006	0.005	0.005	0.002	0.001	0.001
12734S001	7939	0.006	0.005	0.005	0.001	0.001	0.001
14201S002	7834	0.005	0.005	0.005	0.001	0.001	0.001
40104M003	7410	0.005	0.005	0.005	0.001	0.001	0.001
40405M013	7288	0.005	0.006	0.005	0.001	0.001	0.001
40440M001	7091	0.005	0.005	0.005	0.001	0.001	0.001
40442M008	7850	0.006	0.005	0.005	0.001	0.001	0.001
40451M105	7105	0.005	0.005	0.005	0.001	0.001	0.001
40497M001	7110	0.005	0.006	0.005	0.001	0.001	0.001
40499M002	7295	0.006	0.007	0.006	0.001	0.002	0.001
41705M004	7404	0.007	0.006	0.006	0.002	0.002	0.001
50103S007	7843	0.006	0.005	0.006	0.001	0.001	0.001
RMS value		0.006	0.005	0.005	0.001	0.001	0.001

Table 5.4 Precision of the station position and velocity estimates for the preferred observation functionals approach (POF with GPSSV formulation)

DOMES	ID	σ_x (m)	σ_y (m)	σ_z (m)	$\sigma_{\dot{x}}$ (m/year)	$\sigma_{\dot{y}}$ (m/year)	$\sigma_{\dot{z}}$ (m/year)
10002S001	7835	0.006	0.006	0.006	0.001	0.001	0.001
10503S001	7805	0.007	0.006	0.006	0.002	0.001	0.001
12717M001	7543	0.007	0.006	0.006	0.002	0.002	0.002
12734S001	7939	0.007	0.006	0.006	0.001	0.001	0.001
14201S002	7834	0.007	0.006	0.006	0.001	0.001	0.001
40104M003	7410	0.006	0.006	0.006	0.001	0.001	0.001
40405M013	7288	0.006	0.007	0.006	0.002	0.002	0.002
40440M001	7091	0.006	0.006	0.006	0.001	0.001	0.001
40442M008	7850	0.007	0.006	0.006	0.002	0.001	0.001
40451M105	7105	0.007	0.006	0.006	0.002	0.001	0.001
40497M001	7110	0.006	0.007	0.006	0.002	0.001	0.001
40499M002	7295	0.007	0.008	0.007	0.002	0.002	0.002
41705M004	7404	0.008	0.007	0.007	0.002	0.002	0.002
50103S007	7843	0.006	0.006	0.007	0.002	0.002	0.002
RMS value		0.007	0.006	0.006	0.002	0.001	0.001

Table 5.5 to 5.8 shows the results of 3D Helmert transformation parameters with rates for the combination solution obtained from the SV formulation and the POF approach respectively. The magnitude of the translation parameters between VLBI frame and ITRF obtained from the SV formulation are comparatively large. The precision of transformation parameters between SLR frame or GPS frame and

ITRF are lower than those between VLBI frame and ITRF (Table 5.5). This result implies that ITRF solution is not well aligned with the SV VLBI frame, which is not desirable.

Table 5.5 Results of 3D Helmert transformation with rates for the SV formulation

Parameter	VLBI	SLR	GPS
T_x [a]	-8.68 ± 753.96	-2.37 ± 2.49	-1.96 ± 2.49
T_y [a]	-89.46 ± 750.04	0.27 ± 5.68	1.43 ± 5.68
T_z [a]	43.63 ± 746.64	3.25 ± 3.54	1.35 ± 3.54
S [b]	-66.10 ± 4.82	-3.14 ± 4.81	-0.72 ± 4.81
R_x [c]	79.51 ± 27.91	-0.28 ± 5.41	-0.13 ± 5.38
R_y [c]	-4.11 ± 18.54	2.41 ± 2.37	1.65 ± 2.30
R_z [c]	26.53 ± 19.87	-3.46 ± 8.09	-4.25 ± 8.05
$\dot{T}_x$ [a]	-1.12 ± 11.04	-0.07 ± 0.11	-0.20 ± 0.11
$\dot{T}_y$ [a]	-11.84 ± 11.05	0.09 ± 0.15	-0.05 ± 0.14
$\dot{T}_z$ [a]	6.19 ± 10.85	0.73 ± 0.17	0.47 ± 0.16
$\dot{S}$ [b]	-9.20 ± 0.24	-0.19 ± 0.24	-0.20 ± 0.22
$\dot{R}_x$ [c]	11.00 ± 4.49	0.17 ± 0.16	0.10 ± 0.13
$\dot{R}_y$ [c]	-0.16 ± 3.05	0.33 ± 0.19	0.52 ± 0.16
$\dot{R}_z$ [c]	4.03 ± 3.37	0.10 ± 0.30	0.34 ± 0.20

[a] Units are cm for the translations and cm/yr for their rates
[b] Units are ppb (10^{-9}) for the scale and ppb/yr for its rate
[c] Units are cm for the rotations and for cm/yr for their rates (i.e. the rotation in radians is multiplied by the radius of the Earth)

Due to the nature of the POF formulations, no values are given for particular transformation parameters as shown in Table 5.6 to Table 5.8. The magnitude of the transformation parameters generated from the POF approach is generally smaller than those obtained from the SV formulation, except for the translation rate parameters in Y and Z component obtained from POF with GPSSV formulation. This is because the origin and their rates of the ITRF are chiefly defined by SLR technique but not both SLR and GPS technique; hence those two parameters are adjusted accordingly based on the origin of the ITRF as defined by

SLR technique. Their precision counterparts for those three POF formulations are higher than those obtained from the SV formulation.

Table 5.6 Results of 3D Helmert transformation with rates for POF with GPSBL formulation

Parameter	VLBI			SLR			GPS		
T_x [a]	–	±	–	–	±	–	–	±	–
T_y [a]	–	±	–	–	±	–	–	±	–
T_z [a]	–	±	–	–	±	–	–	±	–
S [b]	0.94	±	7.64	-0.63	±	0.71	1.52	±	0.80
R_x [c]	–	±	–	-0.12	±	0.69	–	±	–
R_y [c]	–	±	–	-0.34	±	0.71	–	±	–
R_z [c]	–	±	–	0.59	±	0.97	–	±	–
$\dot{T}_x$ [a]	–	±	–	–	±	–	–	±	–
$\dot{T}_y$ [a]	–	±	–	–	±	–	–	±	–
$\dot{T}_z$ [a]	–	±	–	–	±	–	–	±	–
$\dot{S}$ [b]	-0.23	±	0.96	0.04	±	0.15	0.34	±	0.21
$\dot{R}_x$ [c]	–	±	–	0.04	±	0.13	–	±	–
$\dot{R}_y$ [c]	–	±	–	-0.26	±	0.11	–	±	–
$\dot{R}_z$ [c]	–	±	–	-0.24	±	0.23	–	±	–

[a] Units are cm for the translations and cm/yr for their rates
[b] Units are ppb (10^{-9}) for the scale and ppb/yr for its rate
[c] Units are cm for the rotations and for cm/yr for their rates (i.e. the rotation in radians is multiplied by the radius of the Earth)

Table 5.7 Results of 3D Helmert transformation with rates for POF with GPSBV formulation

Parameter	VLBI			SLR			GPS		
T_x [a]	–	±	–	–	±	–	–	±	–
T_y [a]	–	±	–	–	±	–	–	±	–
T_z [a]	–	±	–	–	±	–	–	±	–
S [b]	1.42	±	8.12	-1.18	±	0.76	1.17	±	0.76
R_x [c]	–	±	–	-0.46	±	0.76	-0.24	±	0.56
R_y [c]	–	±	–	-0.48	±	0.78	-1.29	±	0.56
R_z [c]	–	±	–	0.09	±	1.03	-0.76	±	0.61
$\dot{T}_x$ [a]	–	±	–	–	±	–	–	±	–
$\dot{T}_y$ [a]	–	±	–	–	±	–	–	±	–
$\dot{T}_z$ [a]	–	±	–	–	±	–	–	±	–
$\dot{S}$ [b]	-0.27	±	1.03	0.03	±	0.17	0.06	±	0.17
$\dot{R}_x$ [c]	–	±	–	-0.01	±	0.15	-0.05	±	0.12
$\dot{R}_y$ [c]	–	±	–	-0.20	±	0.16	0.03	±	0.13
$\dot{R}_z$ [c]	–	±	–	-0.17	±	0.27	0.09	±	0.14

[a] Units are cm for the translations and cm/yr for their rates
[b] Units are ppb (10^{-9}) for the scale and ppb/yr for its rate
[c] Units are cm for the rotations and for cm/yr for their rates (i.e. the rotation in radians is multiplied by the radius of the Earth)

Table 5.8 Results of 3D Helmert transformation with rates for POF with GPSSV formulation

Parameter	VLBI			SLR			GPS		
T_x [a]	–	±	–	–	±	–	0.45	±	0.15
T_y [a]	–	±	–	–	±	–	1.22	±	0.15
T_z [a]	–	±	–	–	±	–	-1.82	±	0.15
S [b]	1.11	±	8.13	-1.25	±	0.90	1.10	±	0.90
R_x [c]	–	±	–	-0.50	±	0.82	-0.29	±	0.66
R_y [c]	–	±	–	-0.55	±	0.84	-1.27	±	0.67
R_z [c]	–	±	–	0.06	±	1.10	-0.77	±	0.73
$\dot{T}_x$ [a]	–	±	–	–	±	–	-1.38	±	0.06
$\dot{T}_y$ [a]	–	±	–	–	±	–	-19.63	±	0.06
$\dot{T}_z$ [a]	–	±	–	–	±	–	22.83	±	0.05
$\dot{S}$ [b]	-0.25	±	1.03	0.02	±	0.20	0.10	±	0.20
$\dot{R}_x$ [c]	–	±	–	-0.04	±	0.16	-0.07	±	0.14
$\dot{R}_y$ [c]	–	±	–	-0.23	±	0.17	0.01	±	0.15
$\dot{R}_z$ [c]	–	±	–	-0.23	±	0.28	0.08	±	0.17

[a] Units are cm for the translations and cm/yr for their rates
[b] Units are ppb (10^{-9}) for the scale and ppb/yr for its rate
[c] Units are cm for the rotations and for cm/yr for their rates (i.e. the rotation in radians is multiplied by the radius of the Earth)

5.3.2 Contribution for each technique to the final combination solution

Generalized variance, which is the determinant of the covariance matrix of the estimates, can be used to describe the overall quality of the estimates [Johnson and Wichern, 1992]. To assess the contribution of a particular kind of measurement technique on the solution, the covariance ratio, which is utilized in the identification of influential data [Belsley, 1980], is modified in such a way that only the sum of the diagonal variances is used instead of generalized variance. Hence, this modification, which replaces the multidimensional ellipsoidal volume with a spherical one, highlights more on the variances of the solution.

Let the Overall Variance Ratio (OVR) be defined as,

$$OVR = \frac{tr(\Sigma_x)}{tr(\Sigma_0)} \tag{5-27}$$

where Σ_x is the covariance matrix of the estimates which is obtained from a solution that does not include observations from a particular measurement technique and Σ_0 is the reference covariance matrix of the estimates generated by the whole set of observations. OVR value is interpreted as follows:

1. OVR > 1 indicates a positive contribution of the measurement technique to the final combination solution (i.e. it enhances the quality of the final solution if it is included).
2. OVR < 1 indicates a negative contribution of the measurement technique to the final combination solution (i.e. it worsens the quality of the final solution if it is included).
3. OVR = 1 indicates the technique has no impact on the final combination solution.

Since different types of estimates are included within the covariance matrix, it is subdivided into the covariance matrix for the station positions Σ_P, velocities Σ_V and transformation parameters Σ_T.

The relative contribution of each technique estimated using both the SV and POF formulations are displayed in Table 5.9. It shows that the exclusion of VLBI technique poses an insignificant influence on the overall variances for different kind of estimates. On the other hand, the exclusion of GPS technique on the combined solution represents a considerable increase in the overall variances for station position and velocity estimates.

However, the exclusion of any technique has negligible effect on the overall precision for the transformation parameters based on the POF with GPSBL and POF with GPSBV, but not in the case of the solution with SV and POF with GPSSV. The negative influence of the exclusion of GPS techniques on the overall precision for the station position and velocity estimates obtained from the SV is because the variance component estimation technique makes the GPS observations more dominative through iterative re-weighting which reduces the influence of the observations as provided by SLR and VLBI and hence; lowering the overall precision of the transformation parameters between SLR or VLBI and ITRF. The exclusion of SLR technique also poses a great impact on the overall precision of the station position and velocity estimates obtained from the POF with GPSBL, because SLR is chiefly responsible for defining the geocenter as mentioned in Section 3.3.2.

Table 5.9 Relative contribution of each technique to the combination solution with respect to its corresponding formulation

Approach	Technique excluded	OVR for the positions	OVR for the velocities	OVR for the transformation parameters
SV	VLBI	1.000	1.073	1.000
	SLR	1.000	1.054	1.053
	GPS	1.332	20.379	0.171
POF with GPSBL	VLBI	1.048	0.920	0.959
	SLR	10.911	17.816	0.835
	GPS	2.180	2.366	0.947
POF with GPSBV	VLBI	1.032	1.031	1.024
	SLR	1.927	1.647	1.024
	GPS	7.852	2.136	0.947
POF with GPSSV	VLBI	1.022	1.020	1.003
	SLR	1.189	1.049	15.219
	GPS	5.628	1.540	0.947

5.3.3 Comparison of state vectors and preferred observation functional formulations with the ITRF2000 official solution

It is not appropriate to compare the solution generated from the new approach with the ITRF2000 solution realization, since not all data is utilized to estimate the final combination solution. Nevertheless, it gives a sense of idea on how much the difference between them. The assessment is made through the analysis of the overall quality of the station position and velocity estimates, and the difference among the station position and velocity estimates.

Analysis of the quality of the station position and velocity estimates for the SV and the POF formulations as compared to ITRF2000 official solution

Table 5.10 shows the precision of the station position and velocity estimates for the ITRF2000 solution realization. It displays the precision of station positions and velocities are at millimeter and below millimeter/year level respectively. When it is compared to the solution obtained from the SV and the POF formulations as displayed from Table 5.1 to Table 5.4, it is apparent that the ITRF2000 solution displays a better precision for the station position and velocity estimates in general.

Table 5.10 Precision of the station position and velocity estimates for the ITRF2000 official solution

DOMES	ID	σ_x (m)	σ_y (m)	σ_z (m)	$\sigma_{\dot{x}}$ (m/year)	$\sigma_{\dot{y}}$ (m/year)	$\sigma_{\dot{z}}$ (m/year)
10002S001	7835	0.002	0.001	0.002	0.000	0.000	0.000
10503S001	7805	0.005	0.005	0.005	0.000	0.000	0.001
12717M001	7543	0.002	0.002	0.002	0.000	0.000	0.000
12734S001	7939	0.002	0.002	0.002	0.000	0.000	0.000
14201S002	7834	0.002	0.001	0.002	0.000	0.000	0.000
40104M003	7410	0.002	0.003	0.003	0.000	0.000	0.000
40405M013	7288	0.003	0.005	0.004	0.000	0.000	0.000
40440M001	7091	0.001	0.003	0.003	0.000	0.000	0.000
40442M008	7850	0.002	0.003	0.002	0.000	0.000	0.000
40451M105	7105	0.001	0.002	0.002	0.000	0.000	0.000
40497M001	7110	0.001	0.002	0.002	0.000	0.000	0.000
40499M002	7295	0.002	0.004	0.003	0.000	0.001	0.000
41705M004	7404	0.026	0.028	0.022	0.000	0.001	0.001
50103S007	7843	0.002	0.002	0.002	0.000	0.000	0.001
RMS value		0.007	0.008	0.006	0.000	0.000	0.000

It is difficult to judge the overall precision of the station positions based on the tables because of the relatively low precision of the station with DOMES "41705M004" listed in ITRF2000 official solution when compared to those solution obtained from POF with GPSBV and POF with GPSSV formulations (Table 5.3 and Table 5.4), even though RMS value shows a certain indication. Therefore, OVR, which is introduced in the previous section, is utilized in order to reveal the ratio of overall precision of the station position and velocity estimates obtained through the POF approach and the SV baseline solution to those realized by ITRF2000. But now, the numerator of OVR is the sum of diagonal variance of the covariance matrix estimated through the SV or POF formulations, whereas the denominator is the sum of diagonal variance of the covariance matrix for the ITRF2000 solution realization as a reference. The value of OVR large than one indicates that the overall precision of the station position and velocity estimates obtained based on the new approach is lower than those realized by ITRF2000.

Table 5.11 lists the overall variance ratio of the SV and POF formulations to the reference solution (ITRF2000). It shows that the overall variance of the station position and velocity estimates based on the SV solution is larger than those solution obtained from the POF formulations and ITRF2000 official solution, because it uses the minimum number of constraints to get the solution.

In addition, the overall variance for the velocity estimates of both the POF and the SV formulations are larger than those realized by ITRF2000 because duplicate information of the TRF observations has been eliminated, and hence, lowering the precision of the velocity estimates. Nevertheless, the horizontal velocity estimates for the POF approach are in good agreement in terms of both magnitude and direction as displayed in Figure 5.11 and Figure 5.12.

The overall variances ratio for the position counterparts of POF with GPSBV and POF with GPSSV indicates that they give a better position precision than the ITRF2000 solution because of both the reduction of the useless (or even deleterious) information through the POF with GPSBV and POF with GPSSV formulations and the utilization of generalized condition equations, and hence, increasing the precision of the station with DOMES “41705M004”. However, it is not the case in POF with GPSBL because of the truly independent observation information used in its GPS formulation.

Table 5.11 Overall variance ratio of the SV formulation and the POF approach with respect to ITRF2000 official solution

Approach	OVR for the positions	OVR for the velocities
SV	59.173	28.104
POF with GPSBL	2.046	13.190
POF with GPSBV	0.568	14.609
POF with GPSSV	0.793	20.258

Analysis of the actual differences between station position and velocity estimates against ITRF2000 official solution

Station position and velocity difference in XYZ components from the SV and POF formulation solutions can also be compared to ITRF2000 official solution in addition to the comparison of the precision of the station position and velocity estimates. The station position and velocity estimates along with their precisions are shown in Appendix A2.

Table 5.12 to Table 5.15 indicates the actual position difference in XYZ components obtained from the SV and the POF formulation solutions against the ITRF2000 solution are in agreement within a few centimeters. In general, the station position differences between the POF and ITRF2000 solutions are relatively smaller than the station position differences between the SV formulation and ITRF2000 solution. In addition, the station position differences between POF with GPSBL and ITRF2000 solution is larger than those solutions from POF with GPSBV and POF with GPSSV for the same approach, possibly because only GPS baseline lengths, which are independent of the orientation information, utilized in POF with GPSBL formulation instead of the repetitive usage of the input information in both the POF with GPSBV and POF with GPSSV formulations.

Table 5.12 Station position difference in XYZ components at epoch 1997.0 between the SV formulation and ITRF2000 solution

DOMES	Site Name	ID	ΔX(m)	ΔY(m)	ΔZ(m)
10002S001	GRASSE	7835	0.023	0.023	-0.003
10503S001	METSAHOVI	7805	0.012	0.008	-0.011
12717M001	NOTO	7543	0.012	0.027	-0.009
12734S001	MATERA	7939	0.012	0.026	-0.013
14201S002	WETTZELL	7834	0.010	0.021	-0.014
40104M003	ALGONQUIN	7410	0.042	0.003	-0.027
40405M013	GOLDSTONE	7288	0.028	-0.025	-0.053
40440M001	WESTFORD	7091	0.035	0.001	-0.031
40442M008	FORT DAVIS	7850	0.047	-0.025	-0.028
40451M105	WASHINGTON	7105	0.053	-0.021	-0.018
40497M001	MONUMENT PARK	7110	0.041	-0.038	-0.028
40499M002	RICHMOND	7295	0.056	-0.035	-0.002
41705M004	SANTIAGO	7404	0.061	0.022	-0.022
50103S007	CANBERRA	7843	0.015	-0.034	-0.041
RMS value			0.036	0.025	0.026

Table 5.13 Station position difference in XYZ components at epoch 1997.0 between preferred observation functionals approach (POF with GPSBL) and ITRF2000 solution

DOMES	Site Name	ID	ΔX(m)	ΔY(m)	ΔZ(m)
10002S001	GRASSE	7835	0.013	-0.001	-0.002
10503S001	METSAHOVI	7805	0.016	-0.016	-0.001
12717M001	NOTO	7543	0.008	0.001	-0.004
12734S001	MATERA	7939	0.005	0.001	-0.007
14201S002	WETTZELL	7834	0.003	-0.002	-0.016
40104M003	ALGONQUIN	7410	0.015	0.006	-0.012
40405M013	GOLDSTONE	7288	0.013	-0.026	0.007
40440M001	WESTFORD	7091	0.013	-0.003	0.014
40442M008	FORT DAVIS	7850	0.008	-0.006	-0.004
40451M105	WASHINGTON	7105	0.010	-0.010	0.005
40497M001	MONUMENT PARK	7110	0.004	-0.010	0.008
40499M002	RICHMOND	7295	0.010	-0.031	0.004
41705M004	SANTIAGO	7404	-0.025	0.084	-0.027
50103S007	CANBERRA	7843	0.012	-0.012	0.022
RMS value			0.012	0.026	0.012

Table 5.14 Station position difference in XYZ components at epoch 1997.0 between preferred observation functionals approach (POF with GPSBV) and ITRF2000 solution

DOMES	Site Name	ID	ΔX(m)	ΔY(m)	ΔZ(m)
10002S001	GRASSE	7835	0.013	-0.002	-0.001
10503S001	METSAHOVI	7805	0.016	-0.009	-0.001
12717M001	NOTO	7543	0.003	0.000	-0.007
12734S001	MATERA	7939	0.005	0.000	-0.010
14201S002	WETTZELL	7834	0.007	-0.002	-0.009
40104M003	ALGONQUIN	7410	0.014	0.008	-0.010
40405M013	GOLDSTONE	7288	-0.002	-0.003	-0.019
40440M001	WESTFORD	7091	0.002	0.004	-0.017
40442M008	FORT DAVIS	7850	0.012	-0.006	0.003
40451M105	WASHINGTON	7105	0.019	-0.015	0.000
40497M001	MONUMENT PARK	7110	0.011	-0.013	0.006
40499M002	RICHMOND	7295	0.010	-0.031	0.019
41705M004	SANTIAGO	7404	-0.010	0.025	0.008
50103S007	CANBERRA	7843	-0.002	-0.011	0.018
RMS value			0.010	0.013	0.011

Table 5.15 Station position difference in XYZ components at epoch 1997.0 between preferred observation functionals approach (POF with GPSSV) and ITRF2000 solution

DOMES	Site Name	ID	ΔX(m)	ΔY(m)	ΔZ(m)
10002S001	GRASSE	7835	0.014	-0.001	0.000
10503S001	METSAHOVI	7805	0.016	-0.009	-0.002
12717M001	NOTO	7543	0.003	0.000	-0.007
12734S001	MATERA	7939	0.005	0.000	-0.010
14201S002	WETTZELL	7834	0.006	-0.002	-0.010
40104M003	ALGONQUIN	7410	0.014	0.008	-0.011
40405M013	GOLDSTONE	7288	-0.003	-0.006	-0.017
40440M001	WESTFORD	7091	0.002	0.004	-0.018
40442M008	FORT DAVIS	7850	0.012	-0.007	0.003
40451M105	WASHINGTON	7105	0.019	-0.016	0.000
40497M001	MONUMENT PARK	7110	0.011	-0.014	0.006
40499M002	RICHMOND	7295	0.010	-0.030	0.018
41705M004	SANTIAGO	7404	-0.011	0.026	0.008
50103S007	CANBERRA	7843	-0.003	-0.010	0.018
RMS value			0.010	0.013	0.011

When the horizontal velocities are being compared, those generated from the POF approach displays a good agreement both in direction of velocities and their corresponding magnitudes for all stations. The velocity estimates in Europe calculated from the SV formulation solution are quite consistent with the ITRF2000 solution, except for those stations in United States (Figure 5.5 and

Figure 5.6). Those POF and SV formulation solution results imply an extra NNR-NUVEL-1A condition on the alignment of the orientation rates does not pose a significant change in both the horizontal velocity direction and magnitude for each station.

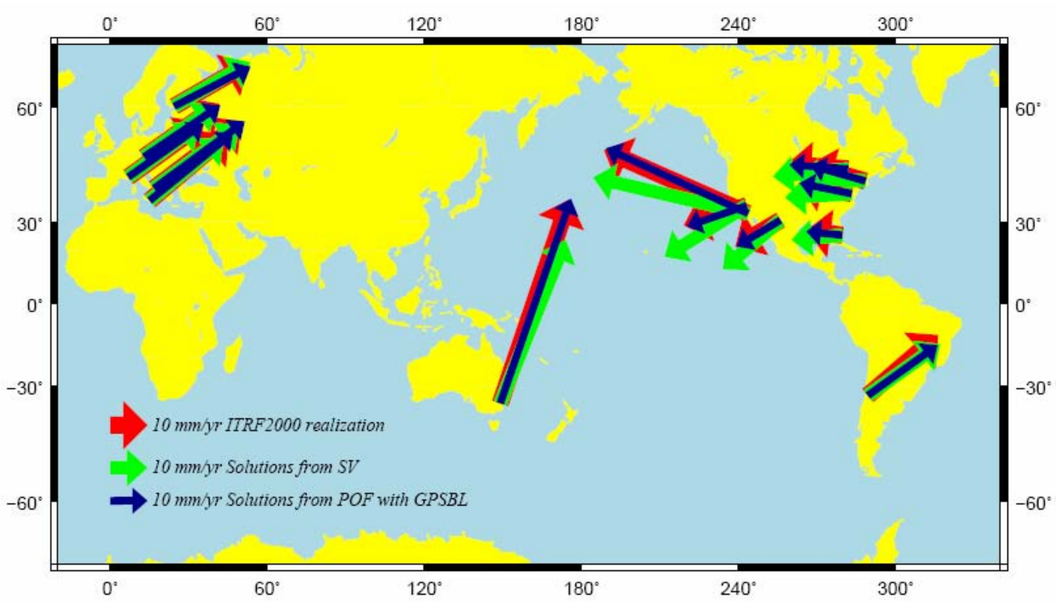

Figure 5.5 Horizontal station velocities for ITRF2000 solution, solutions from State vectors (SV) formulation and from Preferred observation functionals approach (POF with GPSBL)

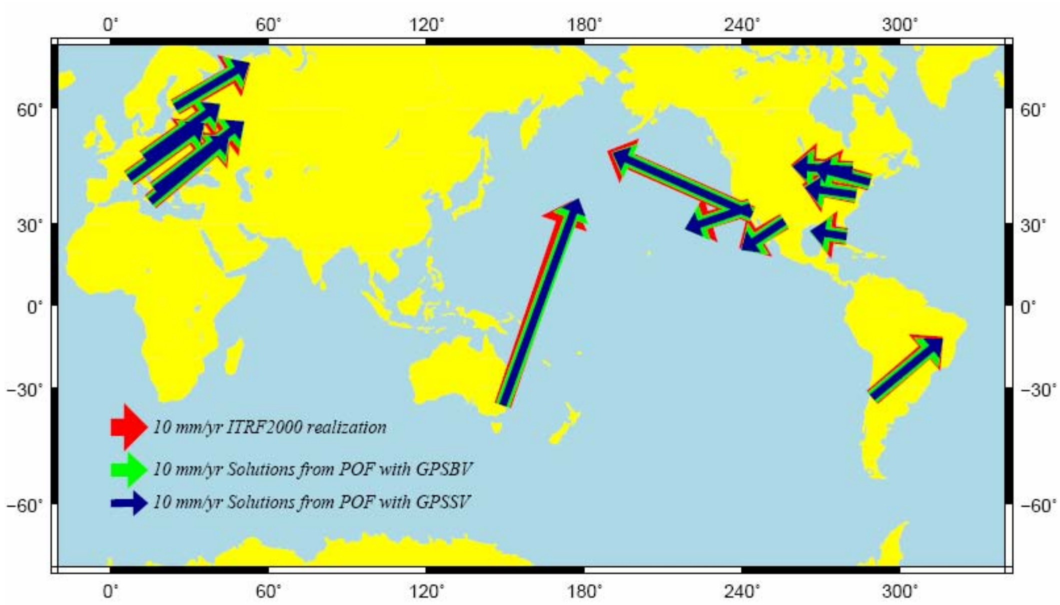

Figure 5.6 Horizontal station velocities for ITRF2000 solution, solutions from Preferred observation functionals approach (POF with GPSBV and POF with GPSSV)

5.4 Summary

In this chapter, studentized residuals were used to detect outliers. Overall, no outlier was found at 99% confidence level. Variance components estimation of the Helmert type was described and used during the combination. A simplified derivation of the variance components estimation together with its approximate formula for the generalized condition was formulated and implemented.

The steps for achieving the combination solutions in this study have also been introduced in section 5.3 so that the whole process involving from the input data preparation to the iterative data sets re-weighting and outlier detection are clearly presented.

Overall, the new formulations gave a better precision for the station position and velocity estimates than those obtained from the SV formulation. It was found that the exclusion of VLBI technique posed a negligible influence on the overall variances for different kind of estimates as displayed in section 5.3.2. When solutions obtained from the SV and the POF formulations were compared to ITRF2000 solution, the overall variance for the velocity estimates of both the POF and SV formulations were comparatively larger than those realized by ITRF2000 for the reason that the duplicate information has not been entered into the combination process.

The overall variance ratio for the position counterparts for both the POF with GPSBV and POF with GPSSV formulations indicated that it gave a better position precision than the ITRF2000 solution because of both the reduction of the useless (or even deleterious) information through the POF with GPSBV and POF with GPSSV formulations and the utilization of generalized condition equations for the adjustment process, and hence, increasing the overall precision.

The difference of the station positions and velocities of the POF approach were also compared to the ITRF2000 solution, it was found that the position differences in magnitude for each coordinate component were at centimeter level, whereas the direction and magnitude of horizontal velocity vectors were in good agreement with the ITRF2000 solution results. This implied the redundant orientation rate condition, which has been applied to the combination for the ITRF2000 solution, did not pose a significant influence on both the horizontal velocity direction and magnitude for each station.

6. CONCLUSION AND FUTURE WORK

6.1 Summary and conclusion

The aim of this thesis was to investigate alternative approach to the estimation of the combined reference frame (ITRF). Attention has been paid on the datum definition of the combined reference frame and the appropriate weighting method for the alternative approach.

The concept of the reference systems, frames, ITRF and its transformation relationship were discussed. In order to gain a better understanding of the whole combination solution process in practice, different types of input data from various space geodesy techniques and implementation strategies were explained in steps. The research topics in the ITRF solution realization were also detailed.

The current least squares adjustment model and related mathematical relationships used in practice and in this study were illustrated. Three new mathematical models were formulated using the concept of preferred observation functionals (POF). The first formulation (POF with GPSBL) emphasized the definition of geocenter and its rates between the combined reference frame (ITRF) and the SLR-based state vector raw solutions; the definition of orientation between the ITRF and the VLBI-based baseline vector solutions; and the conversion of the GPS-based state vector to the baseline length formulation. The second formulation differed from the first through the utilization of GPS baseline vectors and their rate of changes (instead of GPS baseline lengths only), while the third formulation treated the GPS state vectors as observations. Their corresponding statistical models to be used in the generalized condition equations were also formulated. The state vectors (SV) formulation was also presented to obtain the minimum constraint solution for the comparison against the POF approach.

The plot of correlation matrices and the basic statistical measures for the input TRF solutions showed that the constraints are non-uniformly applied to different stations for different TRFs computed by different analysis centers. In some cases, it was found that same station position estimates from different analysis centers for the same technique could be different from each other up to a meter, particularly for VLBI TRF solution computed by GSFC.

The input data was preprocessed to combine various analysis TRF data into one unique set to be used in the combination solutions. The data is also scrutinized for outliers and none was found at 99% confidence level.

A Helmert-type variance components estimation technique was used for re-weighting different data sets during the iterative combination process. While the variance components estimation was well-known in solving observation equations (parametric adjustment), their use for the generalized condition adjustment was not common. The simplified derivation of the variance components estimation together with its approximate formula for the generalized condition was formulated. The statistical formulation of the variance components estimation for the generalized condition adjustment is similar to that of parametric adjustment. This thesis utilized this technique in the new approach.

The precision of the POF formulation combination solution estimates (station state vectors and transformation parameters) were shown to be much better than the combination solution based on SV formulation. It was also found that the contribution for the VLBI TRFs were not significant in the combination solutions obtained from both the SV and POF formulations.

The station position and velocity estimates obtained from the SV and POF formulations were compared with the ITRF2000 solution values. It was found that the overall precision for the station position and velocity estimates based on the SV was comparatively lower, because only minimum constraints were applied to get the solution. The overall precision for the station position and velocity estimates based on POF formulations were, in general, lower than those given by ITRF2000 solution as well for the reason that the replicated information has not been inputted into the combination process. However, both the POF with GPSBV and POF with GPSSV formulations gave a better position precision than the ITRF2000 solution as shown in both the RMS values for each coordinate component and the overall variance thanks to both the reduction of the deleterious information through the POF with GPSBV and POF with GPSSV formulations and the utilization of generalized condition equations for the adjustment process.

The actual difference between solutions obtained from the POF approach and ITRF2000 solution was also compared. It was found that the actual position differences between them in magnitude for each coordinate component are at a maximum of a few centimeters. The horizontal station velocities also showed a good agreement with those in ITRF2000 both in terms of direction and magnitude.

This illustrates the application of the redundant orientation constraints, which has been applied to the combination for the ITRF2000 solution, gives the negligible effect on both the horizontal velocity direction and magnitude for each station. Those results also present the POF approach based on synergetic fusion is an attractive method which deserves further investigation in the solution realization of the ITRF.

6.2 Recommendation of future work

This study is limited to the investigation for those co-located sites with SLR, VLBI and GPS techniques. More observations for stations estimated from different techniques in different co-located site could be included for the inter technique combination process. Since intra technique combination has currently been made by the International DORIS Service (IDS), International GNSS Service (IGS), the International Laser Ranging Service (ILRS) and the International VLBI Service (IVS), the station position and velocity estimates could be served as an input in a direct manner to estimate the combination solutions using the new approach demonstrated in this thesis for further evaluation.

LIST OF REFERENCES

Altamimi, Z., Boucher, C. and Duhem, L. (1993), The worldwide centimetric terrestrial reference frame and its associated velocity field, Advance in Space Research, Vol.13, No.11, pp.151-160.

Altamimi, Z. (2001a), The accuracy of ITRF2000, European Geophysical Society XXVI General Assembly, G6, Nice, France, 25-30 March, 2001.

Altamimi, Z. (2001b), The ITRS and ETRS89 Relationship: New results from ITRF2000. Report on the Symposium of the IAG Subcommission for Europe (EUREF), Dubrovnik, 16-18 May, 2001.

Altamimi, Z., Angermann, D., Argus, D., Blewitt, G., Boucher, C., Chao, B., Drewes, H., Eanes, R., Feissel, M., Ferland, R., Herring, T., Holt, B., Johannson, J., Larson, K., Ma, C., Manning, J., Meertens, C., Nothnagel, A., Pavlis, E., Petit, G., Ray, J., Ries, J., Scherneck, H., Sillard, P. and Watkins, M. (2001c), The Terrestrial Reference Frame and the dynamic Earth, EOS Trans. AGU, 82, 273, 278-279, 2001.

Altamimi, Z. (2001d), Review and Progress of ITRF Datum Definition: New Results from ITRF2000, AGU Fall meeting 2001, San Francisco, USA, 10-14 December, 2001.

Altamimi, Z., Boucher, C. and Sillard, P. (2002a), New trend for the realization of the International Terrestrial Reference System, Advances in Space Research, Vol.30, No.2, pp.175-184.

Altamimi, Z., Sillard, P. and Boucher C. (2002b), ITRF2000: A new release of International Terrestrial Reference Frame for Earth Science Applications, J. Geophys. Res., 107 (B10), 2214, doi:10.1029/2001JB000561, 2002.

Altamimi, Z., Boucher, C., Drewes, H., Ferland, R., Larson, K., Ray, J. and Rothacher, M. (2002c), Combination of Station Positions and Velocities, IERS Technical Note No.30, Proceedings of the IERS Workshop on Combination Research and Global Geophysical Fluids, edited by Bernd Richter, Wolfgang Schwegmann, and Wolfgang R. Dick.

Altamimi, Z., Sillard, P. and Boucher, C. (2003a), The impact of a No-Net-Rotation condition on ITRF2000, Geophys. Res. Lett., 30(2), 1064, doi:10.1029/2002GL016279, 2003.

Altamimi, Z. (2003b), ITRF, GPS permanent stations and the AFREF project, Technical Session TS 6 – Regional Reference Frame I, 2nd FIG Regional Conference, Sheraton Marrakech, Morocco, 2-5 December, 2003.

Altamimi, Z. and Ray, J. (2004), Issues to consider, IERS Combination Pilot Project, Nice Splinter Meeting, 29 April, 2004.

Altamimi, Z and Boucher, C. (2005a), ITRF2004 Strategy. IERS WG on Combination: ITRF2004 and Combination Pilot Project, 3rd meeting of the IERS working group on Combination, 27 April, 2005.

Altamimi, Z., Boucher, C. and Willis, P. (2005b), Terrestrial reference frame requirements within GGOS perspective, Journal of Geodynamics, Vol. 40, Issues 4-5, pp.363-374.

Angermann, D., Thaller, D. and Rothacher, M. (2002), Issues of a Rigorous Combination Part 3: SINEX Combination Campaign, IERS Workshop on Combination Research and Global Geophysical Fluids, Munich, Germany, 18-21 November, 2002.

Angermann, D., Meisel, B., Krügel, M., Müller, H. and Tesmer, V. (2003a), Time series of station positions and datum parameters, Proceedings of the IERS Workshop on Combination Research and Global Geophysical Fluids, Bavarian Academy of Sciences, Munich, Germany, 18 - 21 November 2002, pp.199-201, edited by Bernd Richter, Wolfgang Schwegmann, and Wolfgang R. Dick.

Angermann, D., B. Meisel, M. Krügel, H. Müller and H. Drewes (2003b), Analysis of site position time series derived from space geodetic solutions, AGU Fall Meeting, San Francisco, USA, 8-12 December, 2003.

Angermann, D., Drewes, H., Krunegel, M, Meisel, B., Gerstl, M., Kelm, R., Muller, H., Seemuller, W. and Tesmer, V. (2004a), ITRS Combination Center at DGFI: A Terrestrial Reference Frame Realization 2003, München, Germany, 2004, ISBN 3 7696 8593 8

Angermann, D., Drewes, H., Meisel, B., Krunegel, M and Tesmer, V. (2004b), Towards a refined realisation of the terrestrial reference system, AGU Fall Meeting, San Francisco, USA, 13-17 December, 2004.

Argus, D. F. and Gordon, R. G. (1991), No-net Rotation model of current plate velocities incorporating plate motion model NUVEL-1, Geophys. Res. Lett. 18, 2038-2042, 1991.

Becker, M., Reinhart, E. and Seeger, H. (1997), Realization of the ITRF-94 in Thailand and Malaysia by Use of a Combined Network for Geodynamics and National Survey, International Association of Geodesy Symposia IAG Scientific Assembly, Springer, ed. F.K. Brunner and K. Fritz, Vol. 118, pp.49-56.

Belsley, D. A. (1980), Regression diagnostics: identifying influential data and sources of collinearity, New York: Wiley, 1980.

Beutler, G., Rothacher, M., Schaer, S., Springer, T.A., Kouba, J. and Neilan, R. E. (1999), The International GPS Service, IGS, An Interdisplinary Service in support of Earth Sciences, Advances in Space Research, Vol.23, No.4, pp.631-653.

Beutler, G., Brosche, P., Brzezinski, A., Fukushima, T., Gambis, D., Gross, R., Hefty, J., Huang, C., Malkin, Z., McCarthy, D., Poma, A., Ray, J., Richter, B., Ron, C., Sidorenkov, N., Soffel, M., Wilson, C. and Yatskiv, Ya. (2002), Reports on Astronomy, Vol. XXVA, pp.49-68.

Blewitt, G., Bock, Y. and Kouba, J. (1994), Constraining the IGS polyhedron by distributed processing, in Densification of ITRF Through Regional GPS Networks, edited by J. F. Zumberge and Liu, R., pp.21.37, IGS Cent. Bur., JPL, Pasadena, California.

Blewitt, G., Boucher, C., Davies, P.B.H. et al. (1997), ITRF Densification and Continuous Realization by the IGS, International Association of Geodesy Symposia IAG Scientific Assembly, Springer, ed. F.K. Brunner and K. Fritz, Vol. 118, pp. 8-17.

Bock, Y. and Zhu, S. Y. (1982), On the establishment and maintenance of a modern Conventional Terrestrial Reference System, International Association of Geodesy Symposia IAG Scientific Assembly, Springer, Vol. 5, 7-20 May 1982.

Boucher, C. (1990), Definition and realization of terrestrial reference systems for monitoring earth rotation, International Union of Geodesy and Geophysics and American Geophysical Union, Variations in Earth Rotation, ed. D.D. McCarthy and W. E. Carter, Vol. 51, pp.197-201.

Boucher, C. and Altamimi, Z. (1992), The EUREF Terrestrial Reference System and its first realizations, EUREF Meeting, Bern, Switzerland, 4-6 March, 1992.

Boucher, C. and Altamimi, Z. (1996), International Terrestrial Reference Frame, GPS World, September, 1996, pp.71-74.

Boucher, C., Altamimi, Z., Sillard, P. (1997), The ITRF96 Realization of the International Terrestrial Reference System, International Association of Geodesy Symposia IAG Scientific Assembly, Springer, ed. F.K. Brunner and K. Fritz, Vol. 118, pp. 57-58.

Boucher, C., Altamimi, Z. and Sillard, P (1999), The 1997 International Terrestrial Reference Frame (ITRF97), IERS Tech Note 27, Observatoire de Paris.

Boucher, C., Altamimi, Z., Sillard, P. and Feissel-Vernier, M. (2003), The 2000 International Terrestrial Reference Frame (ITRF2000), IERS Tech Note 31, Observatoire de Paris.

Bruyninx, C., Dousa, J. and Ehrnsperger, W. (1997), The Use of the EUREF Permanent GPS Network for the Maintenance of the European Terrestrial Reference Frame, International Association of Geodesy Symposia IAG Scientific Assembly, Springer, ed. F.K. Brunner and K. Fritz, Vol. 118, pp.18-26.

Buiten, H.J. (1978), Junction of nets by collocation, *Manus. Geodaet.* Vol.3, pp. 253-297.

Carter, W. E. and Robertson, D.S. (1990), Definition of a Terrestrial Reference Frame Using IRIS VLBI Observations: Approaching Millimeter Accuracy, International Association of Geodesy Symposia IAG Scientific Assembly, Springer, ed. C. Boucher and G. A. Wilkins, Vol. 105, pp. 115-122.

Chapter 4, Conventional Terrestrial Reference System and Frame, IERS Conventions 2003.

Davies, P., and Blewitt, G. (2000), Methodology for global geodetic time series estimation: A new tool for geodynamics, J. Geophys. Res., Vol.105, No.B5, pp.11,083-11,100.

Dietrich, R., Dach, R., Engelhardt, G.., Ihde, J., Korth, W., Kutterer, H.-J., Lindner, K., Mayer, M., Menge, F., Miller, H., Müller, C., Niemeier, W., Perlt, J., Pohl, M., Salbach, H., Schenke, H.-W., Schöne, T., Seeber, G., Veit, A. and Völksen, C. (2001), ITRF coordinates and plate velocities from repeated GPS campaigns in Antarctica – an analysis based on different individual solutions, Journal of Geodesy, Vol. 74, pp.756-766.

DGFI Annual Report 2003, 92 pp.

Dong, D., Yunck, T. and Heflin, M. (2003), Origin of the International Terrestrial Reference Frame, J. Geophys. Res., 108 (B4), 2200, doi:10.1029/2002JB002035.

Drewes, H. (1998), Combination of VLBI, SLR and GPS determined station velocities for actual plate kinematic and crustal deformation models, International Association of Geodesy Symposia IAG Scientific Assembly, Rio De Janeiro, 3-9 September 1997, Springer, ed. Forsberg R., Feissel M., Dietrich R. Vol. 119, pp. 377-382.

Feissel-Vernier, M. and Le Bail, K. (2005). Datum definition within and across techniques: station weight factors reflecting their long term stability. IERS WG on Combination: ITRF2004 and Combination Pilot Project. 3rd meeting of the IERS working group on Combination. 27 April, 2005.

Fejes, I., Almar, I., Adam, J. and Mihaly, Sz. (1989), Space VLBI: A new Technique for Unification of Reference Frames, International Association of Geodesy Symposia IAG Scientific Assembly, Springer, ed. C. Boucher and G. A. Wilkins, Vol. 105, pp. 158-165.

Ferland, R., Kouba, J. and Hutchison, D. (2000), Analysis methodology and recent results of the IGS network combination, Earth Planets Space, Vol.52, pp.953-957.

Ferland, R. (2002), Activities of the International GPS Service (IGS) Reference Frame Working Group, International Association of Geodesy Symposia IAG Scientific Assembly, Springer, ed. J. Adam and K -P. Schwarz, Vol. 125, pp. 3-8.

Ferland R., Gendt, G. and Schone T. (2004), IGS Reference Frame Maintenance, IGS 2004 Workshop in Berne, Switzerland, 1 March, 2004.

Fok, H. S., H. B. Iz and Schaffrin, B. (2007), Comparison of Four Geodetic Network Densification Solutions, Survey Review (accepted for publication).

Geodesist's Handbook, Bull. Geod., Vol.66, 128 pp., 1992.

Grafarend, E. and Schaffrin, B. (1974), Unbiased free net adjustment, Survey Review, Vol.22, No.171, pp.200-218.

Hase, H. (1997), Applications of VLBI to Geodesy, Lecture at 2nd VLBI-School, JIVE, Dwingeloo, October 6-10, 1997.

Helmert, F.R. (1924), Die Ausgleichungsrechnung nach der Methode der Kleinsten Quadratic, 3, AUFL., Leipzig/Berlin.

Iz, H. B. (1987), An algorithmic approach to crustal deformation analysis, Report 382, Geodetic and Geo-Information Science, Dept. of Civil and Environmental Engineering and Geodetic Science, The Ohio State University.

Iz, H.B. and H.S. Fok (2004), Alternative ITRF Formulation Based on the Strength of Different Space Geodesy Techniques, Eos Trans. AGU, 85 (47), Fall Meet. Suppl., Abstract G31B-0794.

Jayles, C., Nhun-Fat, B. and Tourain, C. (2006), DORIS: System description and control of the signal integrity, Journal of Geodesy, Vol.8-11, pp.457-472.

Joel, B.O. (2004), Ionospheric studies using VLBI, MSc thesis, Chalmers University of Technology, Sweden

Johnson, R. A. and Wichern, D. W. (1992), Applied Multivariate Statistical Analysis, Prentice Hall, 3rd Edition.

Kar, S. (1997), Long-period variations in the geocenter observed from laser tracking of multiple Earth satellites, Ph.D. dissertation, The University of Texas at Austin, USA.

Kovalevsky, J. and Mueller, I. I. (1989), Introduction. Reference frames in astronomy and geophysics, J. Kovalevsky, I. I. Mueller and B. Kolaczek (Eds.), Kluwer Academic Publisher, Netherlands, 474 pp.

Kuijper, D.C., Ambrosius, B.A.C., Wakker, K.F. (1995), SPOT-2 and TOPEX/POSEIDON precise orbit determination from DORIS Doppler tracking, Adv. Space Res. Vol.16, No.12, pp.45-50.

Leick, A. (2004), GPS satellite surveying, New York: Wiley, 3rd Edition.

McCarthy, D. and Petit, G. (2003), IERS conventions, IERS Tech. Note 32, International Earth Rotation Service Central Bureau, Observatoire de Paris, 2003.

Meisel, B., Angermann, D., Drewes, H., Krugel, M., Muller, H. and Tesmer, V. (2005), The influence of Time Variable Effects on the Terrestrial Reference Frame, EGU General Assembly, Vienna, Austria, 24-29 April 2005.

Mikhail, E.M. (1976), Observations and least squares, New York: IEP.

Montag H., Gendt G. and Wilson P. (1996), On the determination of terrestrial reference frame by SLR and GPS techniques, Journal of Geodynamics, Vol. 22, Issues 1-2, pp.63-77.

Noll, C. and Soudarin, L. (2006), On-line resources supporting the data, products, and information infrastructure for the international DORIS service, Journal of Geodesy, No.8-11, pp.419-427.

Nothnagel, A. (2003), VTRF2003: A conventional VLBI Terrestrial Reference Frame, International VLBI Service for Geodesy and Astrometry, available at http://giub.geod.uni-bonn.de/vlbi/IVS-AC/vtrf2003/vtrf2003.html.

Otsubo, T. and Gotoh, T. (2002), SLR-based TRF contributing to the ITRF2000 project, Second IVS General Meeting (Tsukuba), pp.300-303.

Pearlman, M. R., Degnan, J. J. and Bosworth, J. M. (2002), The International Laser Ranging Service, Advance in Space Research, Vol.30, No.2, pp.135-143.

Petrov, L. (2005), Modeling non-linear motion of geodetic station, EGU General Assembly, Vienna, Austria, 24-29 April 2005

Ray, J. and Altamimi, Z. (2005), Evaluation of co-location ties relating the VLBI and GPS reference frames, Journal of Geodesy, Vol.79, pp.189-195.

Rothacher, M. (2005), Strategies for weekly routine generation of combined IERS products. IERS WG on combination: ITRF2004 and Combination Pilot Project, 3rd meeting of the IERS working group on Combination, Vienna, 27 April, 2005.

Rothacher, M., Thailer, D. and Dill, R. (2004), IERS working group on combination and IERS combination pilot project, EGU 1st General Assembly, Nice, France, 26-30 April, 2004.

Sarti, P., Sillard, P., Vittuari, L. (2004), Surveying co-located space-geodetic instruments for ITRF computation, Journal of Geodesy, Vol.78, pp.210-222.

Schaffrin, B. (1997), Reliabillity measures for correlated observations, Journal of Surveying Engineering, Vol.123, No.3, pp.123-137.

Schillak, S. and Wnuk, E. (2003), The SLR stations coordinates determined from monthly arcs of LAGEOS-1 and LAGEOS-2 laser ranging in 1999-2001, Advances in Space Research, Vol.31, No.8, pp.1935-1940.

Schluter, W., Himlich, E., Nothnagel, A., Vandenberg, N. and Whitney, A. (2002), IVS and its important role in the maintenance of the global reference systems, Advances in Space Research, Vol.30, No.2, pp.145-150.

Schutz, B. E., Eanes R. J., Watkins M. M. and Tapley B. D. (1989), Contribution of SLR to Earth Orientation and Terrestrial Reference Frames, International Association of Geodesy Symposia IAG Scientific Assembly, Springer, ed. C. Boucher and G. A. Wilkins, Vol. 105, pp. 123-130.

Schwegmann, W. and Richter B. (2005), Long time series for ITRF2004 and IERS CPP within the IERS data centre, IERS WG on Combination: ITRF2004 and Combination Pilot Project, 3rd meeting of the IERS working group on Combination, 27 April, 2005.

Sillard, P., Altamimi, Z., and Boucher, C. (1998), The ITRF96 realization and its associated velocity field, Geophys. Res. Lett., Vol. 25, 3223-3226.

Sillard, P. and Boucher, C. (2001), A review of algebraic constraints in terrestrial reference frame datum definition, Journal of Geodesy, Vol.75, pp.63-73.

Smith, D.E., Kolenkiewicz, R., Dunn, P.J. and Torrence, M.H. (1999), Earth scale below a part per billion from Satellite Laser Ranging, International Association of Geodesy Symposia, Vol. 121 Schwarz (ed.), Geodesy Beyond 2000 – The challenges of the First Decade, Springer, pp.3-12.

Snow, K. (2002), Applications of parameter estimation and hypothesis testing to GPS network adjustments, Report 465, Geodetic and Geo-Information Science, Dept. of Civil and Environmental Engineering and Geodetic Science, The Ohio State University.

Soler, T. (1998), A compendium of transformation formulas useful in GPS work, J. Geod. 72:482-490.

Soler, T. and Marshall, J. (2003), A note on frame transformations with applications to geodetic datums, GPS Solutions, Vol.7, pp.23-32.

Soler, T. and Snay, R. A. (2004), Transforming positions and velocities between the International Terrestrial Reference Frame of 2000 and North American Datum of 1983, Journal of Surveying Engineering, Vol. 130, No.2, pp.49-55.

Takahashi, F. et al. (2000), Very Long Baseline Interferometer, Tokyo: Ohmsha, VA: IOS Press Inc.

Tan, S. (2002), Least squares adjustment through reparameterization. Survey Review Vol.36, No.283, pp.362-366.

Tapley, B.D., Schutz, B.E., and Eanes, R.J. (1985), Station Coordinates, Baselines, and Earth Rotation from LAGEOS Laser Ranging: 1976-1984, J. Geophys. Res., Vol.90, pp.9235-9248.

Tavernier, G. Granier, J.P., Jayles, C., Sengenes, P. and Rozo, F. (2003), The current evolution of the DORIS system, Advances in Space Research, Vol. 31, No.8, pp.1947-1952.

Tavernier, G., Fagard, H., Feissel-Vernier, M., Lemoine, F., Noll, C., Ries, J., Soudarin, L. and Willis, P. (2005), The International DORIS Service, Advances in Space Research, Vol.36, Issue 3, pp.333-341.

Tavernier, G., Fagard, H., Feissel-Vernier, M., Le Bail, K., Lemoine, F., Noll, C., Noomen, R., Ries, J.C., Soudarin, L., Valette, J.J. and Willis, P. (2006), The international DORIS service: genesis and early achievements, Journal of Geodesy, No.8-11, pp.403-417.

Theil, H. (1963), On the use of incomplete prior information in regression analysis, Journal of the American Statistical Association, Vol.58, No.302, pp.407-414.

Uotila, U. (1997), Analysis of observations, Lecture Notes, Department of Geodetic Science, The Ohio State University. 168pp.

Vincent, P., Costes, M., Auriol, A., Menard, Y. and Escudier, P. (2002), Impact of the DORIS Precise Orbit Determination System on Climate Change Studies, Acta Astronautica, Vol. 51, No. 1-9, pp.275-283.

Willis, P. and Morel, L. (2001), Present Mean Sea Level indetermination coming from ITRF Reference Frame uncertainties on TOPEX/DORIS orbits, SWT 2001 Poster, available at http://www.aviso.oceanobs.com/documents/ swt/posters2001/willis.pdf

Willis, P., Tavernier, G., Feissel-Vernier, M., Lemoine, F., Noll, C., Ries, J. and Soudarin, L. (2004), The proposed International DORIS Service IAG Proceedings, Vol.128, Springer, Berlin, pp.207-213.

Willis, P., Desai, S. D., Bertiger, W. I., Haines, B. J. and Auriol, A. (2005a), DORIS satellite antenna maps derived from long-term residuals time series. Advances in Space Research, Vol.36, Issue 3, pp.486-497.

Willis, P., Boucher, C., Fagard, F. and Altamimi, Z. (2005b), Applications geodesiques du systeme DORIS a l'Institut geographique national. C.R. Geoscience 337, pp.653-662.

Witchayangkoon, B. (1997), Elements of GPS precise point positioning, Ph.D. dissertation, The University of Maine, Maine, USA.

Yu, Z. C. (1996), A universal formula of maximum likelihood estimation of variance-covariance components, Journal of Geodesy, Vol.70, pp.233-240.

APPENDIX A1 – RESIDUAL PLOTS FOR THE COMBINATION SOLUTION

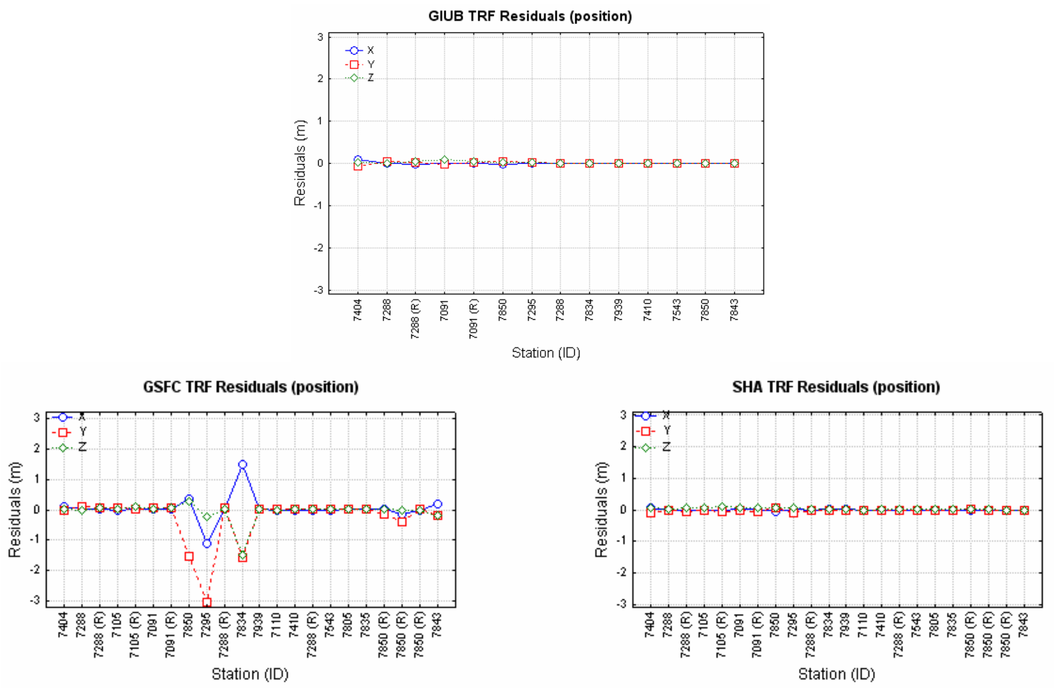

Figure A1.1 A series of residual plots for XYZ positions with respect to each individual VLBI TRF solution in inter-technique combination using state vectors formulation

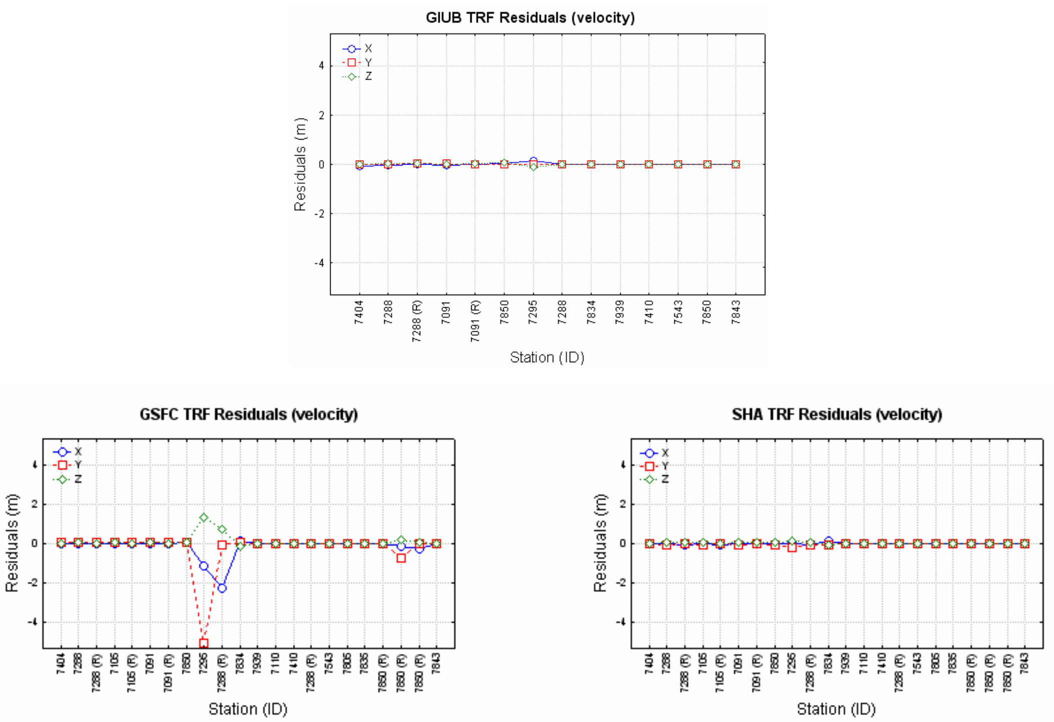

Figure A1.2 A series of residual plots for XYZ velocities with respect to each individual VLBI TRF solution in inter-technique combination using state vectors formulation

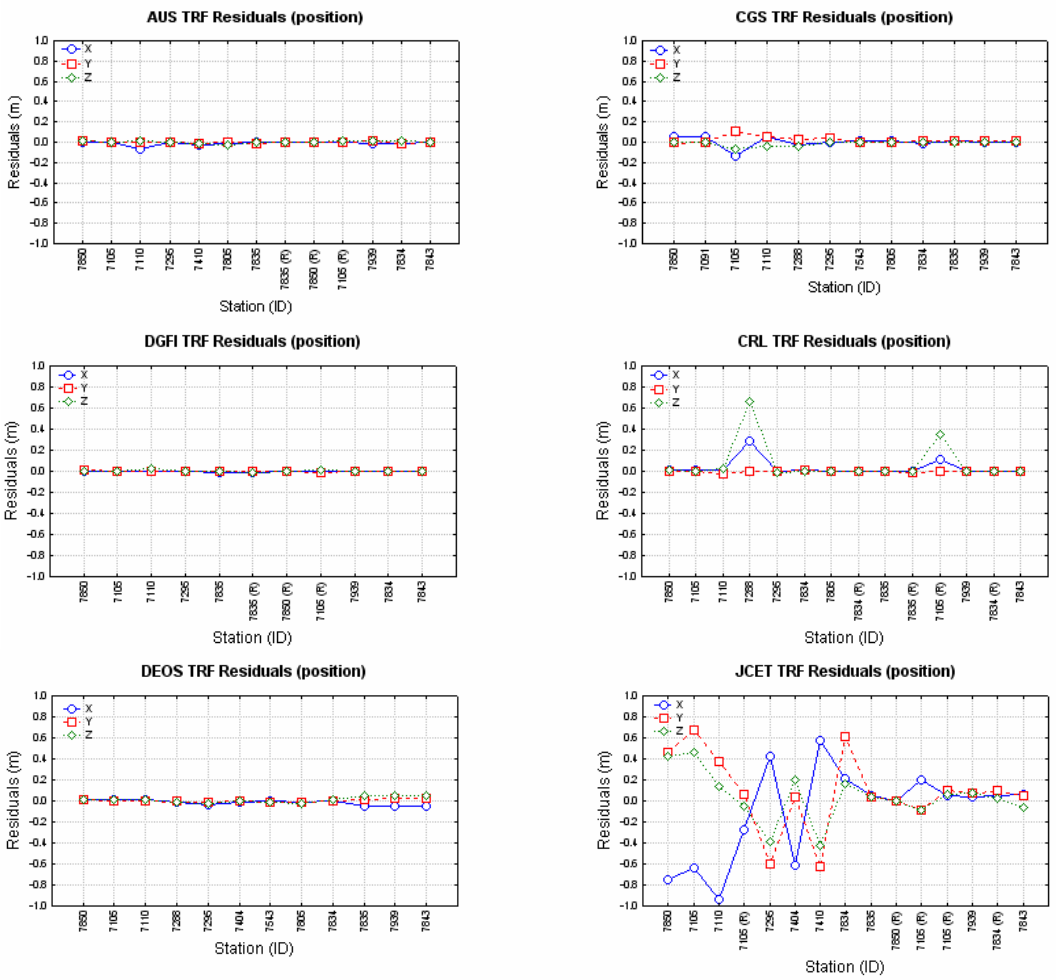

Figure A1.3 A series of residual plots for XYZ positions with respect to each individual SLR TRF solution in inter-technique combination using state vectors formulation

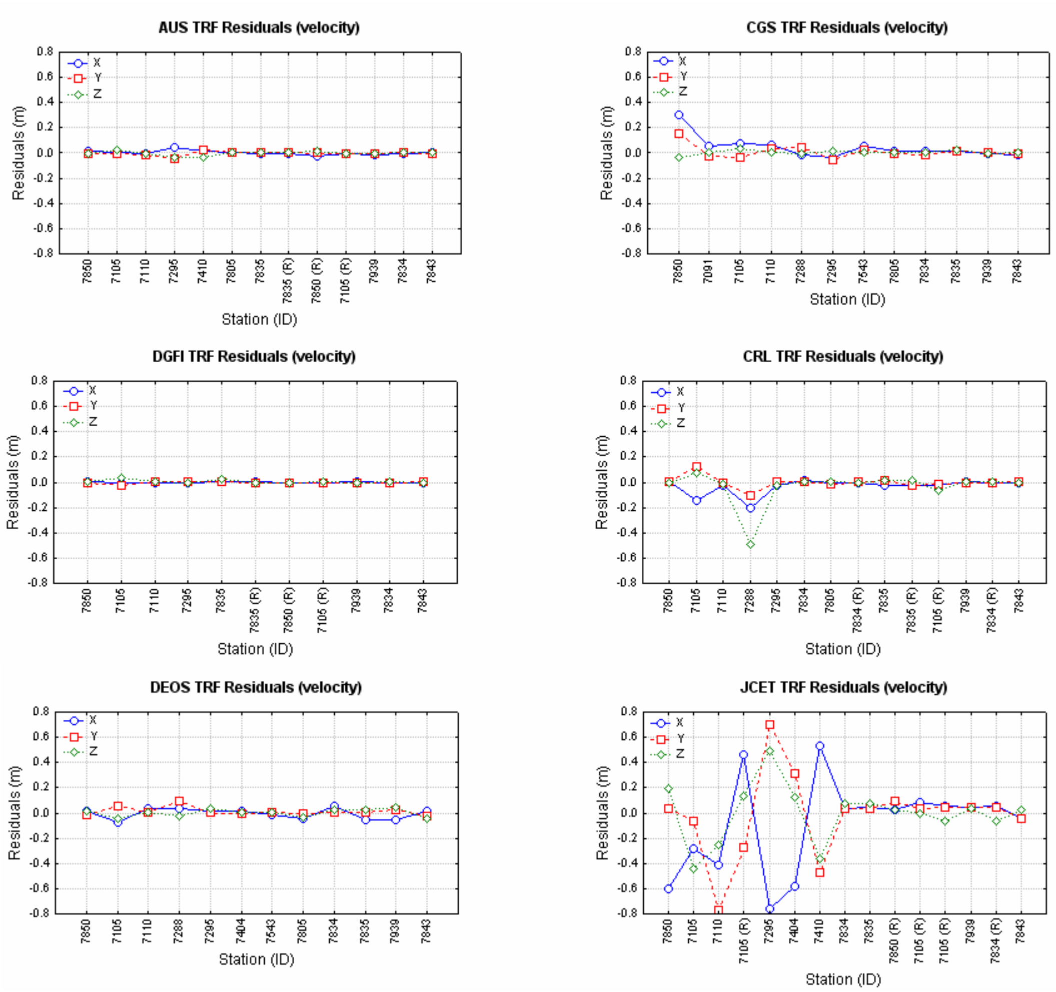

Figure A1.4 A series of residual plots for XYZ velocities with respect to each individual SLR TRF solution in inter-technique combination using state vectors formulation

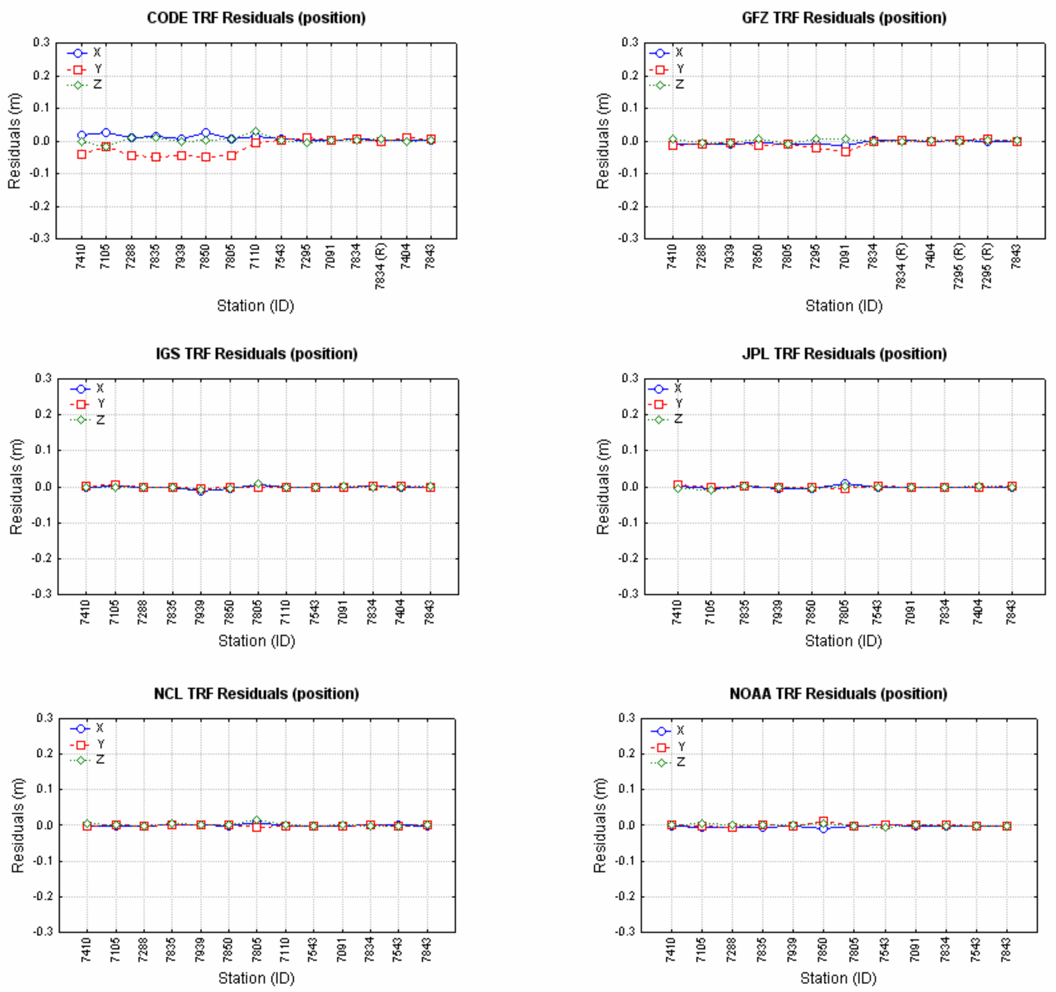

Figure A1.5 A series of residual plots for XYZ positions with respect to each individual GPS TRF solution in inter-technique combination using state vectors formulation

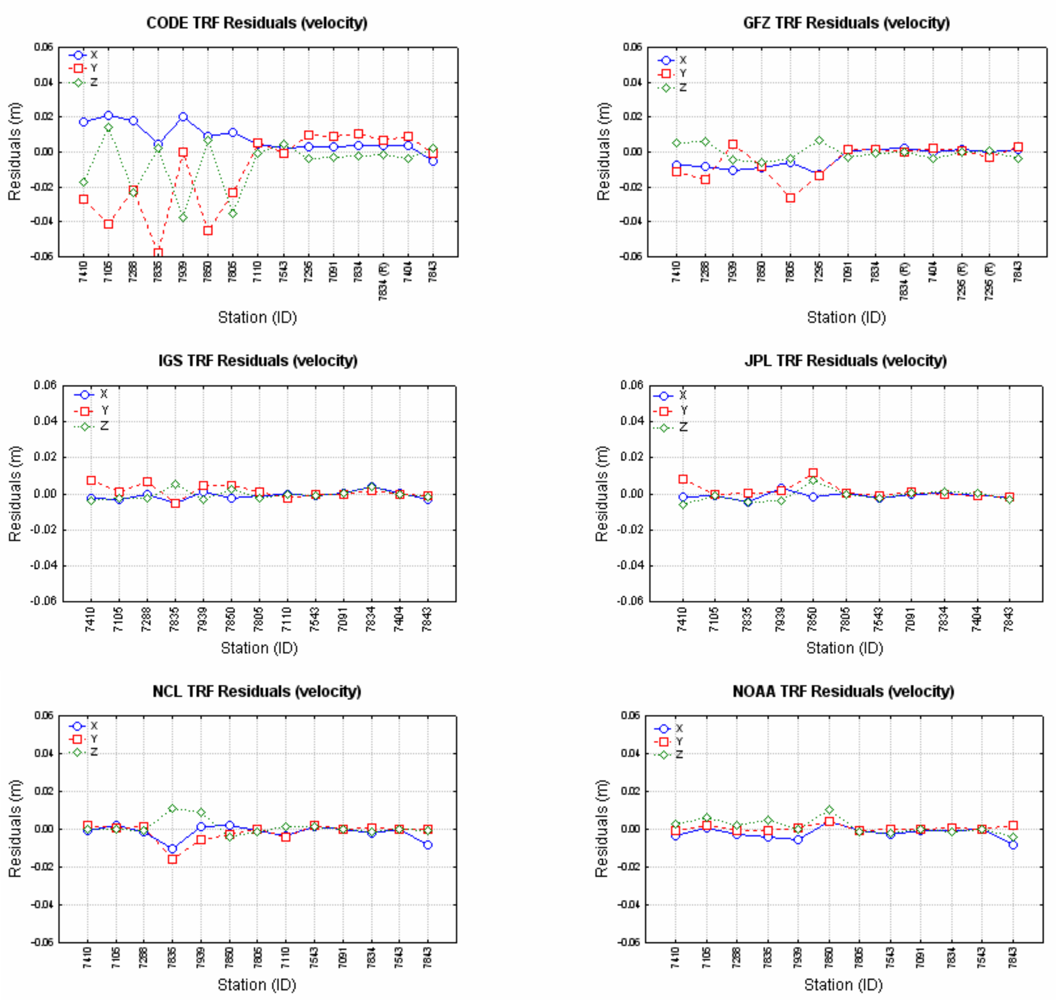

Figure A1.6 A series of residual plots for XYZ velocities with respect to each individual GPS TRF solution in inter-technique combination using state vectors formulation

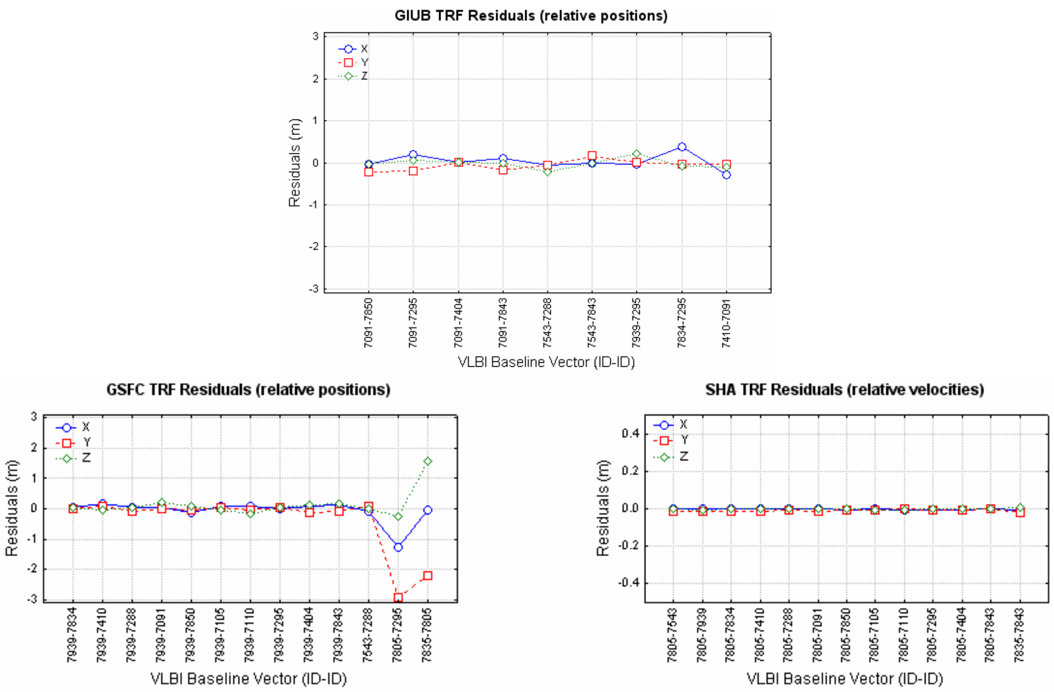

Figure A1.7 A series of residual plots for XYZ relative positions with respect to each individual VLBI TRF solution in inter-technique combination using preferred observation functionals approach (POF with GPSBL)

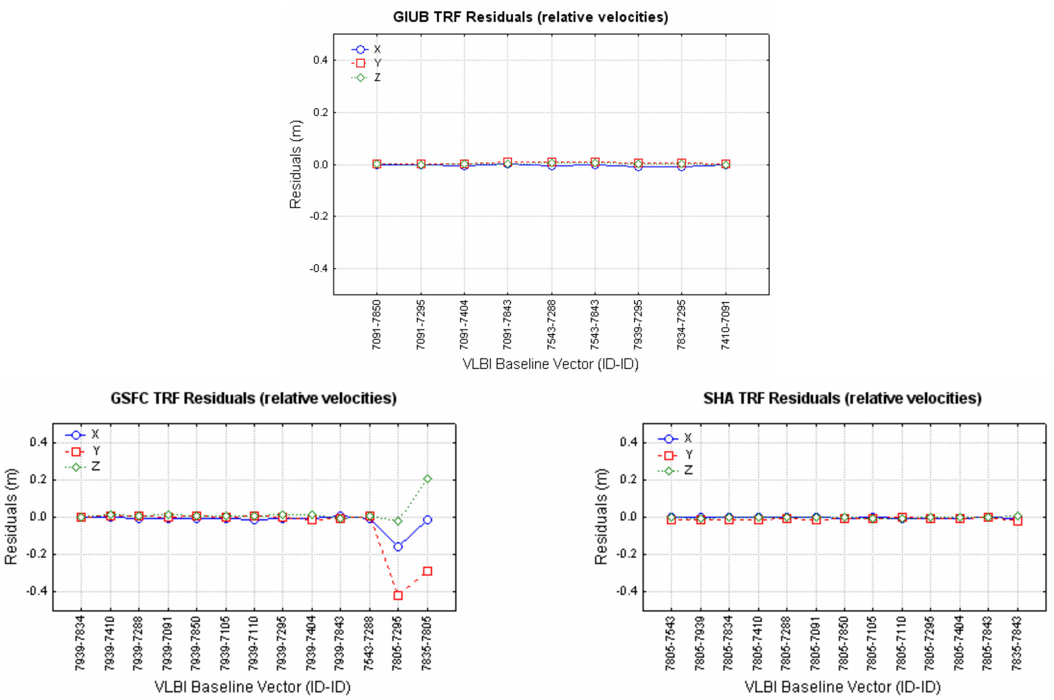

Figure A1.8 A series of residual plots for XYZ relative velocities with respect to each individual VLBI TRF solution in inter-technique combination using preferred observation functionals approach (POF with GPSBL)

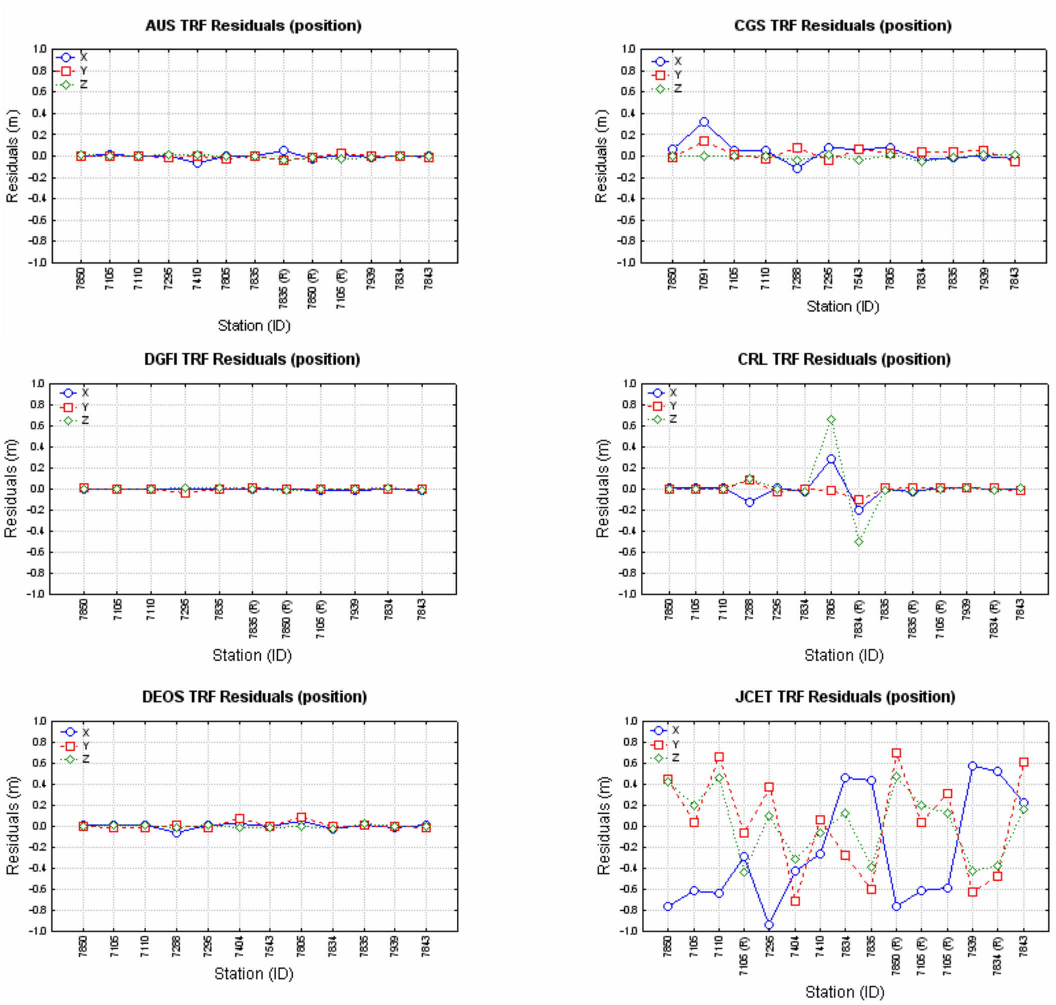

Figure A1.9 A series of residual plots for XYZ positions with respect to each individual SLR TRF solution in inter-technique combination using preferred observation functionals approach (POF with GPSBL)

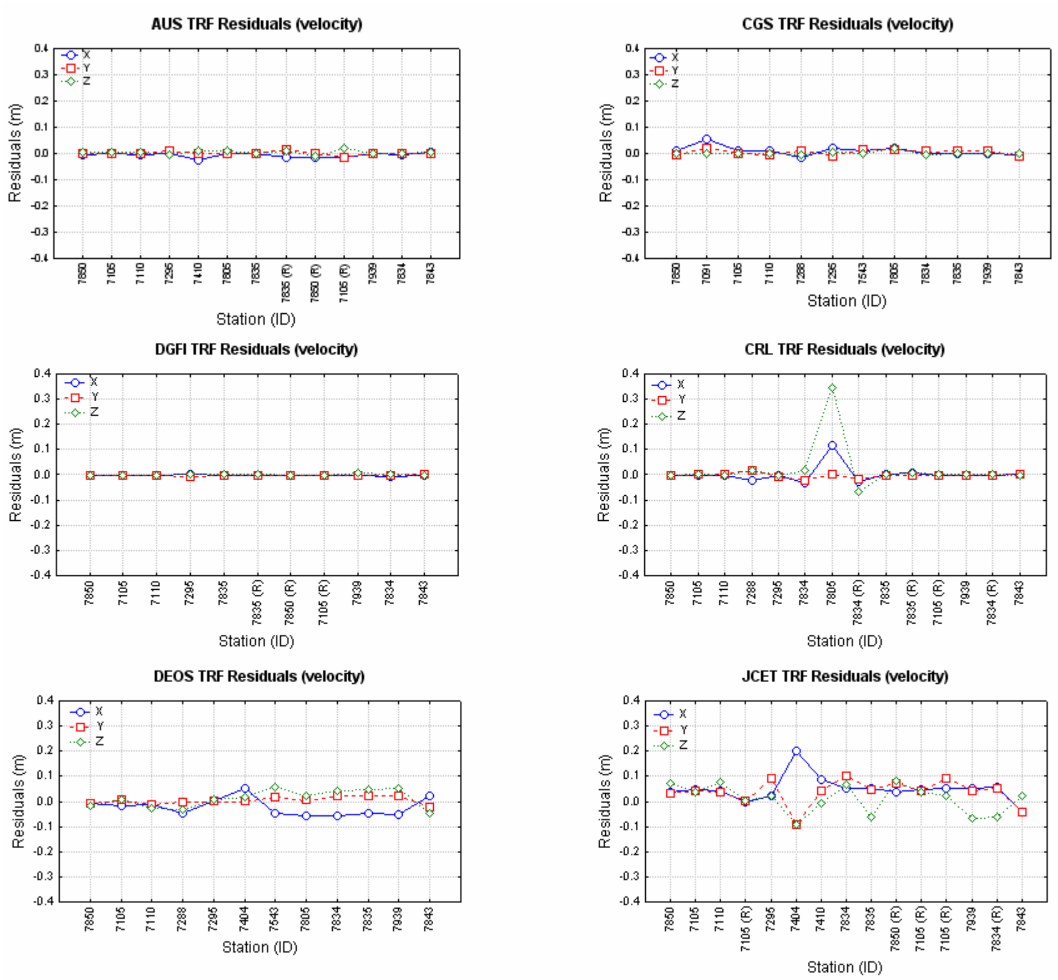

Figure A1.10 A series of residual plots for XYZ velocities with respect to each individual SLR TRF solution in inter-technique combination using preferred observation functionals approach (POF with GPSBL)

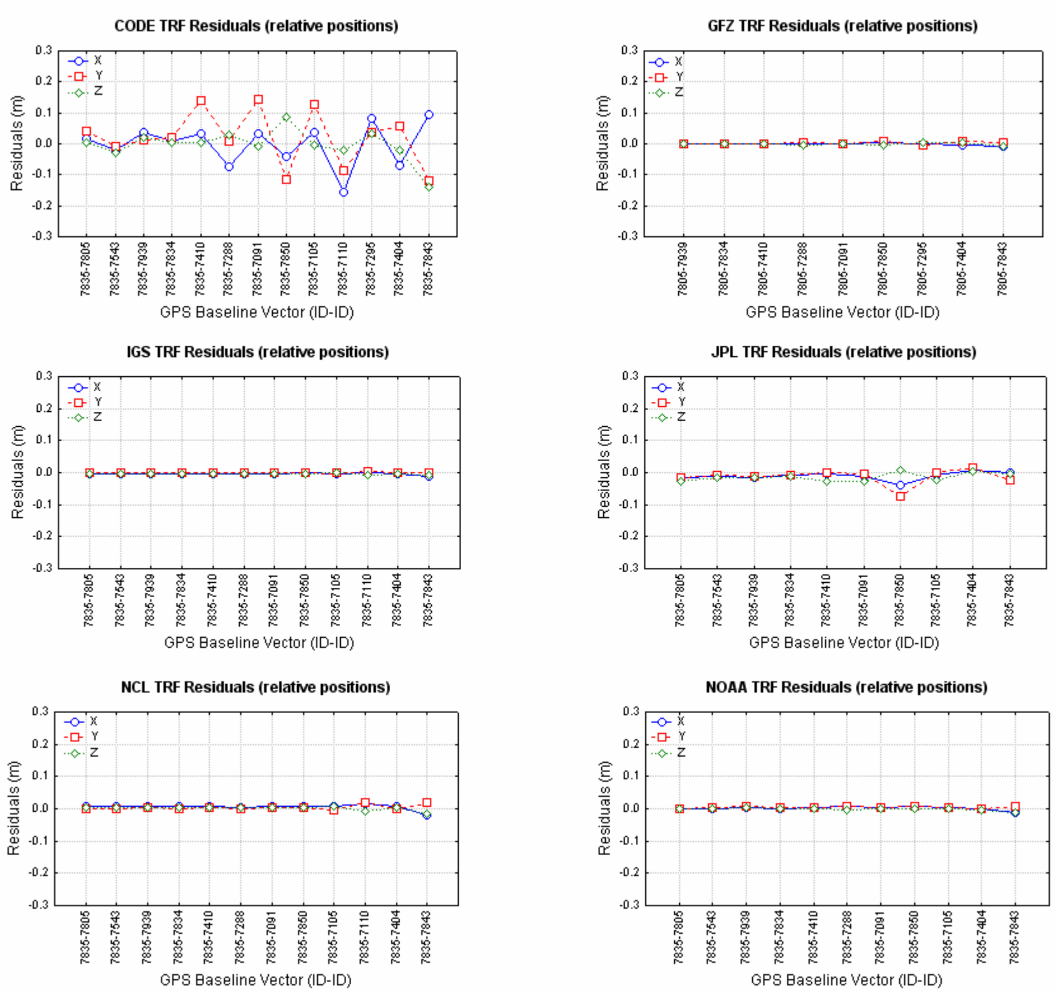

Figure A1.11 A series of residual plots for XYZ relative positions with respect to each individual GPS TRF solution in inter-technique combination using preferred observation functionals approach (POF with GPSBL)

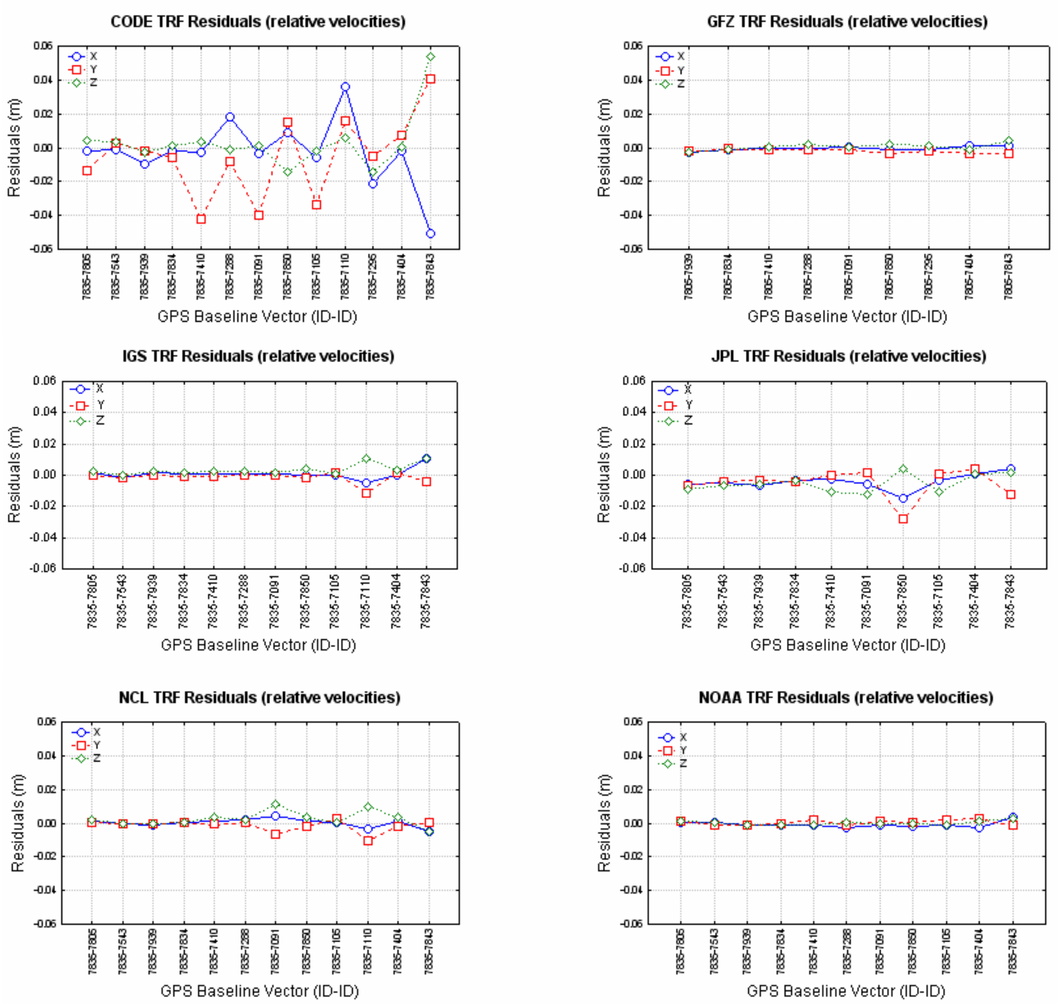

Figure A1.12 A series of residual plots for XYZ relative velocities with respect to each individual GPS TRF solution in inter-technique combination using preferred observation functionals approach (POF with GPSBL)

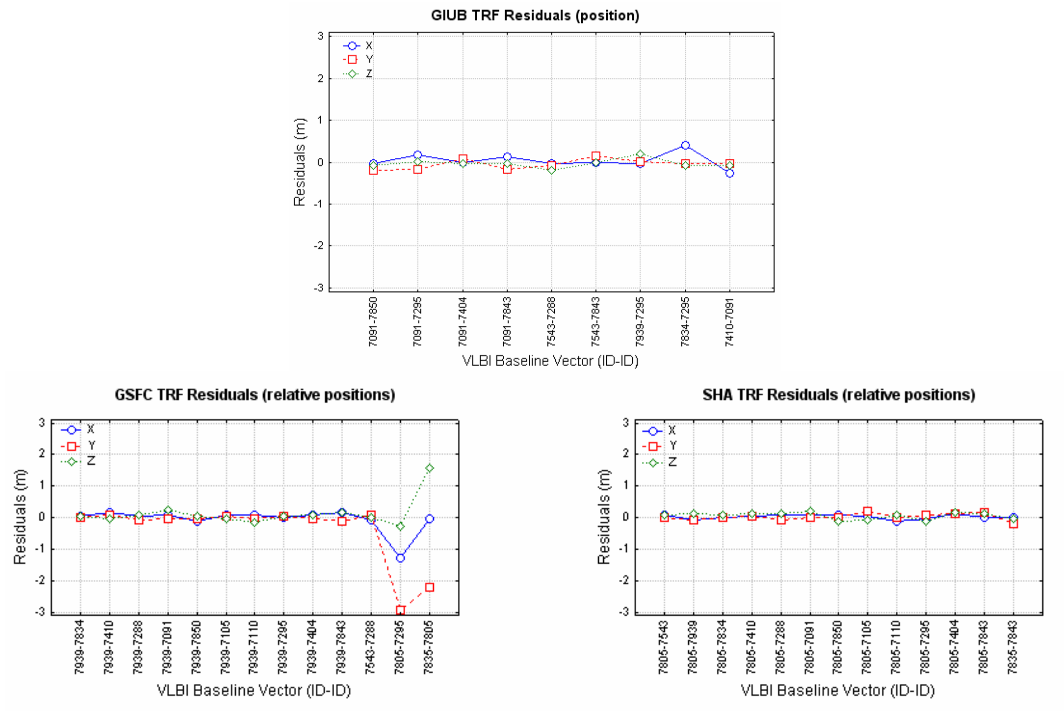

Figure A1.13 A series of residual plots for XYZ relative positions with respect to each individual VLBI TRF solution in inter-technique combination using preferred observation functionals approach (POF with GPSBV)

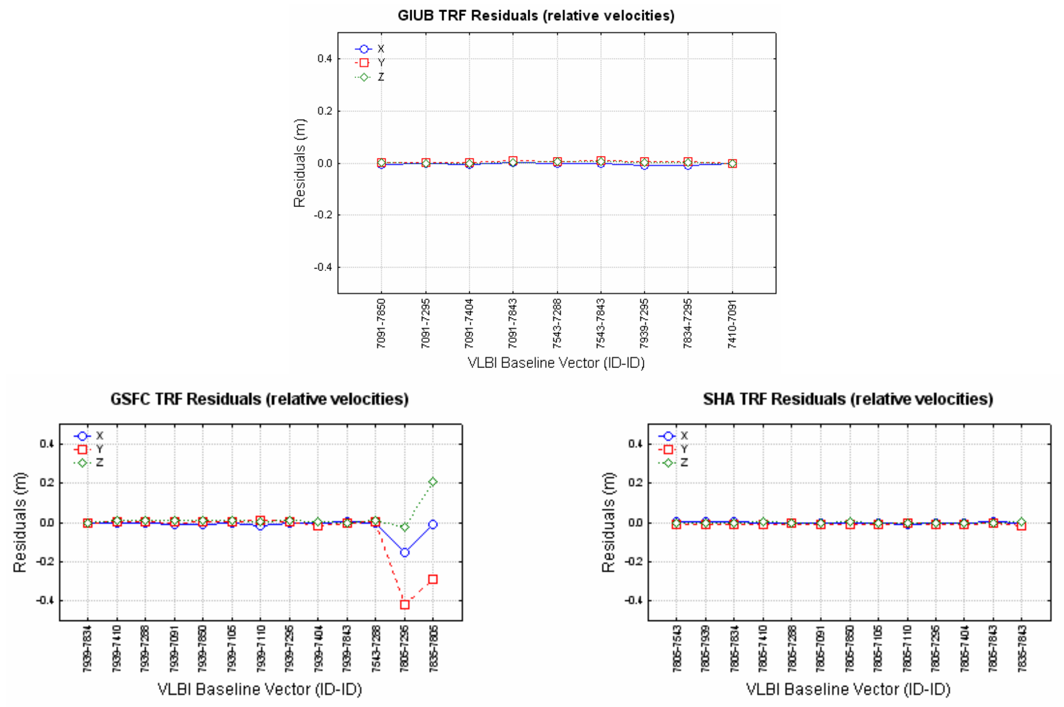

Figure A1.14 A series of residual plots for XYZ relative velocities with respect to each individual VLBI TRF solution in inter-technique combination using preferred observation functionals approach (POF with GPSBV)

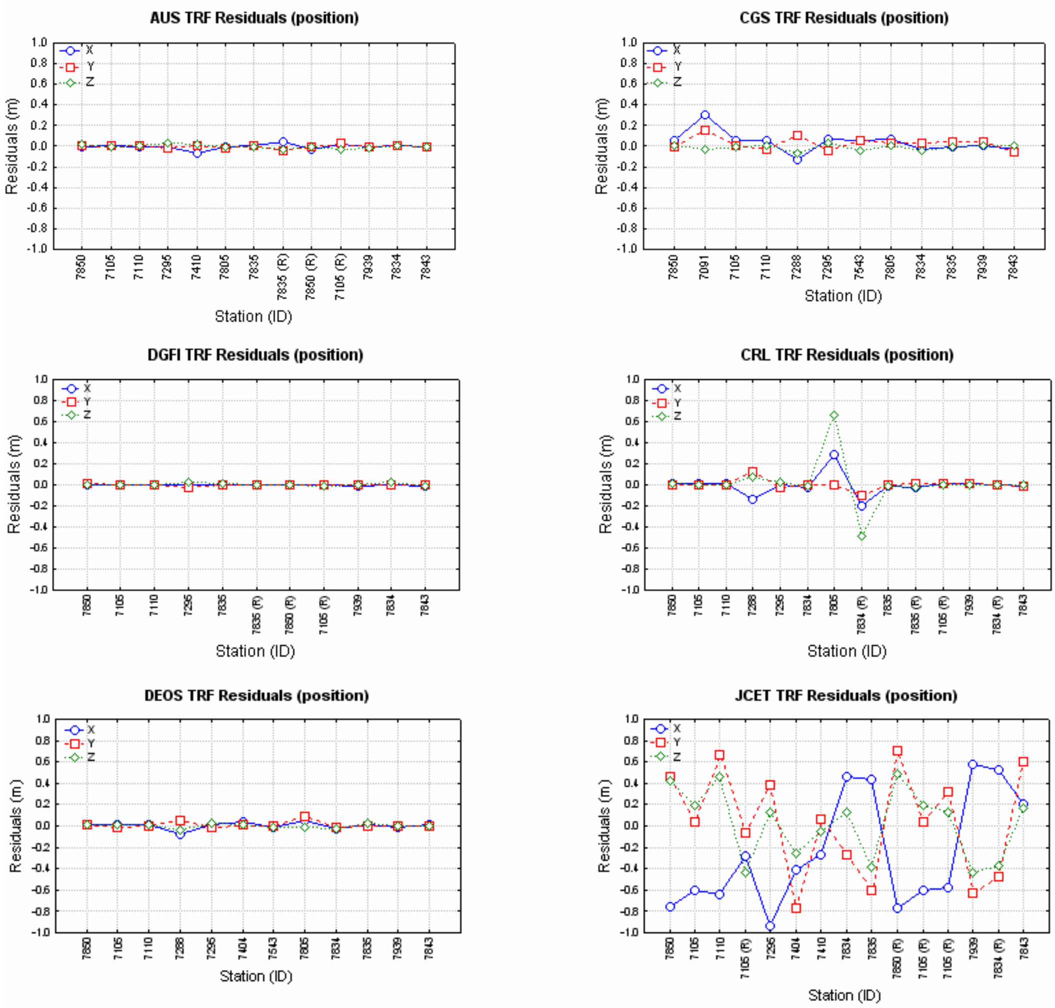

Figure A1.15 A series of residual plots for XYZ positions with respect to each individual SLR TRF solution in inter-technique combination using preferred observation functionals approach (POF with GPSBV)

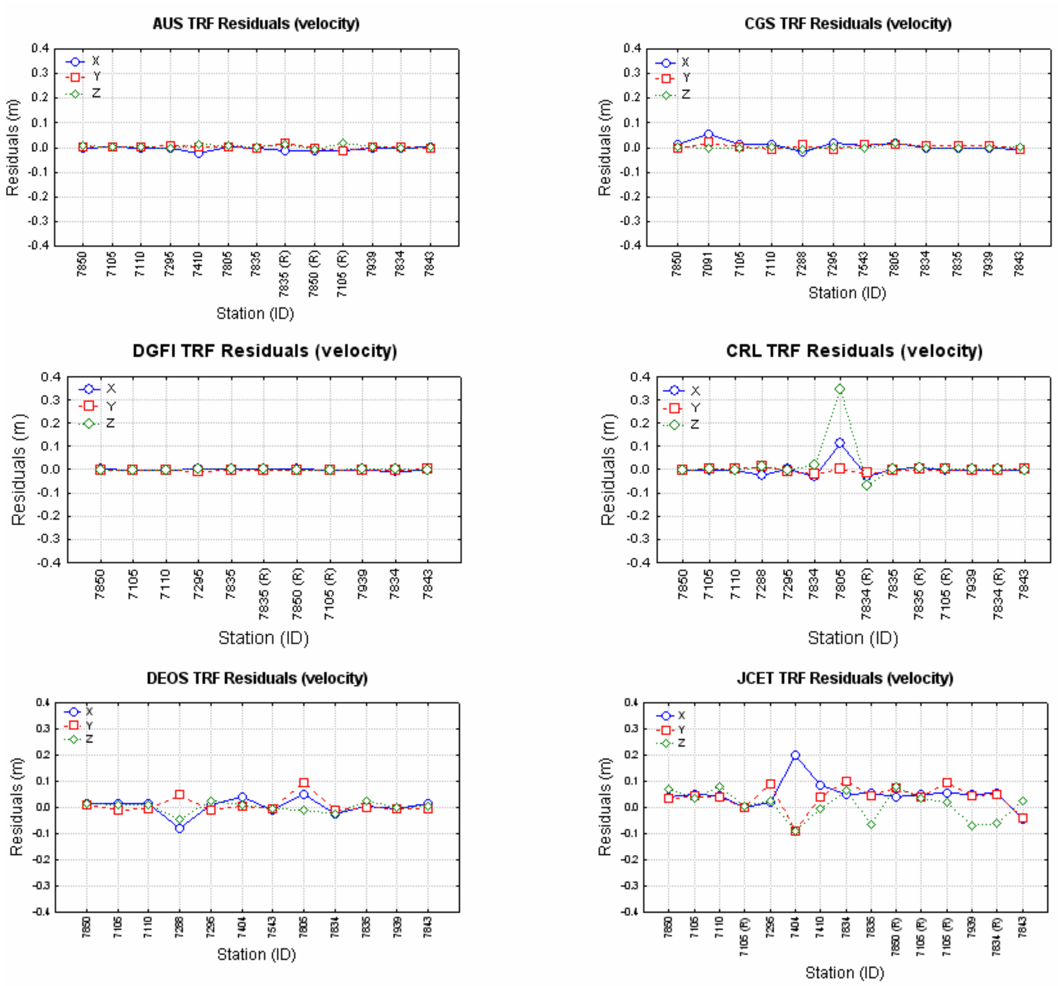

Figure A1.16 A series of residual plots for XYZ velocities with respect to each individual SLR TRF solution in inter-technique combination using preferred observation functionals approach (POF with GPSBV)

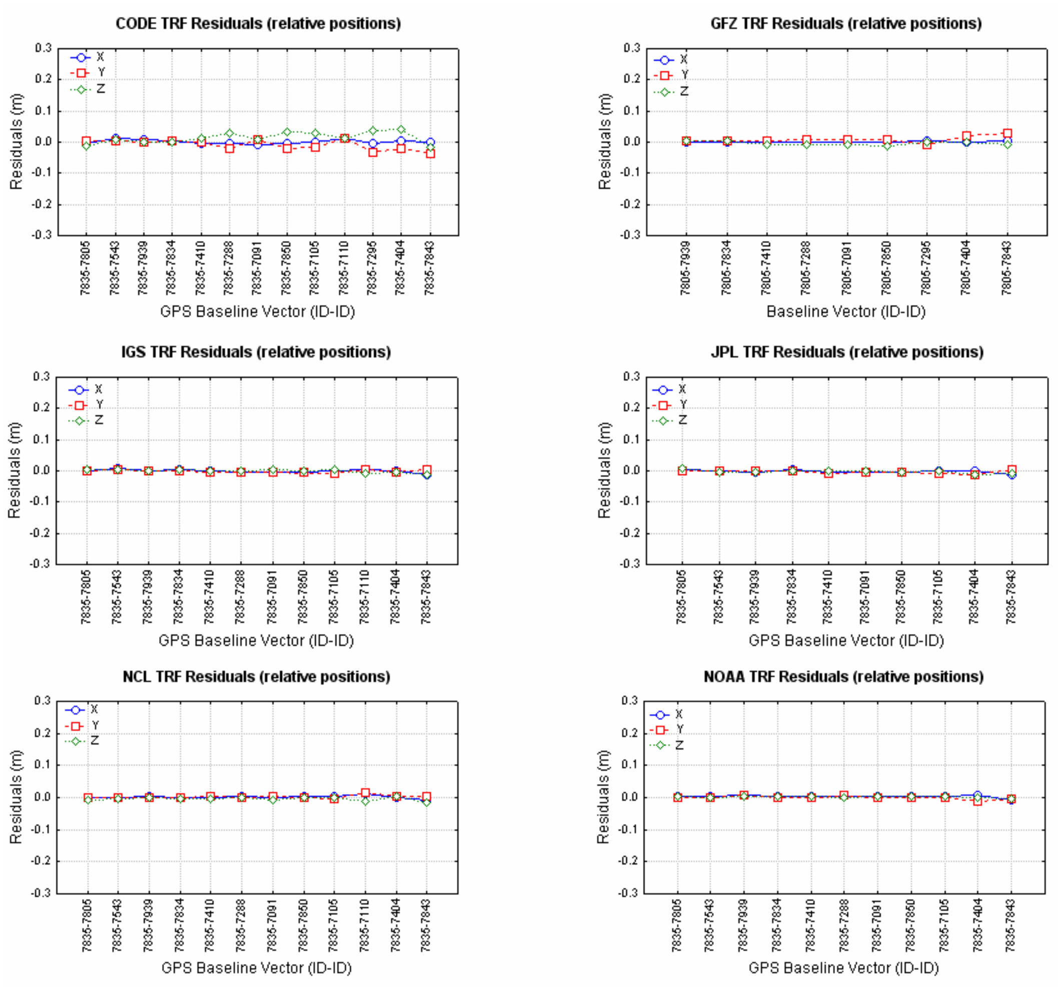

Figure A1.17 A series of residual plots for XYZ relative positions with respect to each individual GPS TRF solution in inter-technique combination using preferred observation functionals approach (POF with GPSBV)

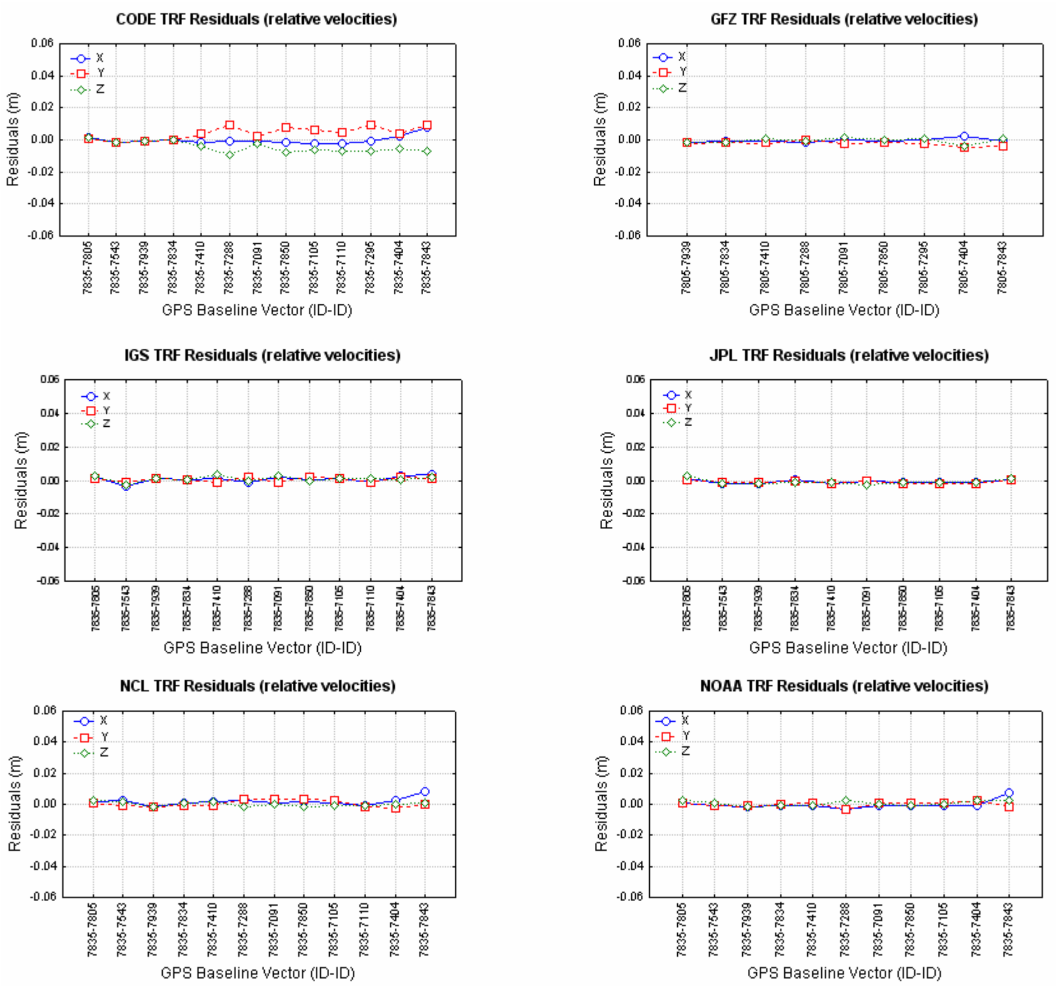

Figure A1.18 A series of residual plots for XYZ relative velocities with respect to each individual GPS TRF solution in inter-technique combination using preferred observation functionals approach (POF with GPSBV)

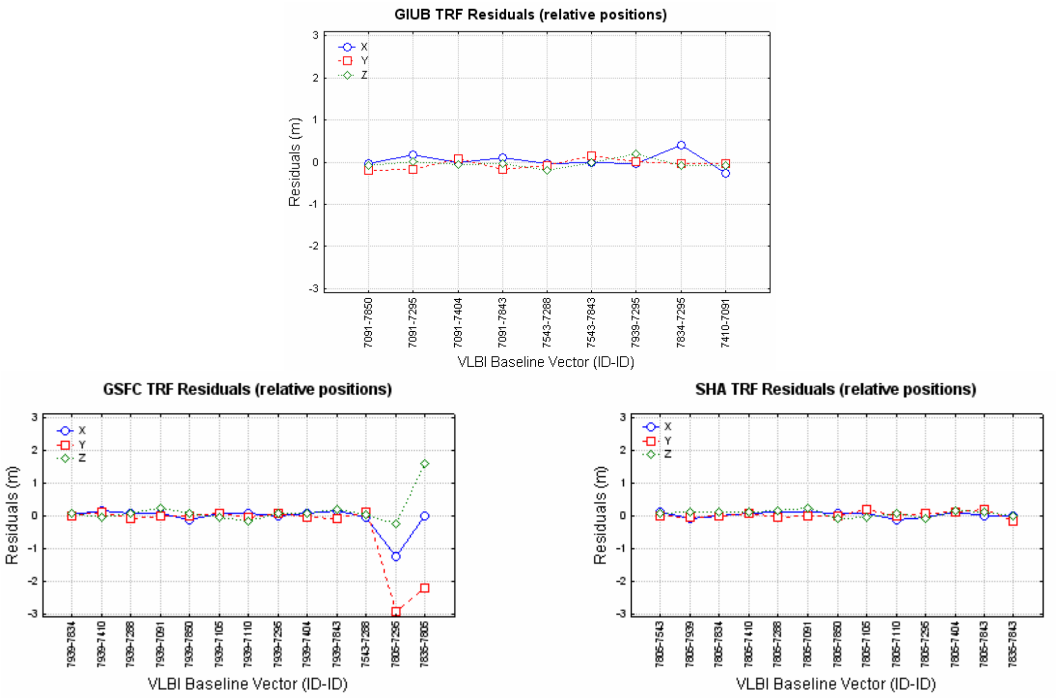

Figure A1.19 A series of residual plots for XYZ relative positions with respect to each individual VLBI TRF solution in inter-technique combination using preferred observation functionals approach (POF with GPSSV)

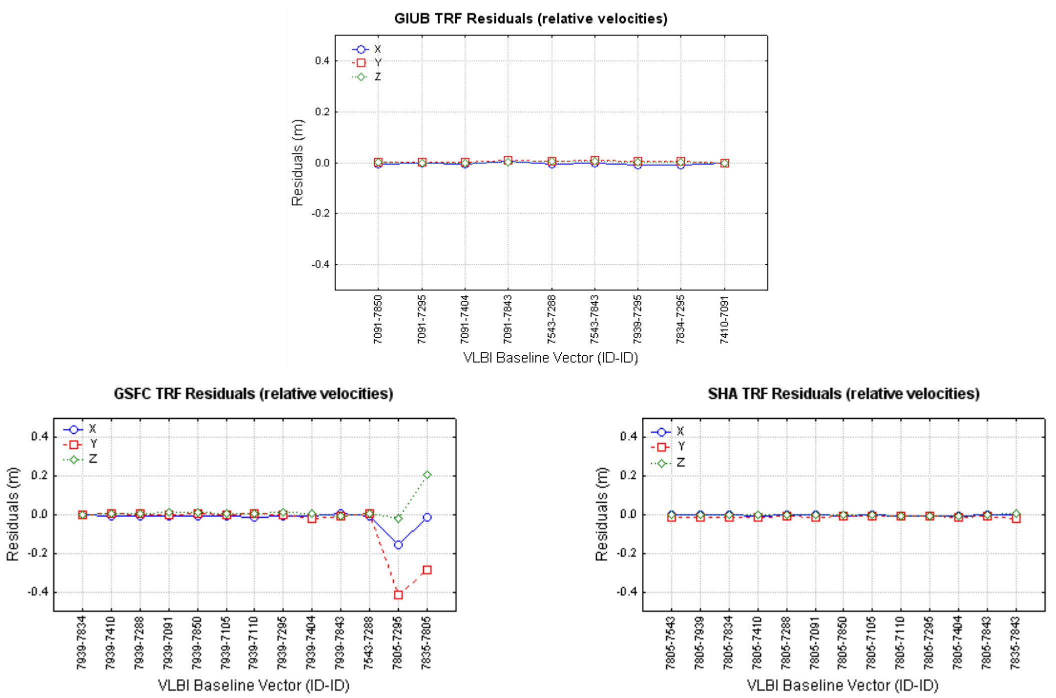

Figure A1.20 A series of residual plots for XYZ relative velocities with respect to each individual VLBI TRF solution in inter-technique combination using preferred observation functionals approach (POF with GPSSV)

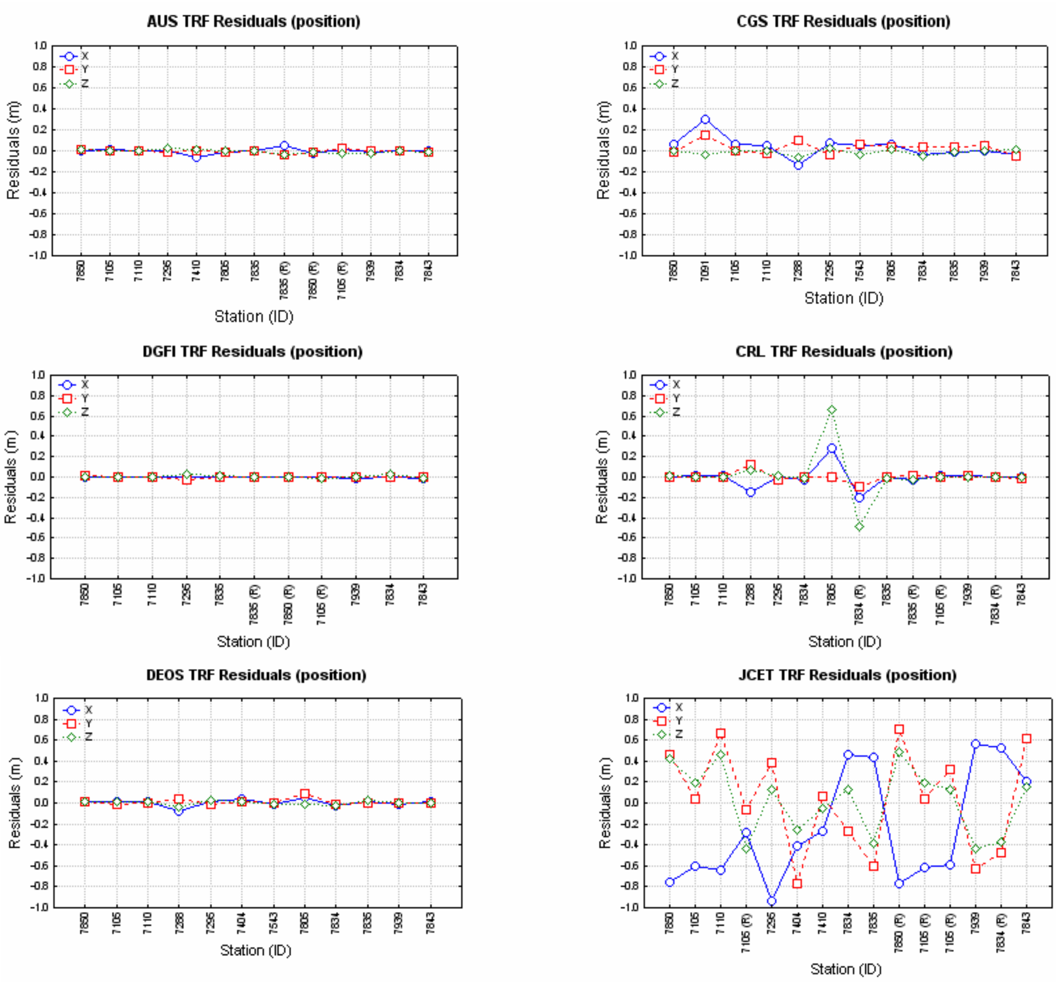

Figure A1.21 A series of residual plots for XYZ positions with respect to each individual SLR TRF solution in inter-technique combination using preferred observation functionals approach (POF with GPSSV)

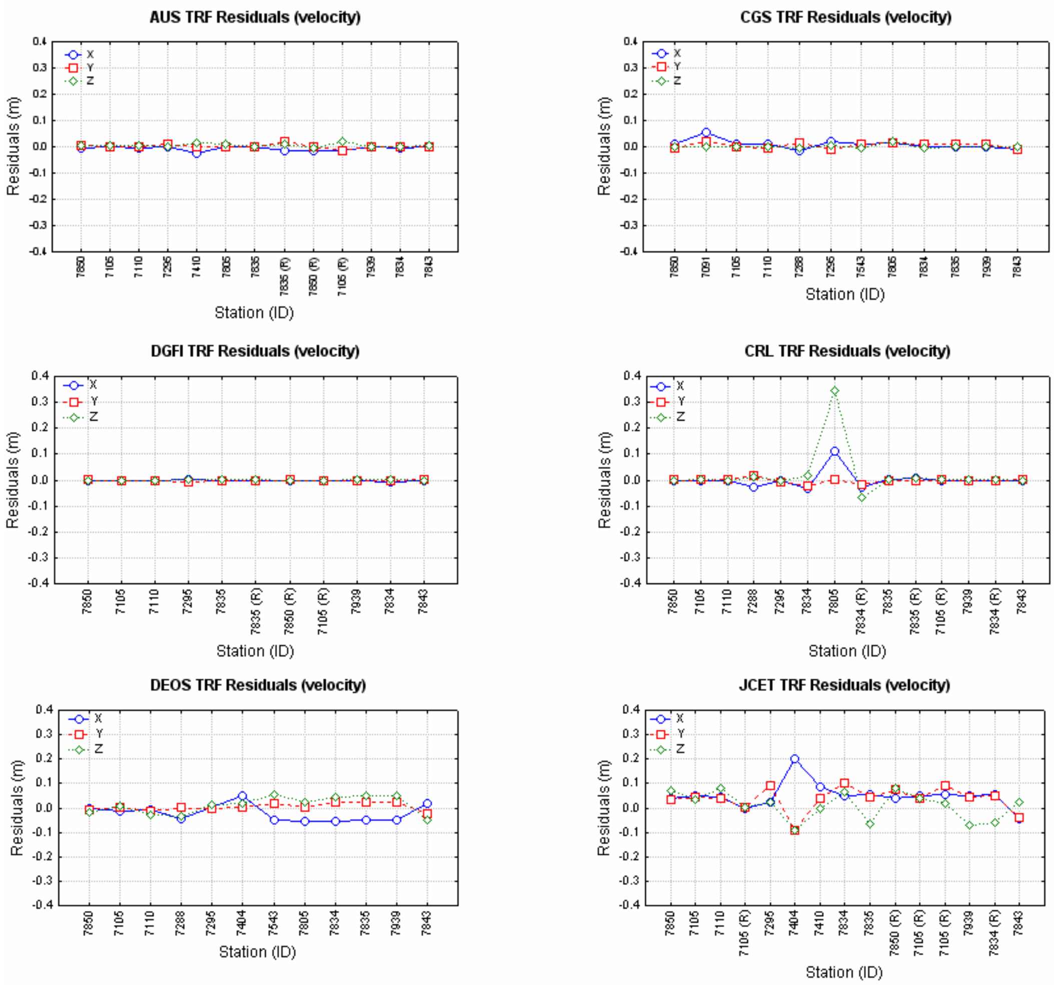

Figure A1.22 A series of residual plots for XYZ velocities with respect to each individual SLR TRF solution in inter-technique combination using preferred observation functionals approach (POF with GPSSV)

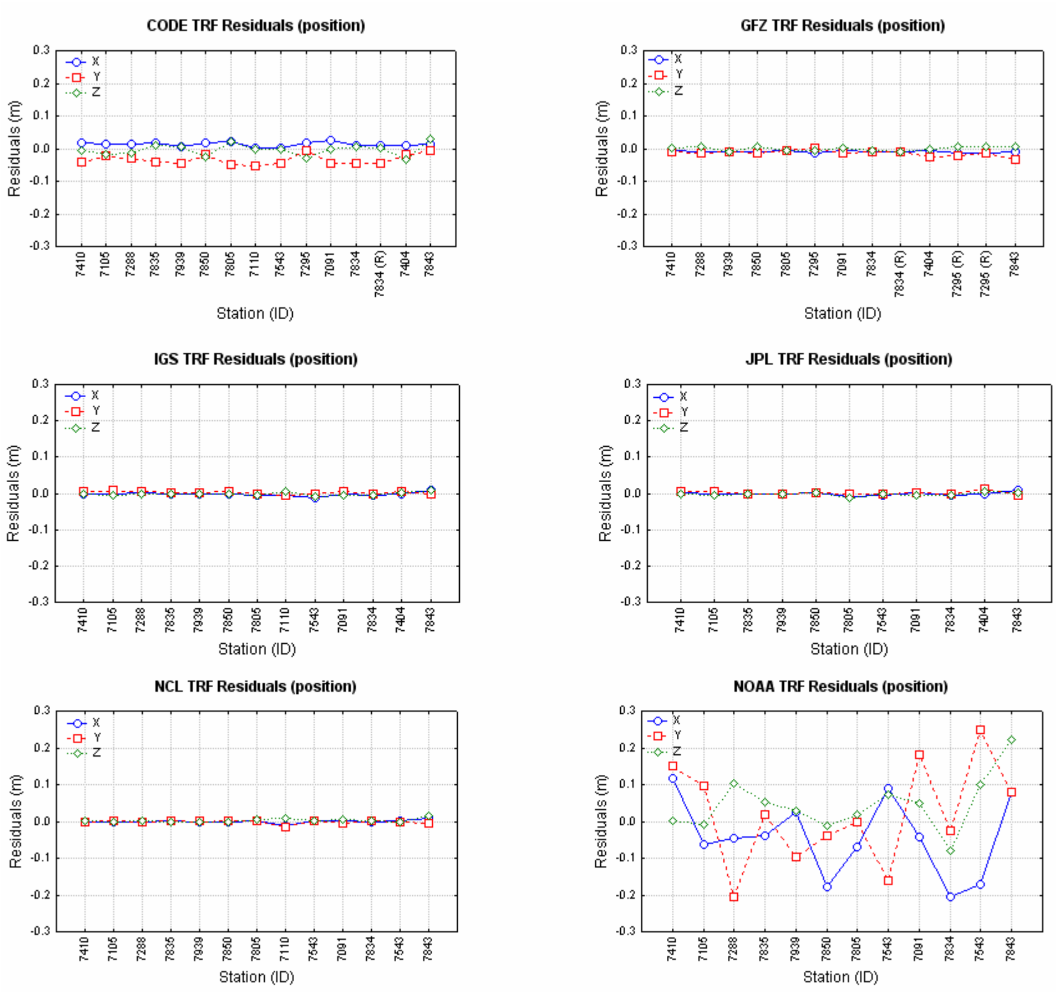

Figure A1.23 A series of residual plots for XYZ positions with respect to each individual GPS TRF solution in inter-technique combination using preferred observation functionals approach (POF with GPSSV)

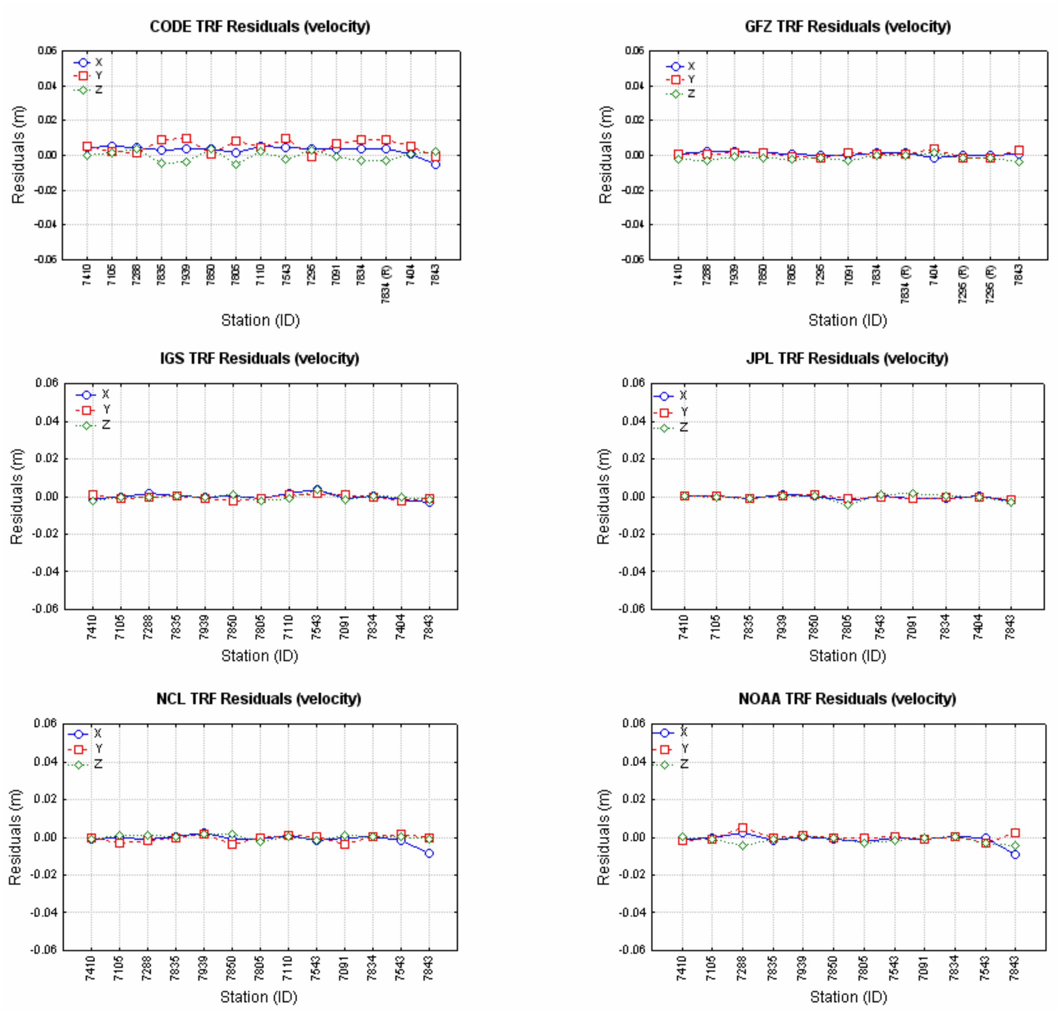

Figure A1.24 A series of residual plots for XYZ velocities with respect to each individual GPS TRF solution in inter-technique combination using preferred observation functionals approach (POF with GPSSV)

APPENDIX A2 – FINAL COMBINATION SOLUTION RESULTS

Table A2.1 Station positions at epoch 1997.0 and velocities estimated using state vector formulation

DOMES	Site Name	ID	X/Vx	Y/Vy	Z/Vz	Standard Deviation		
			----------m/m/year----------					
10002S001	GRASSE	7835	4581691.6643	556159.5618	4389359.4880	0.0184	0.0283	0.0176
			-0.0153	0.0172	0.0069	0.0013	0.0013	0.0014
10503S001	METSAHOVI	7805	2892595.4518	1311807.8133	5512610.8399	0.0157	0.0150	0.0167
			-0.0183	0.0142	0.0051	0.0011	0.0011	0.0010
12717M001	NOTO	7543	4934528.8883	1321133.3873	3806522.7238	0.0204	0.0322	0.0169
			-0.0168	0.0160	0.0117	0.0017	0.0014	0.0015
12734S001	MATERA	7939	4641964.8915	1393070.1214	4133262.3723	0.0193	0.0280	0.0169
			-0.0189	0.0184	0.0115	0.0014	0.0013	0.0014
14201S002	WETTZELL	7834	4075529.8889	931781.4301	4801618.2827	0.0166	0.0217	0.0169
			-0.0159	0.0162	0.0075	0.0012	0.0012	0.0013
40104M003	ALGONQUIN	7410	918213.0525	-4346066.5777	4561957.6581	0.0774	0.0281	0.0491
			-0.0196	-0.0051	-0.0020	0.0020	0.0015	0.0013
40405M013	GOLDSTONE	7288	-2356494.1532	-4646607.6770	3668426.5600	0.0901	0.0590	0.0551
			-0.0228	0.0039	-0.0120	0.0023	0.0019	0.0016
40440M001	WESTFORD	7091	1492453.6303	-4457278.7900	4296815.9361	0.0770	0.0272	0.0499
			-0.0189	-0.0027	-0.0017	0.0020	0.0015	0.0013
40442M008	FORT DAVIS	7850	-1330008.1486	-5328391.6159	3236502.6838	0.0951	0.0494	0.0595
			-0.0162	-0.0010	-0.0125	0.0023	0.0018	0.0015
40451M105	WASHINGTON	7105	1130719.6856	-4831350.5979	3994106.5214	0.0825	0.0299	0.0531
			-0.0181	-0.0016	-0.0034	0.0021	0.0016	0.0013
40497M001	MONUMENT PARK	7110	-2386278.1702	-4802354.1824	3444881.5696	0.0920	0.0597	0.0565
			-0.0336	0.0259	0.0063	0.0024	0.0019	0.0016
40499M002	RICHMOND	7295	961318.9797	-5674091.0287	2740489.6092	0.0930	0.0381	0.0607
			-0.0125	-0.0083	0.0015	0.0022	0.0021	0.0015
41705M004	SANTIAGO	7404	1769714.5499	-5044609.4728	-3468260.5980	0.0849	0.0797	0.0669
			0.0236	-0.0085	0.0063	0.0017	0.0022	0.0017
50103S007	CANBERRA	7843	-4446477.0693	2678126.9768	-3696251.2923	0.0096	0.1213	0.0661
			-0.0361	0.0012	0.0315	0.0018	0.0027	0.0034

Table A2.2 Station positions at epoch 1997.0 and velocities estimated using preferred observation functionals approach (POF with GPSBL)

DOMES	Site Name	ID	X/Vx	Y/Vy	Z/Vz	Standard Deviation		
			m/m/year					
10002S001	GRASSE	7835	4581691.6541	556159.5379	4389359.4883	0.0051	0.0048	0.0050
			-0.0128	0.0188	0.0099	0.0009	0.0010	0.0009
10503S001	METSAHOVI	7805	2892595.4555	1311807.7900	5512610.8503	0.0068	0.0057	0.0082
			-0.0172	0.0148	0.0049	0.0011	0.0012	0.0010
12717M001	NOTO	7543	4934528.8843	1321133.3608	3806522.7293	0.0102	0.0060	0.0089
			-0.0161	0.0189	0.0150	0.0020	0.0012	0.0017
12734S001	MATERA	7939	4641964.8846	1393070.0967	4133262.3781	0.0056	0.0049	0.0054
			-0.0174	0.0202	0.0146	0.0010	0.0010	0.0010
14201S002	WETTZELL	7834	4075529.8814	931781.4069	4801618.2802	0.0052	0.0048	0.0050
			-0.0149	0.0176	0.0091	0.0009	0.0009	0.0009
40104M003	ALGONQUIN	7410	918213.0258	-4346066.5744	4561957.6731	0.0066	0.0056	0.0071
			-0.0157	-0.0026	0.0009	0.0009	0.0011	0.0013
40405M013	GOLDSTONE	7288	-2356494.1685	-4646607.6773	3668426.6192	0.0070	0.0087	0.0111
			-0.0156	0.0051	-0.0050	0.0010	0.0012	0.0013
40440M001	WESTFORD	7091	1492453.6086	-4457278.7941	4296815.9813	0.0065	0.0055	0.0092
			-0.0153	-0.0007	0.0019	0.0009	0.0010	0.0011
40442M008	FORT DAVIS	7850	-1330008.1881	-5328391.5971	3236502.7081	0.0053	0.0051	0.0052
			-0.0123	-0.0003	-0.0064	0.0009	0.0010	0.0010
40451M105	WASHINGTON	7105	1130719.6427	-4831350.5875	3994106.5435	0.0052	0.0047	0.0051
			-0.0145	-0.0003	0.0012	0.0009	0.0010	0.0011
40497M001	MONUMENT PARK	7110	-2386278.2068	-4802354.1542	3444881.6062	0.0051	0.0053	0.0051
			-0.0299	0.0258	0.0147	0.0009	0.0010	0.0010
40499M002	RICHMOND	7295	961318.9340	-5674091.0244	2740489.6158	0.0066	0.0079	0.0069
			-0.0093	-0.0035	0.0020	0.0010	0.0016	0.0013
41705M004	SANTIAGO	7404	1769714.4642	-5044609.4111	-3468260.6027	0.0353	0.0330	0.0245
			0.0225	-0.0073	0.0069	0.0017	0.0022	0.0022
50103S007	CANBERRA	7843	-4446477.0722	2678126.9986	-3696251.2295	0.0051	0.0050	0.0054
			-0.0377	0.0006	0.0444	0.0010	0.0011	0.0011

Table A2.3 Station positions at epoch 1997.0 and velocities estimated using preferred observation functionals approach (POF with GPSBV)

DOMES	Site Name	ID	X/Vx	Y/Vy	Z/Vz	Standard Deviation		
			m/m/year					
10002S001	GRASSE	7835	4581691.6542	556159.5370	4389359.4895	0.0053	0.0051	0.0052
			-0.0128	0.0188	0.0103	0.0012	0.0012	0.0012
10503S001	METSAHOVI	7805	2892595.4559	1311807.7966	5512610.8495	0.0057	0.0050	0.0052
			-0.0178	0.0139	0.0058	0.0012	0.0011	0.0011
12717M001	NOTO	7543	4934528.8795	1321133.3596	3806522.7264	0.0055	0.0052	0.0054
			-0.0165	0.0174	0.0135	0.0015	0.0012	0.0014
12734S001	MATERA	7939	4641964.8849	1393070.0952	4133262.3748	0.0055	0.0051	0.0053
			-0.0182	0.0196	0.0139	0.0012	0.0012	0.0012
14201S002	WETTZELL	7834	4075529.8854	931781.4072	4801618.2872	0.0054	0.0050	0.0052
			-0.0150	0.0173	0.0096	0.0012	0.0011	0.0012
40104M003	ALGONQUIN	7410	918213.0241	-4346066.5728	4561957.6756	0.0054	0.0051	0.0052
			-0.0158	-0.0036	0.0015	0.0012	0.0012	0.0012
40405M013	GOLDSTONE	7288	-2356494.1827	-4646607.6546	3668426.5942	0.0054	0.0057	0.0054
			-0.0172	0.0050	-0.0051	0.0012	0.0013	0.0013
40440M001	WESTFORD	7091	1492453.5980	-4457278.7873	4296815.9502	0.0054	0.0050	0.0053
			-0.0155	-0.0012	0.0018	0.0012	0.0011	0.0012
40442M008	FORT DAVIS	7850	-1330008.1844	-5328391.5965	3236502.7145	0.0055	0.0053	0.0054
			-0.0121	-0.0004	-0.0072	0.0013	0.0012	0.0012
40451M105	WASHINGTON	7105	1130719.6509	-4831350.5928	3994106.5386	0.0054	0.0050	0.0053
			-0.0141	-0.0004	0.0006	0.0012	0.0011	0.0012
40497M001	MONUMENT PARK	7110	-2386278.2003	-4802354.1577	3444881.6037	0.0054	0.0056	0.0054
			-0.0291	0.0258	0.0134	0.0012	0.0012	0.0012
40499M002	RICHMOND	7295	961318.9335	-5674091.0247	2740489.6301	0.0059	0.0074	0.0061
			-0.0093	-0.0045	0.0028	0.0014	0.0017	0.0014
41705M004	SANTIAGO	7404	1769714.4786	-5044609.4696	-3468260.5685	0.0065	0.0059	0.0056
			0.0216	-0.0049	0.0109	0.0016	0.0016	0.0014
50103S007	CANBERRA	7843	-4446477.0859	2678126.9993	-3696251.2332	0.0055	0.0053	0.0058
			-0.0397	0.0005	0.0436	0.0013	0.0013	0.0013

Table A2.4 Station positions at epoch 1997.0 and velocities estimated using preferred observation functionals approach (POF with GPSSV)

DOMES	Site Name	ID	X/Vx	Y/Vy	Z/Vz	Standard Deviation		
			m/m/year					
10002S001	GRASSE	7835	4581691.6553	556159.5372	4389359.4910	0.0063	0.0060	0.0062
			-0.0130	0.0187	0.0102	0.0014	0.0014	0.0014
10503S001	METSAHOVI	7805	2892595.4553	1311807.7963	5512610.8493	0.0067	0.0060	0.0061
			-0.0179	0.0138	0.0057	0.0015	0.0013	0.0013
12717M001	NOTO	7543	4934528.8790	1321133.3597	3806522.7267	0.0065	0.0062	0.0064
			-0.0165	0.0173	0.0135	0.0018	0.0015	0.0017
12734S001	MATERA	7939	4641964.8844	1393070.0952	4133262.3749	0.0065	0.0061	0.0063
			-0.0181	0.0195	0.0142	0.0014	0.0014	0.0014
14201S002	WETTZELL	7834	4075529.8848	931781.4071	4801618.2868	0.0065	0.0059	0.0061
			-0.0148	0.0173	0.0099	0.0014	0.0013	0.0014
40104M003	ALGONQUIN	7410	918213.0242	-4346066.5727	4561957.6748	0.0064	0.0061	0.0062
			-0.0157	-0.0041	0.0020	0.0014	0.0014	0.0014
40405M013	GOLDSTONE	7288	-2356494.1837	-4646607.6577	3668426.5961	0.0064	0.0068	0.0064
			-0.0165	0.0064	-0.0061	0.0015	0.0016	0.0015
40440M001	WESTFORD	7091	1492453.5978	-4457278.7870	4296815.9491	0.0064	0.0060	0.0064
			-0.0154	-0.0014	0.0023	0.0014	0.0014	0.0014
40442M008	FORT DAVIS	7850	-1330008.1842	-5328391.5972	3236502.7142	0.0066	0.0063	0.0064
			-0.0120	-0.0004	-0.0070	0.0015	0.0014	0.0014
40451M105	WASHINGTON	7105	1130719.6509	-4831350.5935	3994106.5391	0.0065	0.0059	0.0063
			-0.0139	-0.0006	0.0004	0.0015	0.0013	0.0014
40497M001	MONUMENT PARK	7110	-2386278.2003	-4802354.1583	3444881.6039	0.0064	0.0066	0.0063
			-0.0290	0.0256	0.0133	0.0015	0.0014	0.0014
40499M002	RICHMOND	7295	961318.9335	-5674091.0240	2740489.6296	0.0069	0.0082	0.0071
			-0.0092	-0.0045	0.0031	0.0016	0.0020	0.0016
41705M004	SANTIAGO	7404	1769714.4778	-5044609.4686	-3468260.5684	0.0076	0.0069	0.0066
			0.0218	-0.0051	0.0109	0.0018	0.0018	0.0016
50103S007	CANBERRA	7843	-4446477.0866	2678126.9999	-3696251.2330	0.0064	0.0062	0.0067
			-0.0401	0.0005	0.0436	0.0015	0.0015	0.0015

Table A2.5 Station positions at epoch 1997.0 and velocities from ITRF2000 official solution

DOMES	Site Name	ID	X/Vx	Y/Vy	Z/Vz	Standard Deviation		
			m/m/year					
10002S001	GRASSE	7835	4581691.6414	556159.5385	4389359.4907	0.0017	0.0008	0.0018
			-0.0131	0.0189	0.0101	0.0003	0.0001	0.0004
10503S001	METSAHOVI	7805	2892595.4395	1311807.8057	5512610.8509	0.0049	0.0045	0.0053
			-0.0160	0.0149	0.0088	0.0003	0.0002	0.0006
12717M001	NOTO	7543	4934528.8762	1321133.3599	3806522.7332	0.0023	0.0015	0.0022
			-0.0173	0.0174	0.0134	0.0004	0.0002	0.0004
12734S001	MATERA	7939	4641964.8795	1393070.0954	4133262.3851	0.0023	0.0015	0.0023
			-0.0188	0.0191	0.0131	0.0003	0.0001	0.0004
14201S002	WETTZELL	7834	4075529.8789	931781.4087	4801618.2964	0.0020	0.0014	0.0024
			-0.0157	0.0172	0.0087	0.0002	0.0001	0.0004
40104M003	ALGONQUIN	7410	918213.0104	-4346066.5805	4561957.6853	0.0024	0.0029	0.0029
			-0.0161	-0.0041	0.0026	0.0001	0.0003	0.0004
40405M013	GOLDSTONE	7288	-2356494.1810	-4646607.6517	3668426.6127	0.0032	0.0049	0.0042
			-0.0161	0.0059	-0.0051	0.0002	0.0003	0.0004
40440M001	WESTFORD	7091	1492453.5956	-4457278.7907	4296815.9674	0.0014	0.0028	0.0029
			-0.0156	-0.0013	0.0026	0.0001	0.0002	0.0003
40442M008	FORT DAVIS	7850	-1330008.1960	-5328391.5907	3236502.7116	0.0018	0.0027	0.0024
			-0.0125	-0.0001	-0.0065	0.0001	0.0003	0.0003
40451M105	WASHINGTON	7105	1130719.6324	-4831350.5774	3994106.5389	0.0008	0.0016	0.0017
			-0.0148	-0.0001	0.0010	0.0001	0.0003	0.0003
40497M001	MONUMENT PARK	7110	-2386278.2108	-4802354.1447	3444881.5980	0.0010	0.0016	0.0016
			-0.0306	0.0255	0.0145	0.0002	0.0003	0.0003
40499M002	RICHMOND	7295	961318.9239	-5674090.9937	2740489.6115	0.0022	0.0035	0.0025
			-0.0097	-0.0013	0.0013	0.0002	0.0005	0.0004
41705M004	SANTIAGO	7404	1769714.4889	-5044609.4949	-3468260.5760	0.0259	0.0282	0.0218
			0.0221	-0.0059	0.0111	0.0004	0.0006	0.0005
50103S007	CANBERRA	7843	-4446477.0840	2678127.0102	-3696251.2509	0.0021	0.0016	0.0022
			-0.0376	0.0011	0.0440	0.0004	0.0003	0.0005